TAMPERE UNIVERSITY OF TECHNOLOGY

TERO-PETRI RUOKO

UV-LIGHT INDUCED DEGRADATION OF POLYPROPYLENE AND POLYSTYRENE – A SPECTROSCOPIC AND DSC STUDY

Master of Science Thesis

Examiners: Professor Helge Lemmetyinen
Adjunct professor Terttu Hukka
Examiners and topic approved in the Faculty of Science and Environmental Engineering Council meeting on 6 June 2012

ABSTRACT

TAMPERE UNIVERSITY OF TECHNOLOGY
Master's Degree Programme in Science and Engineering
RUOKO, TERO-PETRI: UV-light induced degradation of polypropylene and polystyrene – a spectroscopic and DSC study
Master of Science Thesis, 76 pages
August 2012
Major: Chemistry
Examiners: Professor Helge Lemmetyinen and adjunct professor Terttu Hukka
Keywords: Polymer, degradation, UV radiation, photodegradation, photo-oxidation, polypropylene, polystyrene, FTIR, UV-Vis, DSC, DPC, OIT.

Ultraviolet (UV) radiation is an important factor affecting the life-time of polymer products. When polymers are exposed to UV radiation in the presence of oxygen they degrade due to photo-oxidative reactions. The changes in the mechanical properties and appearances of polymers are the result of chemical changes in the polymer structure. The observation of the early chemical changes in the photo-oxidative degradation of polypropylene (PP) and polystyrene (PS) was examined in this thesis.

In this thesis Fourier transform infrared (FTIR) spectroscopy, ultraviolet-visible (UV-Vis) spectroscopy and differential scanning calorimetry (DSC) were used to study the changes that occurred in polypropylene and polystyrene when they were irradiated with a xenon arc lamp in air. The spectroscopic methods were used to observe the chemical changes in the polymer structure and the addition of new chemical groups and DSC was used to observe changes in the thermal properties and oxidative stability of the polymers. Differential photocalorimetry (DPC) was used as a novel method to observe changes in the oxidative stability of polymers with simultaneous irradiation. The DPC results were compared with the DSC results to examine how irradiation affects the oxidative stability of PP and PS.

The largest change observed in the polymer samples during irradiation was the formation of a carbonyl group absorption band in the IR spectra located at $\tilde{\nu} \approx 1720\ \mathrm{cm}^{-1}$. A substantial increase in the absorbance between $\lambda = 270\text{–}350$ nm was observed in the UV-Vis spectra of PS, due mostly to the formation of conjugated double bonds. A small increase in the absorbance between $\lambda = 250\text{–}300$ nm was observed in the UV-Vis spectra of PP, assigned to the formation of carbonyl groups. The melting temperature of PP decreased after irradiation, which was assigned to chain scission. The glass transition temperature of PS rose steadily for the first irradiation sequences, but decreased noticeably during the last one. The increase was assigned to crosslinking whereas the decrease was assigned to either chain scission or the photochain oxidation mechanism. The oxidation induction time (OIT) of PP decreased over 90 % during the first irradiation sequence. The oxidation occurred practically immediately for the irradiated samples, which indicates a large and fast decrease in thermal oxidative stability. The OIT test was not applicable for PS. The oxidation induction temperature (T_{ox}) decreased for PP and increased for PS due to photodegradation. This may be due to changes in the average molecular mass, with a decrease in mass indicating a decrease in the oxidation induction temperature and vice versa.

TIIVISTELMÄ

TAMPEREEN TEKNILLINEN YLIOPISTO
Teknis-luonnontieteellinen koulutusohjelma
RUOKO, TERO-PETRI: UV-valon aikaansaama polypropeenin ja polystyreenin rappeutuminen – spektroskopinen ja DSC tutkimus
Diplomityö, 76 sivua
Elokuu 2012
Pääaine: Kemia
Tarkastajat: Professori Helge Lemmetyinen ja dosentti Terttu Hukka
Avainsanoja: Polymeeri, vanheneminen, UV -säteily, valon aikaansaama vanheneminen, valon aikaansaama hapettuminen, polypropeeni, polystyreeni, FTIR, UV-Vis, DSC, DPC.

Ultraviolettisäteily on tärkeä polymeerituotteiden elinikään vaikuttava tekijä. Kun polymeerejä altistetaan UV-säteilylle hapen läsnä ollessa, ne rappeutuvat valon aikaansaamien hapetusreaktioiden ansiosta. Muutokset polymeerien mekaanisissa ja ulkoisissa ominaisuuksissa aiheutuvat kemiallisista muutoksista polymeerirakenteessa. Tässä diplomityössä tutkittiin varhaisten kemiallisten muutosten havaitsemista polypropeenin (PP) ja polystyreenin (PS) rappeutumisessa valon vaikutuksesta.

Tässä työssä käytettiin Fourier'n muunnos infrapunaspektroskopiaa (FTIR), ultravioletti-näkyvä valo (UV-Vis) -spektroskopiaa sekä differentiaalista pyyhkäisykalorimetriaa (DSC) polypropeenissa ja polystyreenissä tapahtuvien muutosten havaitsemiseen, kun niitä säteilytettiin ksenon-kaarilampulla ilman läsnäollessa. Spektroskopisia menetelmiä käytettiin polymeerirakenteessa tapahtuvien muutosten ja uusien funktionaalisten ryhmien muodostumisen havaitsemiseen, ja DSC:tä käytettiin havaitsemaan muutoksia polymeerien termisissä ominaisuuksissa ja hapettumisen kestossa. Differentiaalista fotokalorimetriaa (DPC) käytettiin uutena menetelmänä muutosten havaitsemiseen hapettumisen kestossa samanaikaisen säteilytyksen kanssa. DPC:llä mitattua hapettumisen kestoa verrattiin DSC:llä mitattuun säteilytyksen vaikutuksen määrittämiseksi PP:n ja PS:n hapettumisen kestossa.

Suurin muutos säteilytetyissä polymeerinäytteissä oli IR-spektreihin aaltoluvulle $\tilde{\nu} \approx 1720\ \mathrm{cm}^{-1}$ muodostunut karbonyyliryhmän absorptiovyö. Polystyreenin UV-Vis-spektreissä havaittiin huomattava absorbanssin kasvu välillä $\lambda = 270\text{–}350\ \mathrm{nm}$, mikä johtui konjugoituneiden kaksoisidosten muodostumisesta. Polypropeenin UV-Vis spektreissä havaittiin pieni absorbanssin kasvu välillä $\lambda = 250\text{–}300\ \mathrm{nm}$, mikä johtui karbonyyliryhmien muodostumisesta. Polypropeenin sulamislämpötila laski säteilytyksen jälkeen, minkä aiheutti polymeeriketjujen katkeaminen. Polystyreenin lasittumislämpötila kasvoi tasaisesti ensimmäiset säteilytysjaksot, mutta laski huomattavasti viimeisen aikana. Kasvu johtui polymeeriketjujen silloittumisesta, kun taas lasku oli seurausta joko ketjujen katkeamisesta tai valoketjuhapettumismekanismista. Polypropeenin hapettumisen alkamisaika (OIT) laski yli 90 % ensimmäisen säteilytysjakson aikana. Säteilytettyjen näytteiden hapettuminen tapahtui käytännössä välittömästi, mikä viittaa huomattavaan ja nopeaan laskuun termisen hapettumisen kestossa. OIT-mittaus ei soveltunut PS:lle. Hapettumisen alkamislämpötila (T_{ox}) laski PP:lle ja kasvoi PS:lle valon aikaansaaman hajoamisen seurauksena. Tämä voi olla seurausta keskimääräisen molekyylimassan muutoksista, jolloin massan lasku vastaa laskua hapettumisen alkamislämpötilassa ja päinvastoin.

PREFACE

This Master of Science Thesis was conducted at the Laboratory of Chemistry at Tampere University of Technology and was examined by professor Helge Lemmetyinen and adjunct professor Terttu Hukka. The thesis was funded by the Academy of Finland.

I would like to thank professor Lemmetyinen and adjunct professor Hukka for their guidance throughout the process of writing this thesis. I would also like to thank professor Lemmetyinen and all of the participants of the UVIADEM project for enabling this opportunity to work at the Laboratory of Chemistry. Special thanks are due to my wife and father for their support throughout my studies.

Tampere, 24 July 2012

Tero-Petri Ruoko
tp.ruoko@gmail.com

CONTENTS

ABBREVIATIONS AND NOTATION

-a	Suffix for an atactic polymer
CI	Carbonyl index
DSC	Differential scanning calorimetry
DPC	Differential photocalorimetry
FTIR	Fourier transform infrared, a type of spectroscopic measurement
HALS	Hindered amine light stabilizer
HI	Hydroxyl index
HPI	Hydroperoxide index
-i	Suffix for an isotactic polymer
ItI	Isotacticity index
PP	Polypropylene
PS	Polystyrene
-s	Suffix for a syndiotactic polymer
IR	Infrared wavelength range of light
OIT	Oxidation induction time
UV	Ultraviolet wavelength range of light
UV-Vis	Ultraviolet-visible wavelength range of light
UVIADEM	UV radiation induced and assisted degradation of materials
Vis	Visible wavelength range of light
λ	Wavelength of electromagnetic radiation
ν	Frequency of electromagnetic radiation
$\tilde{\nu}$	Wavenumber of electromagnetic radiation
A	Absorbance
c	Speed of electromagnetic radiation
E_{exc}	Excited energy state
E_{in}	Initial energy state
E_{ph}	Photon energy
h	Planck constant
ΔH_f	Melting enthalpy
I_0	Incident radiation intensity
I_a	Absorbed radiation intensity
I_r	Reflected radiation intensity
I_t	Transmitted radiation intensity
T	Transmittance
T_g	Glass transition temperature
T_{onset}	Onset temperature of melting
T_{ox}	Oxidation induction temperature
T_m	Peak temperature of melting

1. INTRODUCTION

Many polymers are susceptible to attack by numerous natural and man-made agents; they can degrade by exposure to high temperature, mechanical wear, oxygen and ozone, radiation, moisture and chemical agents. Exposure to these agents can seriously affect the expected lifetime of plastic products. Often a plastic product is exposed to a combination of the degrading agents, resulting in accelerated degradation. [1, pp. 263–264] In this study the degradation caused by a combination of electromagnetic radiation and oxygen, known as photo-oxidation, is studied.

The degradation of plastic materials is traditionally studied using crude mechanical tests which result in the destruction of the sample [1, pp. 186–200]. These methods observe degradation only after the material has degraded thoroughly. Because photodegradation begins in the surface layer before progressing to the bulk of the material, the detection of the early phases of degradation is impractical using these methods.

The purpose of this study is to examine the use of infrared (IR) and ultraviolet-visible spectroscopies (UV-Vis) and differential scanning calorimetry (DSC) in the early phases of the photodegradation of polypropylene and polystyrene. The spectroscopic methods are used to observe the chemical changes that occur during photodegradation whereas differential scanning calorimetry is used to obtain information about the changes in the thermal and physical properties of the polymers. Differential photocalorimetry (DPC) is used as a novel method in examining the effects of simultaneous irradiation on the DSC results. These instrumental methods are useful in the detection of photodegradation, because they are sensitive to the early chemical changes that occur during degradation and are non-destructive or require only minimal sample sizes. The goal of this study is to connect the changes observed in the properties of the materials during photodegradation with the degradation mechanisms of the polymers obtained from previous scientific literature.

The manufacturing methods and general properties of polypropylene and polystyrene are reviewed first in this thesis, after which the interaction between light and matter and the chemical mechanisms of photodegradation are examined as the theoretical background for photodegradation. The instrumental section presents the spectroscopic and DSC instrumental methods and the measurable properties of the polymers used to observe the photodegradation. The sample preparation and weathering and measurement methods are presented after the instrumental section. At the end of this thesis the obtained results are presented and the photodegradation observed in polypropylene and polystyrene are compared.

2. UVIADEM PROJECT

The UVIADEM (ultraviolet induced and assisted degradation of materials) project aims at improving the scientific understanding of the UV radiation induced and assisted degradation of materials. The focus of the project is on the mechanisms of the interactive and wavelength-specific effects of UV radiation on materials, together with other stress agents. The project is funded by the Academy of Finland.

The project is a joint effort between the Metrology Research Institute of Aalto University School of Science and Technology, the Atmospheric radiation research group of the Finnish Meteorological Institute and the Laboratory of Plastics and Elastomer Technology and the Laboratory of Chemistry at Tampere University of Technology. The cooperation between the research partners establishes a cross-disciplinary working environment, fostering active exchange of different views and emergence of new approaches within the research field. The collaboration enables the development and application of improved methodologies in studying the degradation processes, more detailed and focused observation and interpretation of degradation data and establishment of a coherent view on the deficits in the current life time predictions of materials.

The overall goal of the project is to deliver new knowledge on the UV induced and assisted degradation of materials. The objectives that will lead to this goal are:

1. Identifying the different degradation mechanisms, induced or assisted by different stress agents, and predict their temporal evolution in the current and future climates.
2. Determining more accurate action spectra for the UV radiation induced damages, as well as their dependence on temperature and time.
3. Deriving spectrally resolved acceleration factors for UV radiation levels in commonly used artificial ageing environments, as compared to natural weathering conditions.
4. Exploring the feasibility and correlation of selected destructive and non-destructive methods in the characterization of material property changes, especially at the early stage of degradation.
5. Developing a model for estimating the total cumulative environmental stress of a real three dimensional object.

The purpose of this study is to characterize the main chemical reactions involved in the UV degradation mechanism from previous scientific literature (part of objective 1) and

study the applicability of spectroscopic and thermal analytical methods in the early detection of degradation (objective 4).

3. PROPERTIES OF THE STUDIED POLYMERS

The manufacturing methods and basic properties of polypropylene and polystyrene are presented in this chapter. PP and PS are two of the most common thermoplastics, comprising together about 40 % of the total thermoplastics market [1, p. 354].

3.1 Properties of polypropylene

Commercial polypropylene was first produced in 1957. Today it is the largest sales volume polyolefin, comprising approximately a quarter of the total thermoplastics market in 2001 [1, p. 354]. PP is a lightweight, moderately high melting temperature plastic that is mainly used for the manufacturing of pipe, sheet, textile fiber and blow-molded containers. Polypropylene is manufactured from propylene, which is a byproduct of oil production. The structures of propylene and polypropylene are illustrated in Figure 3.1.

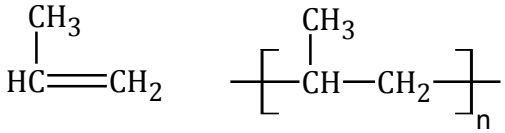

Figure 3.1 *Structures of propylene and polypropylene.*

One of the most important attributes that affects the physical properties of polypropylene, like melting temperature, crystallinity and susceptibility to solvent attack, is tacticity. Tacticity is defined as the orderliness of the succession of configurational repeating units in the main chain of a regular macromolecule, a regular oligomer molecule, a regular block, or a regular chain [2, p. 2292]. Tacticity depicts the relative stereochemistry of adjacent side groups in a polymer backbone.

A macromolecule can be categorized into one of three groups according to its tacticity: an isotactic macromolecule comprises of only one configurational base unit, which has chiral or prochiral atoms in the main chain in a unique arrangement with respect to its adjacent constitutional units; a syndiotactic macromolecule comprises of alternating enantiomeric configurational base units, which have chiral or prochiral atoms in the main chain in a unique arrangement with respect to their adjacent constitutional units or an atactic macromolecule, which is a regular macromolecule in which the configurational base units are not identical [2, p. 2292]. In isotactic polymers the side groups are connected to the same side of the polymer backbone and are all oriented in the same direction, whereas in syndiotactic polymers the side groups have alternate positions and each side group has a different orientation than the one before and after it. In

atactic polymers the side groups are connected randomly to the polymer backbone and don't have a preferred orientation.

Almost all commercial polypropylene is semi-crystalline highly isotactic polypropylene (PP-i), which is the form of PP used in this study. Syndiotactic polypropylene (PP-s) is also semi-crystalline and has some commercial applications, because it has a lower melting point and is more susceptible to solvent attack than PP-i. Atactic polypropylene (PP-a) is a rubbery amorphous polymer at ambient temperature having no important commercial uses. [1, p. 358] Figure 3.2 illustrates the differences between isotactic, syndiotactic and atactic polypropylene. In Figure 3.2 the polymer backbone is depicted as planar, with the methyl groups either in the same plane as the backbone (regular bond) or pointing out of plane, either up (solid wedge bond) or down (hashed wedge bond).

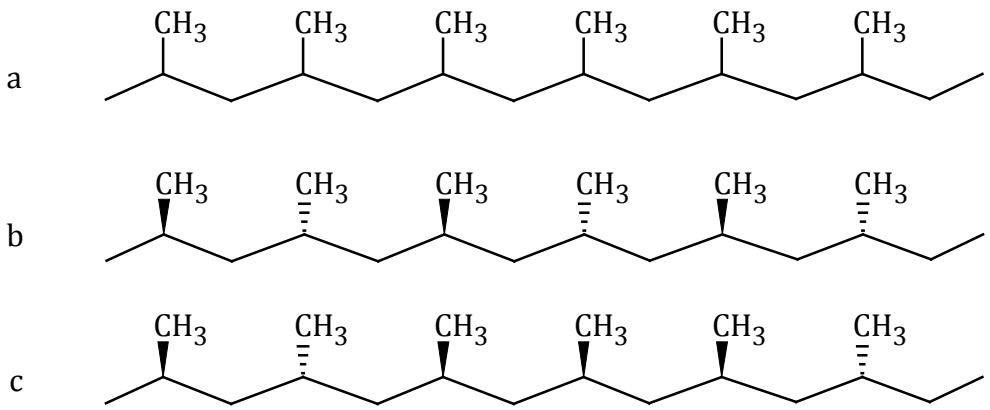

Figure 3.2 *Different types of polypropylene: (a) PP-i, (b) PP-s and (c) PP-a.*

Isotactic polypropylene was first produced by Giulio Natta in 1955 using a stereospecific Ziegler-type catalyst [3, p. 15]. Today most PP-i is manufactured using a Ziegler-Natta catalyst system which consists of crystalline titanium (III) chloride ($TiCl_3$) with a cocatalyst or activator, usually an organoaluminium compound such as diethylaluminium chloride. A metallocene catalyst is most often used to produce syndiotactic polypropylene whereas a Lewis acid or an organometallic compound catalyst produces atactic polypropylene. [1, p. 358]

The polymerization of isotactic polypropylene begins with the initiation phase (1) in which a Ziegler-Natta catalyst attaches to a propylene monomer [3, p. 21].

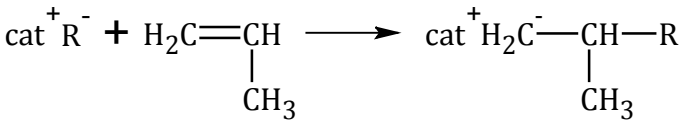

(1)

The initiation phase is followed by the propagation phase (2) in which additional propylene monomers attach between the polymer and the catalyst [3, p. 21].

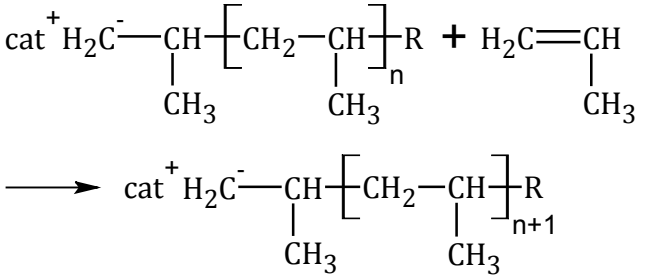

(2)

Polymerization ends in a termination phase which can occur in numerous ways. Termination involving heterolytic splitting of hydrogen (3) may take place in the presence of molecular hydrogen. Mechanism (3) is commonly used to control the degree of polymerization in the commercial manufacturing of PP-i. [3, p. 22]

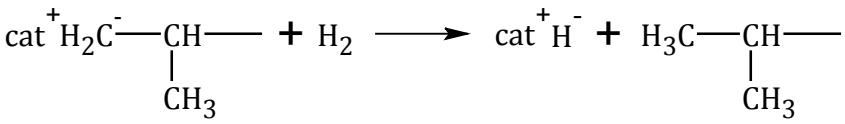

(3)

Other common termination mechanisms are transfer by monomer (4) and transfer of a hydride ion (5). [3, p.22]

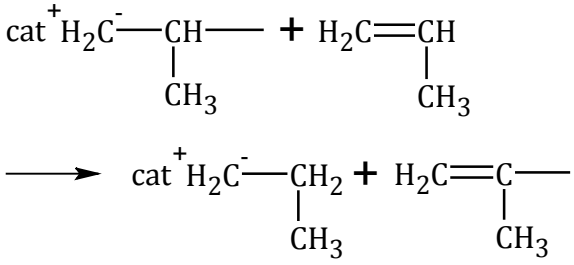

(4)

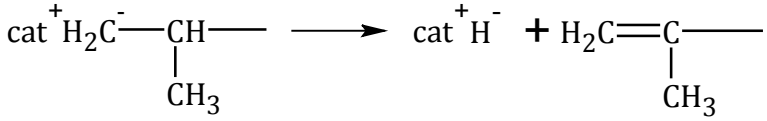

(5)

The catalyst hydride formed in reactions (3) and (5) is an active catalyst species which can initiate further polymerization of PP-i by realkylation with a propylene monomer (6). [3, p.22]

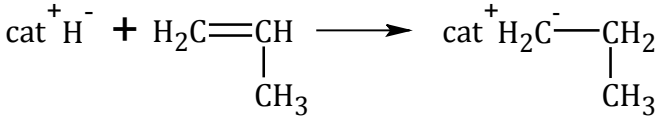

(6)

The termination mechanisms (3)–(5) imply that only terminal methyl or vinylidene groups ($-C(CH_3) = CH_2$) should occur in PP-i. This is supported by infrared measurements, although at higher polymerization temperatures (> 100 °C) terminal vinyl groups ($-CH = CH_2$) can also be detected. [3, p. 22]

The high degree of crystallinity of polypropylene, typically $60-80$ %, and high melting point of 165 °C (for fast cooled processed samples) are a consequence of a helical conformation that minimizes steric strain. The polymer backbone twists around its

main axis to form a 3_1 helix of the methyl side groups, which corresponds to a regular alternation of *trans* and *gauche* bonds. [3, pp. 47–58] Although isotactic polypropylene is highly crystalline due to its helical structure, it comprises of a mixture of crystalline isotactic and amorphous atactic segments. Typical commercial PP-i samples contain 90 % or more isotactic segments [3, p. 51].

3.2 Properties of polystyrene

Commercial polystyrene was first produced in quantity in 1938. Today styrenic polymers, principally general purpose and impact grades of polystyrene (PS-GP and PS-HI, respectively), comprise a sixth of the total thermoplastics market. Polystyrene is a brittle, high glass transition temperature polymer that is mainly used for packaging and insulation materials in the form of a foam or bead. Polystyrene is manufactured from styrene, which in turn is manufactured by the dehydrogenation of ethylbenzene. The structures of styrene and polystyrene are illustrated in Figure 3.4. [1, p. 359]

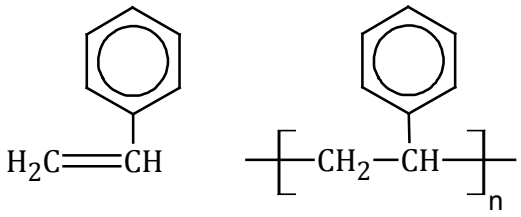

Figure 3.4 *Structures of styrene and polystyrene.*

Almost all commercial polystyrene is amorphous atactic polystyrene (PS-a), which is the form of PS used in this study. Isotactic PS (PS-i) is moderately crystalline but is also more brittle and expensive than PS-a, having no commercial applications. Like isotactic polypropylene, PS-i was first produced by Giulio Natta in 1955 using Ziegler-Natta catalysts. Syndiotactic polystyrene (PS-s) is also semi-crystalline and more expensive to produce than PS-a, but has better high temperature performance, toughness, lower permeability and good chemical resistance. It has potential applications in electrical and electronic applications. It was first produced in 1986 using metallocene polymerization. [1, p. 360]

Atactic polystyrene is wholly amorphous. It's relatively high glass transition temperature of 90 °C is a consequence of the phenyl substituents as side groups, which act as steric hindrances to the motion of the polymer that generally raises the glass transition temperature of a polymer.

Atactic polystyrene is manufactured by free-radical polymerization in bulk or suspension using peroxides or trace oxygen as initiators. Peroxides contain a labile group $(-\mathrm{O}-\mathrm{O}-)$ which can be broken by heat or irradiation. Other possible initiator species include azo $(-\mathrm{N}=\mathrm{N}-)$ and disulfide $(-\mathrm{S}-\mathrm{S}-)$ compounds. The decomposition of the initiator species, dissociation, is the first step of initiation in the polymerization of

polystyrene. Formula (7) shows the decomposition of benzoyl peroxide which is used as an example initiator. [1, p. 31]

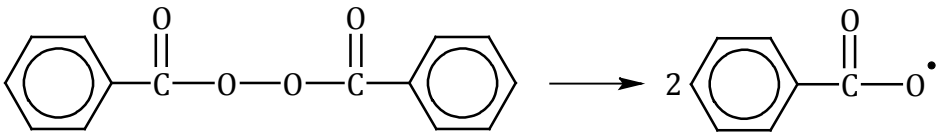

(7)

The second step of initiation is called association, in which a styrene monomer is attached to the initiator radical [1, p. 31]:

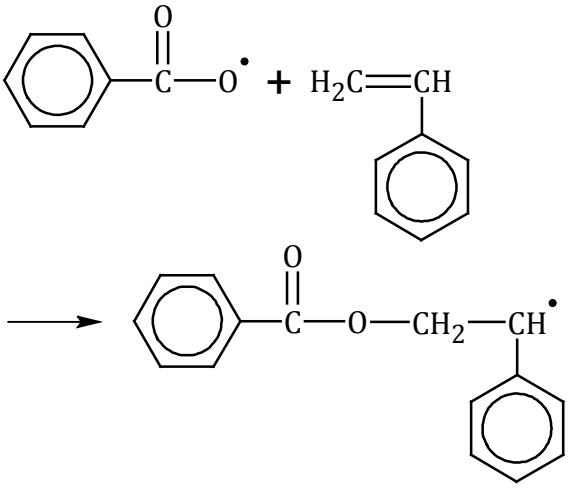

(8)

In the propagation phase additional styrene monomer units attach to the polystyrene radical [1, p. 32]:

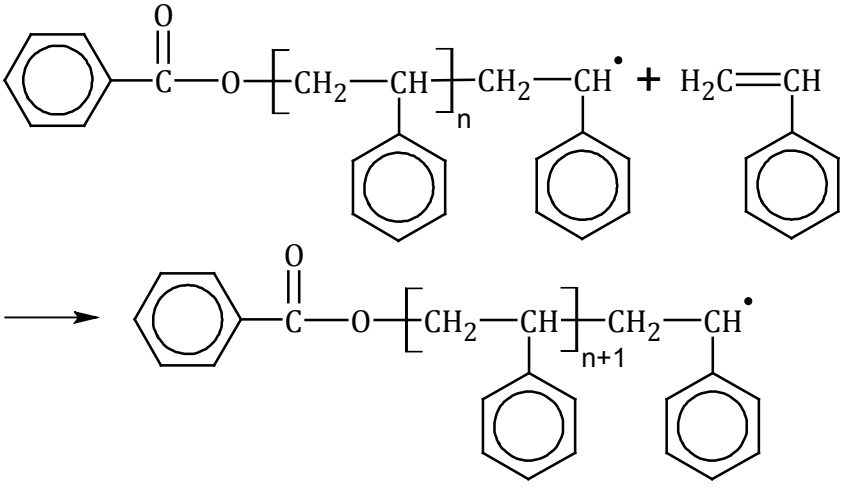

(9)

As with polypropylene, the termination of the polymerization of polystyrene can occur in numerous ways. Common termination reactions in the polymerization of polystyrene are combination, disproportionation and chain transfer. Combination is the main termination reaction in the polymerization of polystyrene. In a combination reaction two polystyrene macroradicals react to form a single polystyrene macromolecule [1, p. 32]:

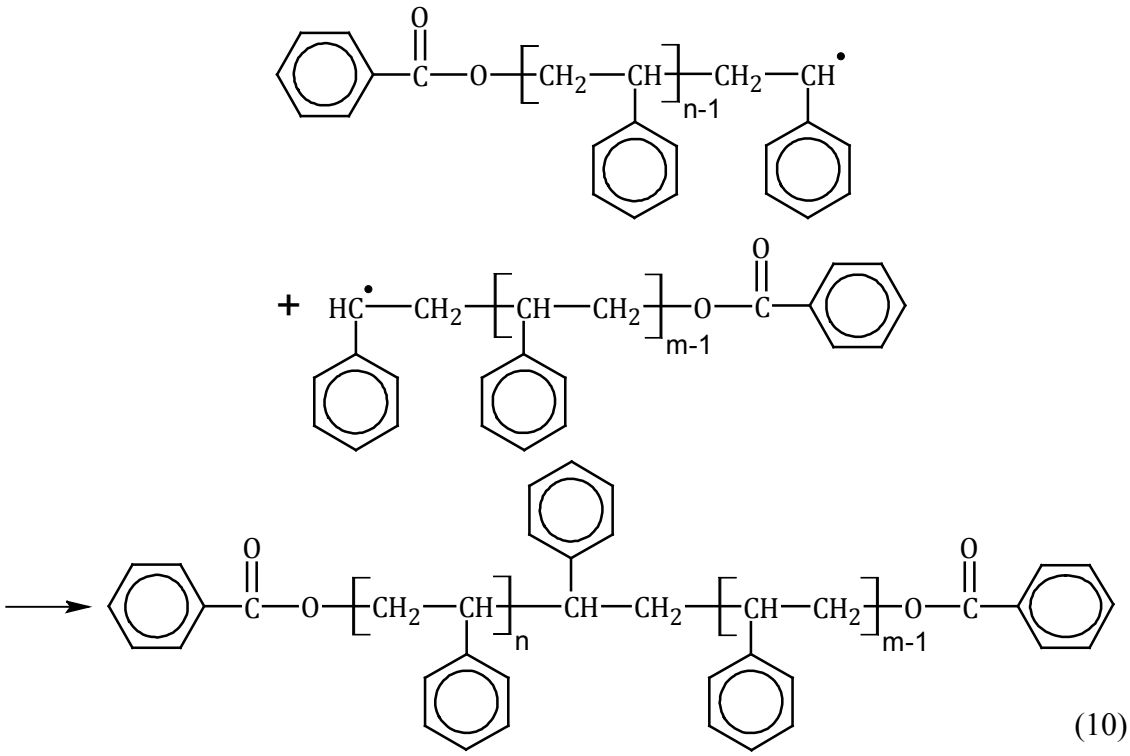

(10)

In a disproportionation reaction two polystyrene macroradicals react to form two polystyrene macromolecules [1, p. 33]:

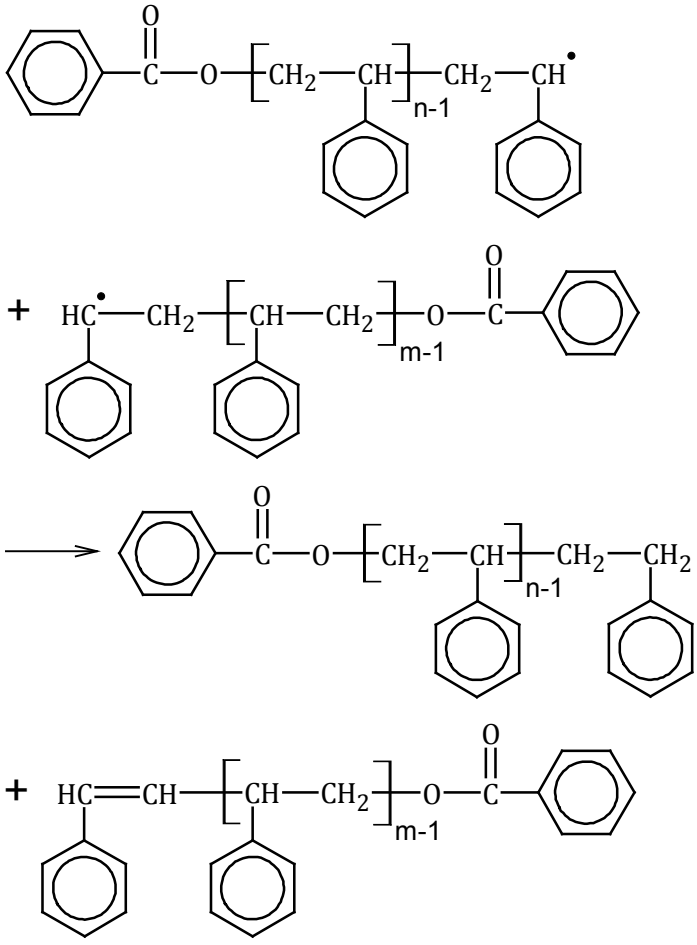

(11)

In a chain transfer reaction a polystyrene macroradical abstracts a hydrogen atom from an initiator, monomer, polymer or solvent molecule, for all of which I − H stands for in equation (12). Note that the radical molecule formed in (12) can act as an initiator for polymerization. [1, p. 34]

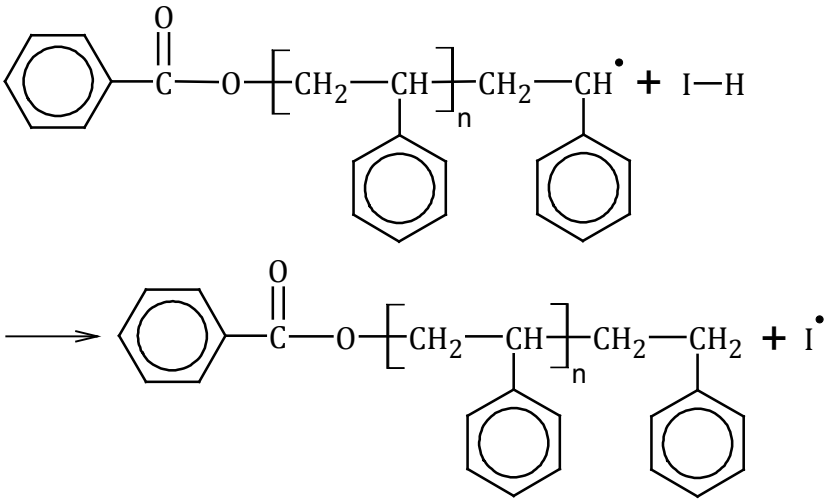

(12)

The termination mechanisms (10)–(12) imply that polystyrene can contain benzoyl peroxide or benzene as a terminal group. The benzene end group can also be connected to either a saturated or unsaturated carbon group. In all termination mechanisms at least one end of a polystyrene molecule contains the initiating free-radical group of the initiator molecule. Thus the initiator becomes part of the polystyrene molecule, in comparison with catalytically polymerized polypropylene, in which the catalyst is removed from the polymer. [1, p. 33]

4. PHOTODEGRADATION OF POLYMERS

The purpose of this chapter is to review the interaction between light and matter and the basic mechanisms of polymer photodegradation with the focus on the specifics of the photodegradation of polypropylene and polystyrene. Different methods of stabilizing polymers against photodegradation are also reviewed in this chapter.

4.1 Absorption of radiation

The absorption of radiation is based on the electrical interactions between the electric field of radiation and the electrons of matter. The electric field of a photon can interact with the dipole moment of an atom or a molecule, exciting the atom or molecule to a higher energy state by effectively absorbing the photon energy. Because both the energy of a photon and the energy levels of matter are quantized, absorption of radiation can occur only if the energy difference between the excited and initial energy states of the absorbing matter equals or is less than the photon energy, as in formula (13)

$$E_{exc} - E_{in} = E_{ph} = h\nu = \frac{hc}{\lambda} = hc\tilde{\nu}, \tag{13}$$

in which E_{exc} and E_{in} are the absorbing matter's excited and initial energy states respectively, E_{ph} is the photon energy, h is the Planck constant and ν is the frequency, c the speed, λ the wavelength and $\tilde{\nu}$ the wavenumber of electromagnetic radiation. An excited atom or molecule can return to the electrical ground state by emitting a photon with the same or less energy as the exciting photon, by losing part or all of the excitation energy as heat or by chemical changes.

When radiation is absorbed by matter the photon energy is converted into the movement of the valence or binding electrons. The chemical bond or structure that is excited depends directly on the energy of the absorbed photon. Ultraviolet (UV, $\lambda = 100\text{–}400$ nm) [4] and visible (Vis, $\lambda = 400\text{–}700$ nm) [4] radiation can excite the electrons in the atomic electron orbitals to a higher energy level whereas infrared (IR) radiation ($\lambda = 10^3\text{–}10^6$ nm) can excite the vibration of the bonds between atoms in a molecule [5].

The absorption of radiation by a chemical compound in the ultraviolet and visible wavelength regions relates to the structure of the compound. The selective absorption of radiation by organic compounds depends on the compounds electronic structure, or more accurately the electron vacancies in the molecule. Completely saturated compounds that contain only carbon and hydrogen absorb radiation only in the vacuum

ultraviolet range ($\lambda < 200$ nm), so polypropylene should not absorb ultraviolet or visible radiation. The absorption spectrum shifts towards visible light if an organic compound contains double bonds, but e.g. polystyrene (in which the benzene rings shift the absorption spectrum) should still only absorb radiation well into the mid ultraviolet range ($\lambda \lesssim 260$ nm). [6, p. 15] The fact that commercial polymers degrade under natural light, which contains only wavelengths over 290 nm [7, p. 587], suggests that some other chemical groups must be acting as chromophores, absorbing radiation and initiating the degradation. Despite the inclusion of antioxidants and other stabilizers, trace amounts of hydroperoxide and ketone chromophores exist in practically all commercial polymers, extending the absorption spectrum of the polymers well over $\lambda = 200$ nm [6, p. 134].

Absorption spectroscopy measures the amount of radiation that is absorbed at a specific wavelength. When the surface of matter is irradiated, part of that radiation is reflected, another part is absorbed and the remaining part is transmitted through the matter. The sum of reflected, absorbed and transmitted intensities (I_r, I_a and I_t, respectively) is equal to the incident intensity (I_0)

$$I_0 = I_r + I_a + I_t. \tag{14}$$

Transmittance is the ratio of the transmitted and incident intensities,

$$T = I_t/I_0, \tag{15}$$

and absorbance is the base 10 logarithm of the reciprocal of transmittance

$$A = \log_{10}(1/T) = \log_{10}(I_0/I_t). \tag{16}$$

It is important to note, that in this study the vertical axes of the measured absorbance spectra are base 10 logarithmic.

4.2 General hydroperoxide mechanism for polymer degradation

The general photo-oxidative degradation mechanism of polymers is largely similar to that which occurs in the thermo-oxidative degradation. Polymer degradation is initiated by the formation of polymer radicals (P$^{\cdot}$), which is necessary for rapid polymer oxidation:

$$\mathrm{PH} \rightarrow \mathrm{P}^{\cdot} + \mathrm{H}^{\cdot} \tag{17}$$

Reaction (17) can be initiated by e.g. radiation, heat, mechanical treatment or chemical reactions, such as a direct reaction with ozone. Initiation by a direct reaction with mo-

lecular oxygen is highly improbable, but polymer radicals formed by e.g. UV radiation react readily with oxygen molecules by addition to form peroxy polymer radicals:

$$\mathrm{P^{\cdot} + O_2 \rightarrow POO^{\cdot}} \tag{18}$$

The rate of addition of oxygen to a radical depends on the structure of the polymer, so different polymers form peroxy radicals at different rates during degradation. [6, p. 98]

A peroxy radical can abstract hydrogen from a polymer molecule to form polymer hydroperoxides:

$$\mathrm{POO^{\cdot} + PH \rightarrow POOH + P^{\cdot}} \tag{19}$$

The rate constant of reaction (19) is a composite of several possible hydrogen abstraction reactions. These reactions are sensitive to steric and polar effects of the abstracting radical and are also temperature dependent. Peroxy radicals are strongly resonance stabilized, and abstract tertiary bonded hydrogen in preference to secondary or primary bonded. [6, p. 98]

Polymer hydroperoxides decompose under irradiation according to the following three reactions:

$$\mathrm{POOH \rightarrow P^{\cdot} + {}^{\cdot}OOH} \tag{20}$$

$$\mathrm{POOH \rightarrow PO^{\cdot} + {}^{\cdot}OH} \tag{21}$$

$$\mathrm{POOH \rightarrow POO^{\cdot} + {}^{\cdot}H} \tag{22}$$

The energy of light with wavelength $\lambda > 300\,\mathrm{nm}$ ($> 400\,\mathrm{kJ/mol}$) is sufficient to cleave $\mathrm{PO-OH}$ and $\mathrm{P-OOH}$ bonds (dissociation energies 180 and $290\,\mathrm{kJ/mol}$, respectively), but hardly $\mathrm{POO-H}$ bonds (dissociation energy $380\,\mathrm{kJ/mol}$). The large differences in bond dissociation energies means that with solar UV irradiation reaction (21) will dominate, with reaction (20) also occurring to some extent and reaction (22) occurring only little. [6, pp. 98–99]

Polymer molecules can react with the alkoxy radicals formed in reaction (21) to form hydroxyl groups:

$$\mathrm{PO^{\cdot} + PH \rightarrow POH + P^{\cdot}} \tag{22}$$

The hydroxyl groups can be formed along the polymer chain or on its end groups, but forming on the end groups is rare. [6, pp. 99–100]

Carbonyl and aldehyde groups can be formed in polymer degradation in a number of ways. A β-scission process of an alkoxy radical that is formed in reaction (21) plays an

important role in the back-bone scission of polymer chains and in the alkyl radical formation at the chain ends [6, p. 100]:

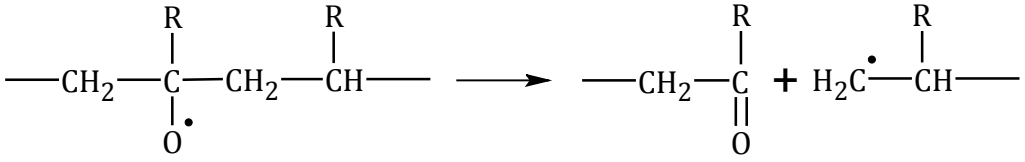

(23)

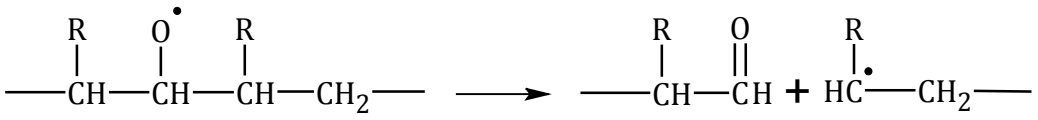

(24)

The reactive hydroxyl radicals formed in the decomposition of hydroperoxide groups can abstract labile atoms, e.g. tertiary bonded hydrogen from a carbon atom under certain restricted cage like conditions. An intermediate biradical is formed which transforms into a carbonyl group [6, pp. 100–101]:

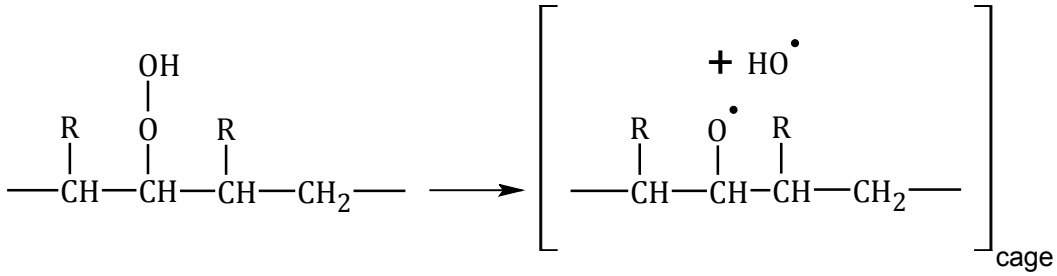

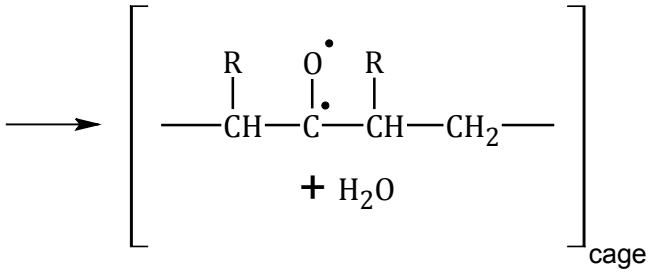

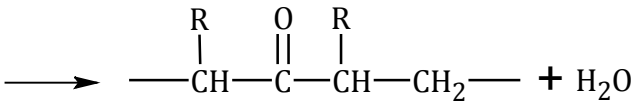

(25)

A reaction between two polymer alkoxy radicals can produce simultaneously a carbonyl and a hydroxyl group by disproportionation:

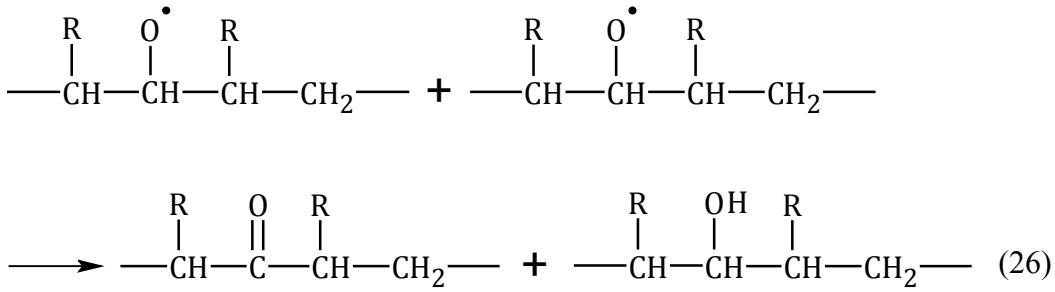

(26)

Carbonyl groups, like the ones that are formed in reactions (23)–(26), are partially responsible for the absorption of UV radiation at wavelengths over 300 nm in saturated polymers. These groups can be formed in the manufacturing process or by photodegradation if low wavelength UV radiation is present. The introduction of carbonyl groups results in the shift of the absorption spectrum towards higher wavelengths, resulting in accelerated photodegradation. Carbonyl groups also take part in many photochemical reactions present in the degradation of polymers. These reactions are classified as Norrish reactions of types I, II and III. [6, p. 48–49]

In the type I Norrish reaction a bond between the carbonyl group and the adjacent α-carbon is homolytically cleaved. The cleavage can occur by two possible reactions [6, p. 49]:

$$\mathrm{RCOR'} \rightarrow \mathrm{RCO^{\cdot}} + \mathrm{^{\cdot}R'} \rightarrow \mathrm{R^{\cdot}} + \mathrm{CO} + \mathrm{^{\cdot}R'} \tag{27}$$

$$\mathrm{RCOR'} \rightarrow \mathrm{R^{\cdot}} + \mathrm{R'CO^{\cdot}} \rightarrow \mathrm{R^{\cdot}} + \mathrm{CO} + \mathrm{^{\cdot}R'} \tag{28}$$

The type II Norrish reaction is a nonradical intramolecular process, in which a cyclic six-membered intermediate is formed. Abstraction of a hydrogen atom from the γ-carbon results in the decomposition of the intermediate into an olefin and an alcohol or aldehyde:

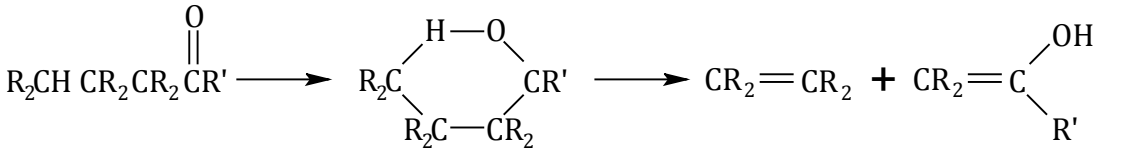

(29)

The type II Norrish reaction can also involve an intramolecular process with a longer chain segment in polymers. [6, p. 49]

The type III Norrish reaction is also a nonradical intramolecular process, which involves a transfer of a β-hydrogen atom. It results in the formation of an aldehyde and an olefin through scission of the $\mathrm{C-C}$ bond adjacent to the carbonyl group [6, p. 49]:

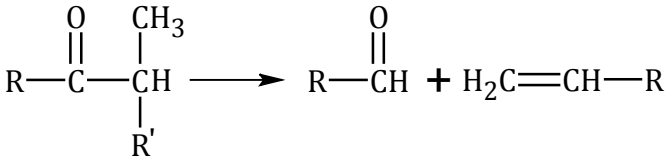

(30)

The radicals formed in the degradation of polymers can be terminated by numerous different combination reactions between two polymer radicals, in which inactive products are formed:

$$POO^{\cdot} + POO^{\cdot} \rightarrow POOP + O_2 \tag{31}$$

$$POO^{\cdot} + P^{\cdot} \rightarrow POOP \tag{32}$$

$$P^{\cdot} + P^{\cdot} \rightarrow P - P \tag{33}$$

When the oxygen pressure is high, the termination reaction follows reaction (31) almost fully. At low oxygen pressure other termination reactions take place to some extent. In the degradation of solid polymers when sufficient oxygen content cannot be maintained reaction (32) becomes significant. Polymer radicals can couple mutually as in reaction (33) and form crosslinks with polymer peroxy radicals. [6, pp. 101–102]

Chain scission and crosslinking can occur simultaneously in the same polymer sample during the degradation process. Scission can make a solid polymer into a thin liquid and crosslinking can make the polymer sample brittle. These mechanisms are mainly responsible for the changes in the macro scale properties of a polymer, e.g. changes in the elongation at break. The relative amounts of scission and crosslinking depend on the polymer's chemical and physical structures, so different polymers and even the same polymer with a different tacticity can exhibit different behavior in the macro scale degradation. [6, p. 102]

4.3 Photodegradation mechanism of polypropylene

In the ideal case polypropylene contains only $C-H$ and $C-C$ bonds, and thus shouldn't absorb radiation at wavelengths over 200 nm. Trace amounts of impurities, consisting mostly of extrinsic terminal carbonyl groups, are formed in the manufacturing process of commercial polypropylene and can act as initiators to the degradation mechanism of polypropylene.

A polypropylene molecule with a mid-chain carbonyl group (polyketone type A) can form one carbon monoxide molecule and two polymer radicals via a Norrish type I reaction like in reactions (27) and (28) [6, p. 138; 7]:

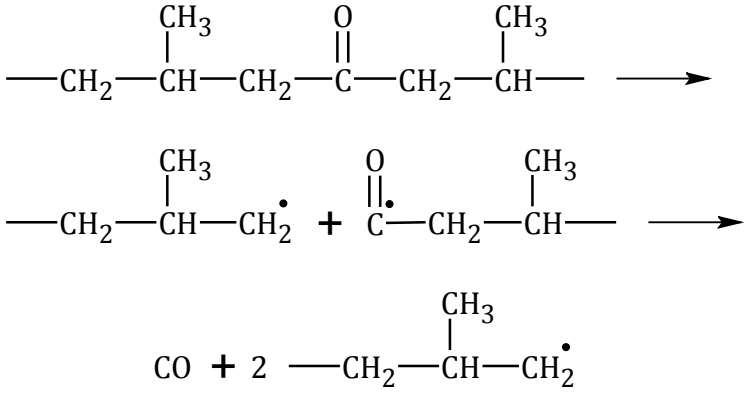

(34)

A polypropylene molecule with a chain end carbonyl group (polyketone type B) can form one acetone molecule and an unsaturated polymer chain end via a Norrish type II reaction (29) [6, p. 138; 7]:

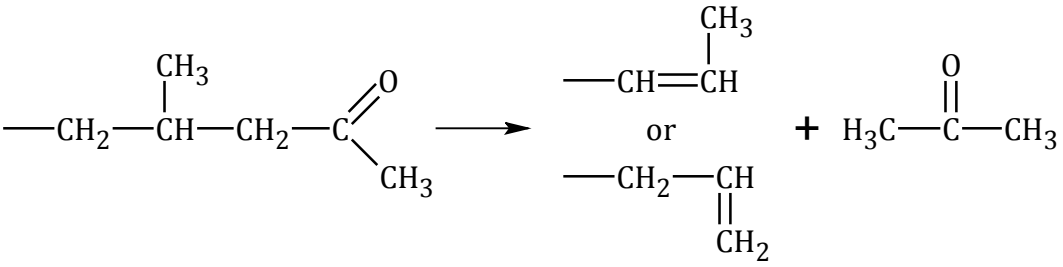

(35)

The polymer radicals that are formed in the Norrish type I reaction (34) act as initiators for the degradation mechanism of polypropylene. Polypropylene's degradation mechanism after initiation is the same as the general hydroperoxide mechanism described in reactions (18)–(31). The whole degradation pathway can be illustrated by the following sequence [6, pp. 135–140]:

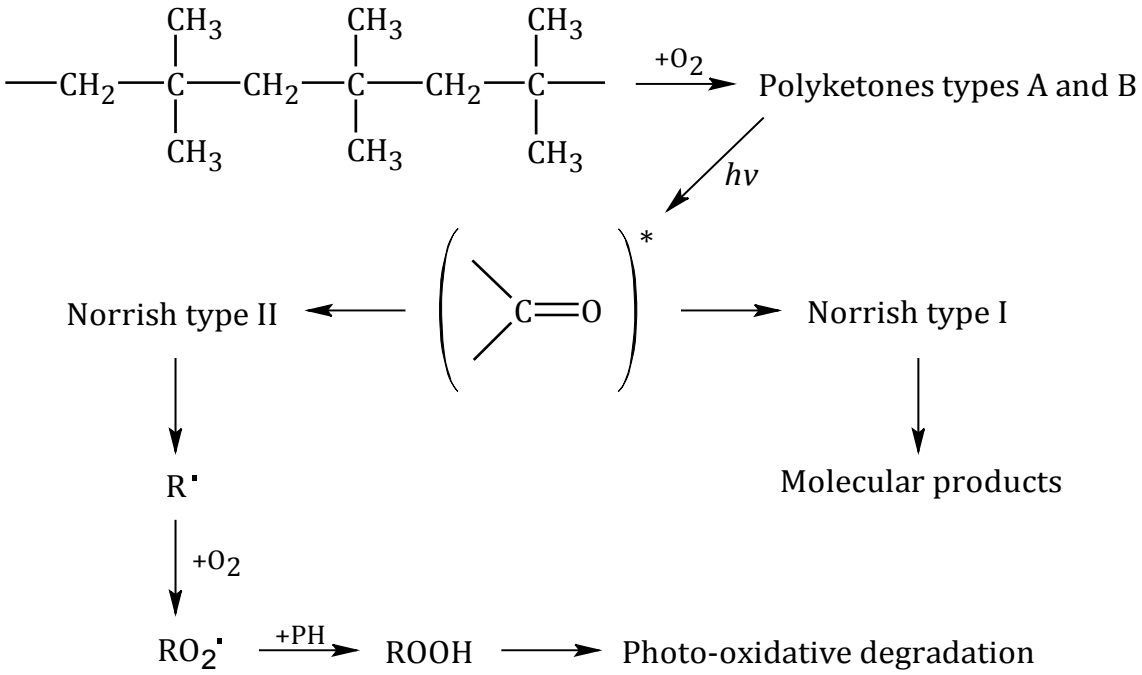

Figure 4.1 *The photodegradation pathway of polypropylene. Adapted from [6, p. 140]*

Prevention of the photodegradation of polypropylene can only be achieved by preventing the photolysis of polymer hydroperoxides or by deactivating the excited states of carbonyl and hydroperoxide groups.

Photodegradation of polypropylene is mainly restricted to the amorphous portions of the polymer. This is due to the much greater mobility of the molecules in the amorphous regions compared to the crystalline regions and an easier diffusion of oxygen.

4.4 Photodegradation mechanism of polystyrene

In each repeating unit of polystyrene there is a phenyl chromophore that shifts the absorption spectrum of PS towards the visible region, up to $\lambda \approx 260$ nm. When PS is irradiated with UV radiation the phenyl ring is excited, after which the excitation energy is transferred to the nearest $C-H$ bond, resulting in the cleavage of a hydrogen radical and the formation of an alkyl-type radical:

$$-CH_2-CH(Ph)-CH_2-+h\nu \rightarrow -CH_2-C^{\cdot}(Ph)-CH_2-+^{\cdot}H \qquad (36)$$

When PS is irradiated in room temperature, double bonds are formed. This leads to an equilibrium reaction in which a more stable allyl-type radical (37) is produced from the alkyl-type radical (36) with a 3:1 ratio, respectively. [8, p. 43]

$$-CH_2-C^{\cdot}(Ph)-CH=CH(Ph)-CH_2- \qquad (37)$$

Commercial grades of polystyrene contain extrinsic terminal carbonyl groups and segments with conjugated double bonds that act as chromophores. These chromophoric groups shift the edge of the action spectrum of radical formation in polystyrene up to $\lambda \approx 440$ nm, which is well into the visible region. The type of the radicals formed in polystyrene during photodegradation depends on the irradiation wavelength. In addition to reaction (36), in the irradiation of polystyrene with wavelengths over 300 nm hydroxyl radicals are produced.

$$-\mathrm{CH(Ph)} - \mathrm{C^{\cdot}OH} - \mathrm{CH(Ph)} - \tag{38}$$

Unlike in (36), the formation of this radical does not include the formation of a hydrogen radical. Irradiation with wavelengths over 360 nm leads to the generation of allyl radicals (37) with a conjugated chain that contains four monomer units. [8, pp. 44–45]

In the presence of oxygen all of the radicals formed in the irradiation of polystyrene follow reaction (18) and turn into peroxy radicals. Some of the peroxy radicals form polymer hydroperoxides according to reaction (19), forming mainly terminal carbonyl groups and double bonds through chain scission:

$$\begin{aligned} &-\mathrm{CH_2} - \mathrm{(C(Ph)OOH)} - \mathrm{CH_2} - \mathrm{CH(Ph)} - \\ &\rightarrow -\mathrm{CH_2} - \mathrm{C(Ph)} = \mathrm{O} + \mathrm{CH_2} = \mathrm{C(Ph)} - + \mathrm{H_2O} \end{aligned} \tag{39}$$

The most intense process in the photodegradation of polystyrene is the absorption of oxygen and the release of gaseous products carbon dioxide and water. The release of $\mathrm{CO_2}$ and $\mathrm{H_2O}$ is not connected to the general hydroperoxide degradation mechanism, but a different photochain mechanism that is associated with chromophoric radicals formed in the initial stages of degradation. Approximately 10 % of the degradation of polystyrene is associated with the general mechanism described above, with up to 90 % occurring via the photochain mechanism. [8, pp. 47–49]

The specifics of the photochain degradation mechanism are not fully understood yet. It is initiated by the excitation of peroxy radicals formed according to reaction (18). The excitation can occur by either irradiation or energy transfer from other chromophores. The photodegradation of the peroxy radicals involves the dissociation of the $\mathrm{C-H}$, $\mathrm{C-C}$ and $\mathrm{O-O}$ bonds, the appearance of $\mathrm{CO_2}$ and $\mathrm{H_2O}$ and the formation of a new polymer radical ($\mathrm{R^{\cdot}}$), which oxidizes into a one monomer unit shorter peroxy radical than the initial radical. The photochain degradation mechanism is in essence a process, in which the photodissociation of the peroxy radical and the oxidation of the polymer radical occur repetitively. It can be viewed as a mechanism in which the polymer burns from the chain end like a candle. Because compounds that contain a benzene ring are not formed in the photochain mechanism, the phenyl group is also dissociated in the photochain mechanism. [8, pp. 47–48]

4.5 Stabilization against photodegradation

The stabilization of polymers against photodegradation involves either the retardation or elimination of the photochemical processes that occur during irradiation. There are several different methods of photostabilization, and the choice of method is dependent on the polymer and application. Accurate knowledge of the stabilization mechanism is of immense commercial value, because a single stabilizer can multiply the expected lifetime of a polymer product. The most important methods of photostabilization are the screening or absorbing of UV radiation by stabilizing agents and the use of antioxidants, which react with the polymer radicals, stopping the degradation process by forming inactive products.

Screening of radiation is a process in which the stabilizing activity is the prevention of the penetration of radiation into the polymer material, limiting the degradation process to the surface. The screening agent is usually an inorganic pigment, most often a metal oxide that is opaque to UV radiation, reflecting the radiation away from the polymer surface. UV radiation screening is an effective photostabilization method, but the screening agent can change the physical properties of the polymer. Chemical changes can also occur, because metal oxides can act as catalysts for the hydroperoxide degradation mechanism of certain polymers. UV screeners are mostly used as a surface coating. Different polymers are not protected to the same degree by a given pigment because of differences in the absorption spectra of polymers and pigments. [6, pp. 363–363]

Some organic compounds, like phtalocyanines or coumarins, are often used as absorbers of UV radiation. These stabilizer compounds absorb the incident UV radiation and discharge the energy in a form that is not harmful to polymers, e.g. by releasing the energy as heat or as luminescence of higher wavelength radiation. Organic UV absorbers are often volatile compounds, so their concentration can diminish with time. Many fluorescent compounds are also susceptible to photodegradation. [6, pp. 363–380]

Organic compounds that prevent or stop the oxidation process by reacting chemically are known as antioxidants. Antioxidants function by inhibiting the propagation phase of the general hydroperoxide mechanism. The antioxidant molecule (AH) interferes with the propagation reactions (18) and (19) mainly by two reactions, chain transfer, (40) and (41), or termination, (42) and (43):

$$R^{\cdot} + AH \rightarrow RH + A^{\cdot} \tag{40}$$

$$RO_2^{\cdot} + AH \rightarrow ROOH + A^{\cdot} \tag{41}$$

$$A^{\cdot} + RO_2^{\cdot} \rightarrow RO_2A \tag{42}$$

$$2A^{\cdot} \rightarrow A_2 \tag{43}$$

Antioxidants react faster with peroxy radicals (41) than with polymer radicals (40), making reaction (41) the main inhibition reaction. The products formed in reactions (42) and (43) are inactive with regards to photodegradation. Like organic stabilizers, many antioxidants absorb light in the UV region. Some antioxidants are also prone to photo-degradation themselves, sometimes causing very complex photochemical reactions in the polymers [6, p. 412, 418]. The most commonly used antioxidants today are hindered amine light stabilizers (HALS), which act as free radical scavengers.

5. INSTRUMENTAL METHODS

The instrumental methods used in this study are reviewed thoroughly in this chapter. Spectroscopic methods are used to study the absorption of ultraviolet, visible and infrared radiation of the polymer sample and calorimetric methods are used to study the thermal properties of the polymers. Variables that can be deduced from the changes in the measured properties are also reviewed. These variables give important information about the degree and phase of degradation.

5.1 Fourier transform infrared spectroscopy

Fourier transform infrared spectroscopy (FTIR) is an instrumental technique that measures the amount of IR radiation reflected from or transmitted through a sample. It is used mainly to solve the composition of organic compounds. In this study it is used to detect chemical changes that occur during the photodegradation of polypropylene and polystyrene. The principle of infrared spectroscopy, the design of the FTIR spectrometer and the degradation indices calculated from the measured spectra are reviewed in this chapter.

5.1.1 Principle of infrared spectroscopy

Infrared radiation refers to the part of electromagnetic radiation that is between visible and microwave regions, comprising approximately of the wavelength range $\lambda = 700\ \text{nm} - 1\ \text{mm}$ [4]. Wavenumbers are often used as a measure of the energy of IR radiation instead of wavelength (13). Wavenumbers are the reciprocal of wavelength, often expressed as inverse centimeters (cm^{-1}). The wavelength of radiation can be calculated from wavenumbers using equation (44)

$$\lambda(\text{nm}) = \frac{10^7}{\tilde{\nu}(\text{cm}^{-1})}. \tag{44}$$

Infrared radiation with wavenumbers of $10000 - 100\ \text{cm}^{-1}$ is absorbed and converted into molecular vibration [5]. This is why IR radiation is often called heat radiation. The absorption of IR radiation is quantized, but vibrational absorption spectra appear as bands instead of lines, because a single vibrational transition is accompanied by a number of rotational transitions. Infrared spectroscopy focuses mainly on the vibrational-rotational absorption bands occurring between $4000 - 400\ \text{cm}^{-1}$. [9, p. 71]

There are two types of molecular vibrations, stretching and bending. A stretching vibration is a rhythmical movement along the bond axis in which the distance between the atoms is increasing or decreasing. A bending vibration can consist of a change in the bond angle between bonds with a common atom or the movement of a group of atoms in relation to the remainder of the molecule. The vibration of a molecule can cause a change in the charge distribution of the bond, thus changing the dipole moment of the molecule. This change forms an electric field that can couple with the oscillating electric field of the incident radiation, causing the radiation to be absorbed. Only the vibrations that result in a rhythmical change in the dipole moment of a molecule can be seen in IR spectroscopy. In general, functional groups that have a strong dipole give rise to strong absorptions in the IR range. [9, p. 72–74]

A vibrating bond can be seen as a harmonic oscillator, which means that the frequency, or wavenumber, of a specific bond depends on the atomic masses and the force constant of the bond. Thus different compounds absorb radiation at different wavenumbers, making it possible to distinguish different molecules using IR spectroscopy.

5.1.2 Fourier transform infrared spectrometer

Figure 5.1 is a schematic drawing of a Fourier transform infrared spectrometer.

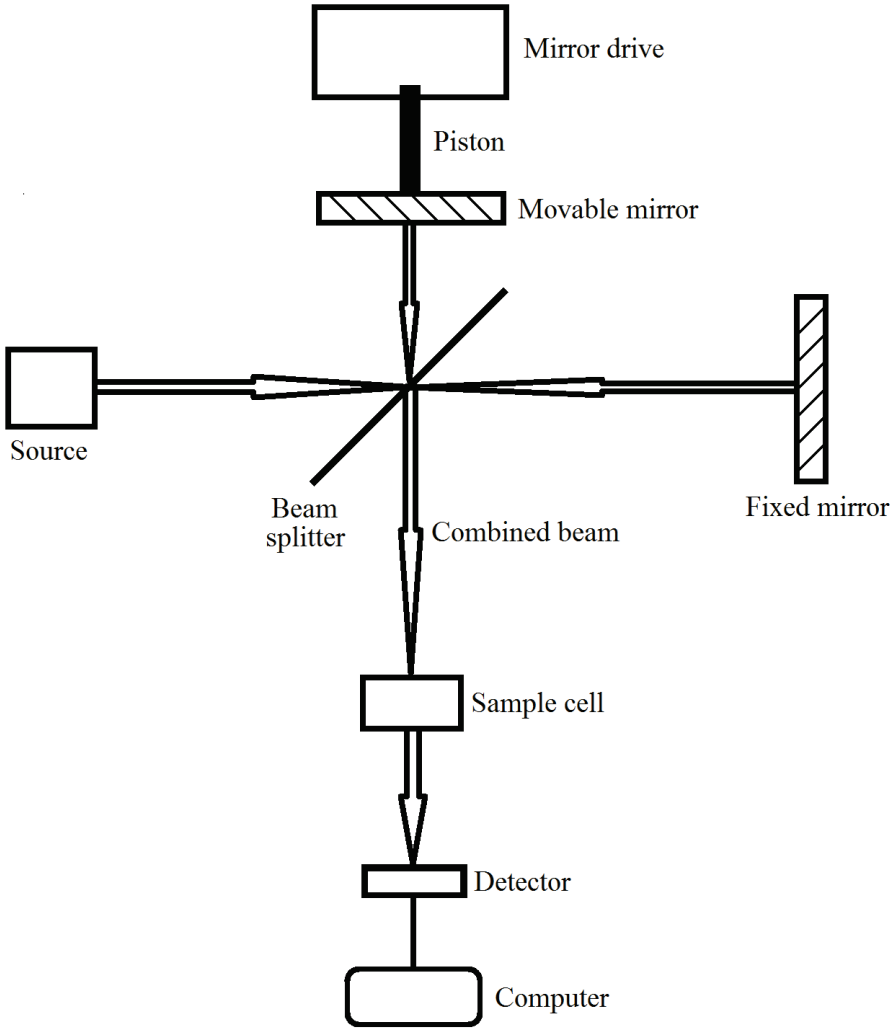

Figure 5.1 *A schematic drawing of a Fourier transform spectrometer. Adapted from [9, Figure 3.4]*

The source emits a beam of radiation which contains all desired IR wavenumbers, generally those of $4000-400\ \mathrm{cm}^{-1}$ (corresponding to wavelengths of $2500-25000\ \mathrm{nm}$). When the beam reaches the beam splitter it is split into two separate beams, of ideally equal intensity, that travel separate paths. One beam reflects from a fixed mirror making its pathway of fixed length, the other beam reflects from a movable mirror making its pathway of variable length. During the measurement the movable mirror is moved continuously, resulting in a varying path difference called retardation. This varying distance results in a varying phase difference between the two beams. The varying phase difference results in a sequence of constructive and destructive interferences when the beams are combined, thus resulting in varying intensities of the combined beam, which contains approximately half of the intensity of the original beam at most. The detector measures the intensity of the radiation reaching it after which a computer forms an interferogram of the measured intensities as a function of time. Fourier transform is a mathematical method that converts the measured interferogram from the time domain into

one spectral point on the frequency domain. A Fourier transform is performed at successive points throughout the movement of the moving mirror, giving rise to the complete IR spectrum. [9, pp. 76–77]

Passage of the combined beam through a sample subjects the compound to a broad band of energies. In principle one broad banded pass of radiation through the sample gives rise to a complete IR spectrum. Generally the IR spectrum is comprised of a number of scans that are averaged to remove random absorption artifacts. In addition the background must be subtracted from the measured spectrum, so that only the absorption of the sample is shown in the spectrum. [9, pp. 76–77]

There are two major advantages to using FTIR spectroscopy instead of a general scanning spectrometer. Because all information of the spectrum can be obtained by just one scan, the measurement time is diminished greatly. A scanning spectrometer also needs a monochromator, which has entrance and exit slits that restrict the amount of light that passes through it. On a FTIR spectrometer the throughput of IR radiation is determined solely by the source and the beam splitter. [9, p. 77]

5.1.3 Degradation indices

FTIR spectroscopy can detect the functional groups that are formed in the photodegradation process. The visible absorptions are caused by the formation of hydroperoxide groups (reaction (19)), hydroxyl groups (reactions (22), (26) and (29)), carbonyl groups (reactions (23)–(26), (29) and (30)) and double bonds (reaction (37)). Hydroperoxide and hydroxyl groups and double bonds form wide absorption bands, whereas carbonyl groups form distinct narrow absorption bands. The carbonyl bands are close to each other, forming a superposition band from the separate absorption bands formed by the different carbonyl species.

The relative positions of the absorption bands of the functional groups formed in photodegradation are well known: hydroxyl and hydroperoxide groups absorb at $\tilde{\nu} = 3600\text{–}3200\ \mathrm{cm^{-1}}$, carbonyl groups absorb at $\tilde{\nu} = 1800\text{–}1650\ \mathrm{cm^{-1}}$ and double bonds absorb at $\tilde{\nu} = 1000\text{–}800\ \mathrm{cm^{-1}}$ [6, p. 129, 175; 10; 11]. The accurate positions of the specific absorption bands are dependent on the polymer species.

A degradation index is defined as the ratio of the maximum absorbance of an absorption band of a functional group divided by the absorbance of a reference band. Carbonyl (CI), hydroperoxide (HPI) and hydroxyl (HI) indices are used to follow the progress of the photodegradation process. The reference absorption band must be chosen so that it does not change due to degradation. The absorption bands associated with the methylene (CH_3) and ethylene (CH_2) groups are useful for this purpose, because they are the most plentiful functional groups visible in the IR spectra of polypropylene and polystyrene.

FTIR can also be used to measure the relative amount of isotacticity in polypropylene. The isotacticity index (ItI) is defined as the ratio between the absorbance of a band that is caused by the isotactic helical regions ($\nu = 998\ \mathrm{cm^{-1}}$) and a reference band.

Nuclear magnetic resonance (NMR) measurements can be used to observe the absolute amounts of isotactic and atactic segments in polypropylene. It has been shown that the isotacticity change calculated from FTIR spectra is linear with the one measured with NMR, although FTIR gives consistently lower isotacticity values [12, 13]. The isotacticity index is related to the crystallinity of polypropylene [14], so it is used as a proxy to measure the changes in the crystallinity of polypropylene during photodegradation.

5.2 Ultraviolet-visible spectroscopy

Ultraviolet-visible spectroscopy is an instrumental technique that measures the amount of ultraviolet and visible light reflected from or transmitted through a sample. It is used to measure the energies of the transitions of valence electrons in the atomic or molecular orbitals to higher energy levels. Molecules can absorb UV radiation if they contain either π- or n-electrons that can be excited to a higher anti-bonding molecular orbital.

In this study UV-Vis spectroscopy is used to measure the change in the amount of absorbed UV and visible radiation. The design of the UV-Vis spectrometer and the way to detect changes in the amount of conjugated double bonds from the measured spectra are reviewed in this chapter.

5.2.1 Ultraviolet-visible spectrometer

Figure 5.2 is a schematic drawing of a double beam UV-Vis spectrometer.

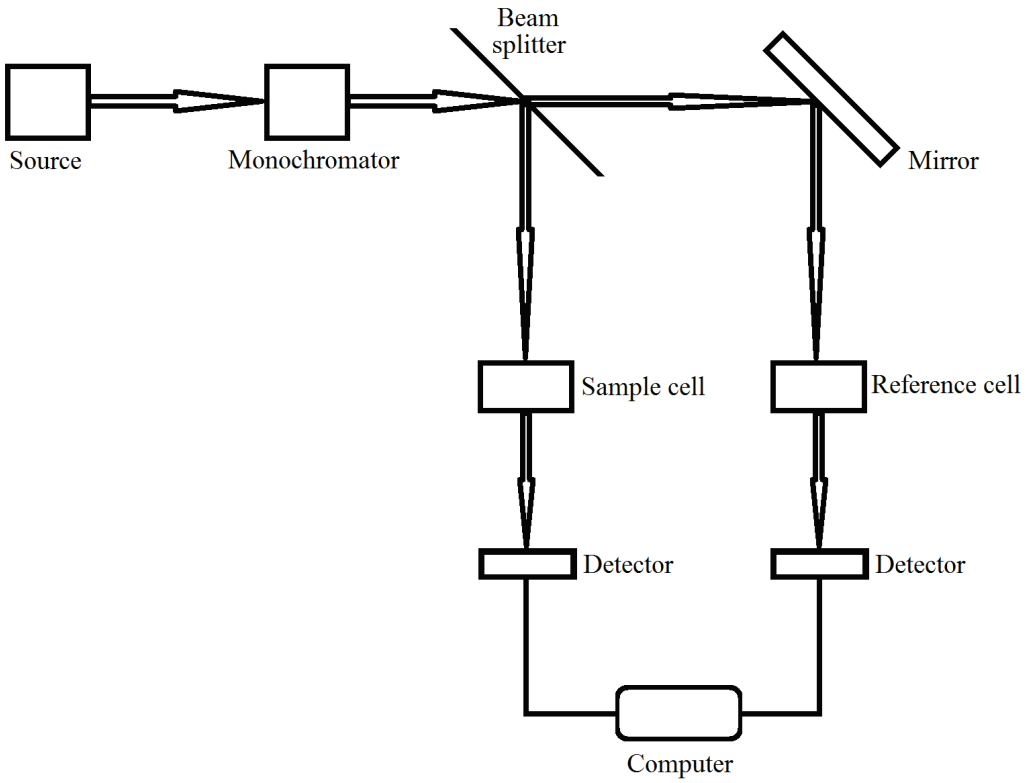

Figure 5.2 *A schematic drawing of a simplified double beam UV-Vis spectrometer.*

The light source of the UV-Vis spectrometer contains two different lamps, typically a deuterium lamp for UV and a tungsten lamp for visible wavelengths. The monochromator is constructed of numerous slits and prisms or gratings that allow only a short wavelength range of radiation to pass through. The monochromator is tunable, so that the whole UV-Vis spectrum can be obtained. The monochromatic radiation travels through the sample and reference after which its intensity is measured with a detector.

In a double beam spectrometer the monochromatic beam is split into a sample and a reference beam. The sample beam travels through the sample cell and the reference beam travels through the reference cell, which contains a similar cuvette and solvent for liquid samples or is empty for solid samples. The measured intensity of the reference beam is taken as the radiation intensity that reaches the sample I_0 and the measured intensity of the sample beam is taken as the transmitted radiation intensity from the sample I_t. The UV-Vis spectrum is then calculated from the measured intensities using equations (14–16).

5.2.2 Observation of double bonds

It is well known that polystyrene exhibits yellowing during photodegradation. The yellowing is caused by the formation of conjugated double bonds in the polymer molecules and low molecular weight organic degradation products that contain a conjugated double bond system. [6, pp.169–170; 8; 15; 16]

The change in the amount of conjugated double bonds that are formed in the polymer molecules can be measured directly with UV-Vis spectroscopy. The approximate wavelength at which conjugated double bonds in polystyrene absorb UV radiation can be approximated by

$$\lambda_n = [280 + 30 \times (n - 1)], \tag{45}$$

where n is the number of double bonds in the conjugated system [16]. In this study the exact wavelengths for conjugated systems with two, three and four double bonds are taken as $312\ \mathrm{nm}$, $328\ \mathrm{nm}$ and $368\ \mathrm{nm}$, respectively [15]. The absorbances at the aforementioned wavelengths are taken as the conjugated double bond indices.

5.3 Differential scanning calorimetry

Differential scanning calorimetry is the most widely used instrumental technique for determining the thermal properties of different materials. A DSC analyzer measures the energy changes that occur in thermal transitions when a sample is heated, cooled or held in isothermal conditions, as well as the temperature where the transition occurs. The transitions observable with DSC include melting, crystallization, glass transition and oxidative degradation. [17, pp. 2–3] The sample size needed for a DSC measurement is

as low as 1– 2 mg. Typically the DSC measurement is performed with sample sizes in the range of 2– 40 mg [18].

In this study DSC is used to measure the changes that occur due to photodegradation in the melting temperature and heat of fusion of polypropylene, the glass transition temperature of polystyrene and the degradative stability of both polymers. The design of the calorimeter used and the basics of observed thermal transitions are reviewed in this chapter.

5.3.1 Heat flux DSC

The purpose of DSC is to determine the heat flow, i.e. the flow of energy into or out of the sample as a function of temperature or time. The unit in which heat flow is typically presented is mW, which can be normalized to the size of a specific sample, when the heat flow is presented in W/g. Because measuring the heat flow directly is not plausible, DSC instruments generally measure the temperature difference between a sample and a reference pan, from which the heat flow can be calculated.

Figure 5.3 is a schematic drawing of a heat flux DSC instrument.

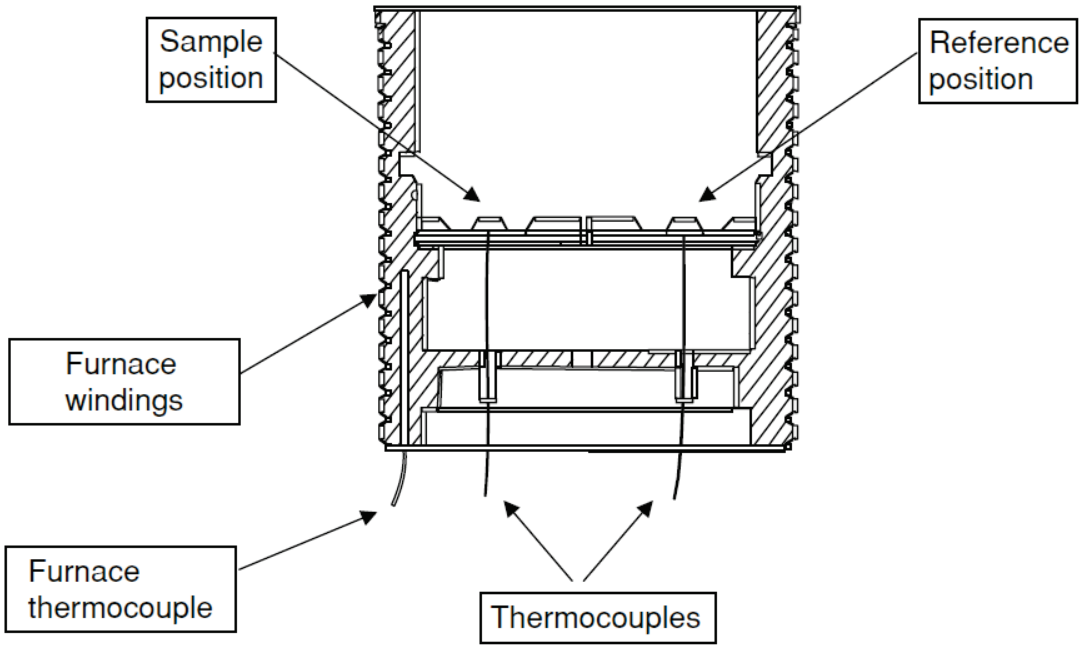

Figure 5.3 *A schematic drawing of a heat flux DSC instrument [17, Figure 1.26]*

Heat flux DSC is a single furnace design with multiple thermocouples for each of the sample and reference pans located in the same furnace. The reference pan is typically an empty pan of the same type as the sample pan. When thermal transitions happen in the sample, a temperature difference is formed between the sample and reference pans. On continued heating or cooling the temperature difference decreases as the system approaches thermal equilibrium in accordance with the time constant of the system. Typi-

cal heat flux DSC instruments can be used in the temperature range from -150 °C up to 700 °C. [17, pp. 47–48]

The temperature difference between the sample and reference pans is the basic parameter that is measured in heat flux DSC. The instrument is calibrated so that the temperature difference signal is converted to a heat flow equivalent which is displayed as a function of temperature or time, known as a thermoanalytical curve. [17, pp. 47–48]

5.3.2 Differential photocalorimetry

Many chemical reactions can be initiated by irradiation, specifically with UV radiation. Differential photocalorimetry is a method used to study the effects of radiation on the thermal transitions or chemical reactions in materials. DPC is often used in the study of light curable coatings, adhesives and dental materials. [17, p. 248]

The DPC instrument is typically a UV irradiation system attached to a commercial DSC instrument, so no extensive modifications are needed to an existing instrument. DPC enables the study of the effects of temperature, radiation intensity and wavelength sensitivity to be studied at the same time. The DPC instrument is typically an exterior lamp, whose intensity and wavelength range can be controlled. The lamp is connected to the DSC instrument by fiber optics. [17, p. 48]

The temperature of the DSC furnace must be controlled precisely for reliable results. This means that the lid of the furnace must be specifically made for a DPC system to enable both precise temperature control and the passage of radiation to the sample.

5.3.3 Glass transition temperature

The glass transition temperature (T_g) is a temperature above which amorphous materials are fluid or rubbery and below which they are immobile and rigid. Amorphous materials like polystyrene, although often hard and brittle, are not solids, which refers to crystalline materials. In temperatures under their glass transition temperature they are in a frozen liquid state, where molecular movement can occur over long time periods. Material in this state is defined as a glass, and when above the glass transition temperature as being in a rubbery state. The glass transition is observed in DSC as a discontinuity in the thermoanalytical curve. [17, p. 22]

The full nature of the glass transition is not fully understood. One explanation of the glass transition is the consideration of energy involved in movement. At very low temperatures molecules have insufficient energy to move and materials are immobile and hard. As the material is heated a long chain molecule will exhibit small transitions where rotations and vibrations of side groups or chains can begin. Eventually a temperature is reached where molecules of the structure can move independently resulting in significant softening of the material which is designated as the glass transition. [17, p. 23] It is not yet known if a true phase change of the material is associated with the glass transition.

The glass transition is not confined to fully amorphous materials. Semi-crystalline materials can also exhibit a glass transition, but as the crystallinity of the material increases the glass transition weakens. A glass transition does not occur in fully crystalline materials.

5.3.4 Temperature and enthalpy of melting

The melting of crystals is one of the most commonly measured thermal transitions with DSC. The melting process appears as an endothermic band (endotherm) in the thermoanalytical curve, because the material absorbs energy in order for the crystals to melt. The shape of the melting band depends on the properties of the crystalline material; single crystals form narrow and well defined melting bands whereas semi-crystalline polymers form wide melting bands due to a number of different crystal sizes. Two different values depict the melting temperature of a crystalline material: the onset temperature of the melting band (T_{onset}) or the maximum band value temperature (T_m). The maximum value of the melting band is typically taken as the melting temperature for semi-crystalline materials like polypropylene, because the onset of the melting is less reproducible for wide melting endotherms. [17, pp. 18–20]

Integrating over the melting band gives the melting enthalpy (ΔH_f) of the sample. The melting enthalpy can be used to calculate the crystallinity of the polymer. The crystallinity is calculated as the ratio of the measured melting enthalpy and a calculated melting enthalpy for a theoretical fully-crystalline polymer.

5.3.5 Oxidation induction time and temperature

DSC can be used to determine the oxidative stability of materials by measuring the time or temperature in which degradation begins in an oxidative environment. It is used often for in the study of plastics intended for use in high temperature or other oxidative environments.

The oxidation induction time (OIT) is measured with an isothermal test in which the sample is exposed to air or oxygen at an elevated temperature. The sample is first heated in an inert atmosphere to the test temperature, which is above the melting temperature of the sample or for amorphous plastics above the glass transition temperature, typically in the range of 180– 210 °C. The test temperature is kept constant. After the heat flow has stabilized, the inert atmosphere is switched to either air or oxygen. The time from switching of the atmosphere to the onset of the degradation exotherm is measured as the OIT. [19]

The oxidation induction temperature (T_{ox}) is a dynamic test in which the oxidizing atmosphere (air or oxygen) is present for the whole duration of the test. The sample is heated from an ambient temperature up to 400 °C. The onset temperature of the degradation exotherm is measured as the T_{ox}. [19] Both the oxidation induction time and temperature are direct measures of the stability against thermal degradation. In this study they are used to solve how photodegradation affects the thermal stability.

6. POLYMER SAMPLES

The polymer samples and their preparation and weathering methods are presented in this chapter. All polypropylene and polystyrene samples were prepared and weathered using the same methods and parameters. The raw material and samples were obtained from the Laboratory of Plastics and Elastomer technology at Tampere University of Technology.

6.1 Raw polymer materials

Moplen HP501L was used as the raw material for the polypropylene samples. It is an unstabilized polypropylene, intended for use as caps & closures, house wares and furniture. The polymer was received as opaque white granules.

BASF Polystyrol 143 E was used as the raw material for the polystyrene samples. It is a general purpose grade unstabilized polystyrene, intended for use as handles, gloss layer on food packaging and blending with other polystyrene grades. The polymer was received as transparent granules.

The general properties of Moplen HP501L and BASF Polystyrol 143 E are presented in table 6.1.

Table 6.1 *The general properties of Moplen HP501L polypropylene and BASF Polystyrol 143 E polystyrene.*

Property	PP, Moplen HP501L	PS, BASF Polystyrol 143 E
Weight average molecular mass (kg/mol)	250 [20]	308 [21]
Polydispersity index	4,0 [20]	3,3 [21]
Density (kg/m^3)	900	1043
Melt flow rate	6,0 g/10 min	10 cm^3/10 min
Tensile modulus (MPa)	1500	3300
Stress at break (MPa)	34	46
Strain at break (%)	> 50	2
Charpy notched impact strength at 23 °C (kJ/m^2)	3,5	3
Ball indentation hardness at 358 N/30 s (MPa)	74	150

Only the properties obtained for both polymers are listed in table 6.1.

6.2 Sample preparation

Polymer samples for the spectroscopic studies were manufactured by compression moulding. The amount of light absorbed by a sample depends on its concentration, i.e. with solid samples the thickness of the sample. If a sample is too thick the bands and bands measured with transmission spectroscopy can saturate, causing the spectrum to deform. The differences in thickness between samples affect the diffusion of oxygen into the sample, as well as the consistency of the measurements during photo-oxidation. In order for the results to remain as consistent as possible, the spectroscopic studies were measured from thin pressed films.

The pressed films were prepared using a Specac constant thickness film maker. The thickness of the films was chosen to be 50 μm to enable diffusion of oxygen into the whole sample, instead of just the surface layer. Each film was made from approximately 110 ± 5 mg of granules, typically 4 PP or 6 PS granules. The granules were centered in the film maker, between two pieces aluminium foil with the reflecting sides towards the granules. The film maker was heated up to 200 °C with Specac heated platens inside a Perkin-Elmer laboratory press. The granules were kept between the platens at 200 °C for 2 minutes, after which a pressure of 4000 kg was applied with the press. After 3 minutes under pressure and heat the samples were set to cool for two minutes in the film makers cooling cradle, after which they were sealed for 3 days in an airtight polyethylene bag and set into a dark drawer with ambient temperature to wait for the weathering studies.

The polymer samples used in the DSC studies were made by the Plastics and Elastomer laboratory of Tampere University of Technology. The samples were $0{,}45 \pm 0{,}05$ mm thick and 20 cm times 30 cm large rectangular sheets compression moulded in a hydraulic press heated to 210 °C. These samples were used in the DSC studies, because their thickness was suitable for the standardized oxidation induction tests. The weight of a pan sized sample piece was on average approximately 10 ± 2 mg, suitable for performing a DSC measurement with only one sample piece. Not needing to use multiple sample pieces for a DSC measurement allows for a better thermal connection between the pan and sample, resulting in more consistent results.

6.3 Artificial weathering method

The polymer samples were weathered artificially by irradiating them with a Luzchem Research Inc. XE-LMP xenon arc lamp. The lamp housing had an optical system to focus the light into a slowly spreading circular beam. The xenon lamp was used without any wavelength filters to accelerate the degradation progress of the samples.

The results obtained with this method cannot be compared directly to the results obtained from samples degraded by natural light, because the xenon lamp emits lower wavelength radiation (approximately $\lambda > 250$ nm in air) than present in natural light

($\lambda > 290$ nm). This method was used for the greatly accelerated photodegradation process, in order to demonstrate the use of the instrumental methods in the detection of polymer photodegradation.

The samples were attached to the center of the xenon lamp's beam in a cardboard frame at a distance of 65 cm from the lamp, after which they were irradiated. Measurements were performed at suitable time frames during the irradiation cycle. The power of the lamp at the sample distance was measured before and after each irradiation sequence with a Coherent Powermax LM-10 thermopile sensor attached to a Coherent Fieldmax II-TOP power and energy meter. The LM-10 sensor can be used in the wavelength range of $\lambda = 250$ nm– 10,6 µm, which corresponds well with the output range of the xenon lamp. The irradiance of the lamp at the sample distance was calculated by dividing the measured power with the LM-10's sensor area, the radius of which is $18{,}20 \pm 0{,}05$ mm. The average power of the lamp at this distance was $67{,}85 \pm 0{,}10$ mW, which corresponds to an average irradiance of $260{,}8 \pm 0{,}4$ W/m^2. The small standard error of the mean irradiance indicates that the irradiance was constant throughout the sample irradiation cycle.

7. MEASUREMENT METHODS

The precise measurement methods and instruments are presented in this chapter. The measurements were performed according to standardized test methods when applicable.

7.1 Spectroscopic measurements

The spectroscopic measurements were performed according to the international standard ISO 10640:2011 [22]. All IR and UV-Vis spectra of the samples were measured in the absorbance mode.

Five separate 50 µm thin PP and PS films were prepared for the spectroscopic measurements. The samples were irradiated together and the measurements were taken from the center portions of the pressed 50 µm thin films at suitable time intervals.

The FTIR spectra of the samples were measured with a PerkinElmer Spectrum One FT-IR Spectrometer. The background and sample spectra were measured for wavenumbers of $4000-400\ \mathrm{cm^{-1}}$ with a resolution of $4\ \mathrm{cm^{-1}}$ and were averaged over 16 scans. The samples were attached into a thick paper specimen holder, with an round aperture of 10 mm. The same sample holder was used for all of the FTIR measurements.

The UV-Vis spectra of the samples were measured with a double beam Shimadzu UV-3600 UV-VIS-NIR spectrometer. The background and sample spectra were measured between $250-800$ nm with a resolution of 1 nm. The samples were positioned in a solid specimen holder, with a rectangular aperture with a width of approximately 10 mm.

7.2 DSC measurements

The measurement conditions and temperature programs used in the DSC measurements are reviewed in this chapter. The DSC measurements were performed according to the international standards ISO 11357-1 [18] and 11357-6 [19].

The DSC measurements were performed on a Mettler Toledo DSC820 calorimeter. The calorimeter was calibrated according to the instructions given in ISO 11357-6 [19] with a two point calibration using the melting temperatures and enthalpies of indium and tin in a nitrogen atmosphere. The DPC instrument was attached to the calorimeter during every measurement to enable reliable comparison between measurements with and without the UV lamp switched on. All samples were cut from the pressed polymer sheets and set into 40 µl aluminium pans, with bottom pins for manual centering inside

the furnace. The aluminium pans were left unsealed to enable a fast change of the sample compartments atmosphere and the free passage of UV radiation from the DPC lamp to the sample. All measurements were performed three times for both PP and PS at each irradiation time.

7.2.1 Measuring the glass transition temperature of PS

The glass transition of polystyrene exhibits a distinct enthalpic relaxation band simultaneously with the glass transition. The band disappears after one heating over the glass transition temperature range, so the polystyrene samples were heated twice to obtain the glass transition temperature from the second heating run.

The measurements were performed under a stable nitrogen flow of 60 ml/min. The polystyrene samples were first heated from 20 °C to 150 °C with a heating rate of 20 °C/min after which they were immediately cooled back to 20 °C with a faster cooling rate of 40 °C/min. The samples were held isothermally at 20 °C for one minute to stabilize the heat flow after which the samples were heated again from 20 °C to 150 °C with a heating rate of 20 °C/min.

7.2.2 Measuring the oxidation induction time and the melting of PP

The oxidation induction time was measured by heating the sample from 20 °C to at least 180 °C with a heating rate of 20 °C/min and a nitrogen flow of 60 ml/min, after which the rest of the test was isothermal. The heat flow was allowed to stabilize for three minutes before the gas flow was changed from nitrogen to an oxygen flow of 60 ml/min. The gas flow was changed manually, because nitrogen and oxygen were applied to the sample through the same gas pipe. The onset of oxidation was determined as the intercept point of extrapolated tangents from the baseline and the oxidation exotherm. The time from the gas change to the onset of the oxidation was measured as the OIT. The OIT was determined for both polypropylene and polystyrene in multiple test temperatures from 180 °C upwards at 10 °C intervals to determine a test temperature which resulted in an OIT between 10 and 60 minutes for unirradiated samples.

The OIT test was performed in a temperature higher than the melting point of polypropylene so that the whole melting endotherm was visible in the heat flow trace. The melting temperature and enthalpy were determined from the initial heating up to the OIT test temperature. A straight line that was extrapolated over the melting endotherm was used as the baseline for melting. The melting enthalpy was obtained by calculating the area between the heat flow trace and the melting baseline.

The OIT measurements were repeated with UV irradiation. The UV lamp's shutter was opened exactly when the furnace reached the OIT test temperature. The DPC system consisted of a Hamamatsu Lightningcure L8333-02 LC5 mercury-xenon UV spot light source with an optical filter that allowed the pass-through of radiation with wavelengths between $\lambda = 280 - 400$ nm. The UV radiation was directed to the sample and reference pans with a Y-shape quartz light guide. The DPC furnace had a lid with three

quartz glass covers to enable the irradiation of the sample, one glass forming the top of the lid and one glass over the sample and reference pans each in the bottom of the lid. The LC5 lamp was used at 10 % power, which resulted in sample irradiance of $5 \pm 1\ \mathrm{W/m^2}$ through the furnace lid, measured with a Hamamatsu C6080-03 UV power meter. The irradiance was intentionally set low to be able to observe subtle changes due to the irradiation. If the lamp's power was set higher, the resulting higher UV irradiance forced the oxidation to occur practically immediately in the UV-OIT measurements.

7.2.3 Measuring the oxidation induction temperature

The oxidation induction temperature was measured by heating the sample from 20 °C up to as high as 350 °C with a heating rate of 20 °C/min and an oxygen heat flow of 60 ml/min. The sample was always heated up to a maximum temperature that was at least 30 °C higher than the steepest point of the oxidation exotherm. The T_{ox} was determined as the onset temperature of the oxidation exotherm. The onset of oxidation was determined using the same method as in the determination of the OIT.

The T_{ox} measurements were repeated with UV irradiation. The DPC measurement parameters were the same as in the OIT measurements with UV irradiation.

8. RESULTS AND OBSERVATIONS

The observed changes and results obtained from the IR and UV-Vis spectra and thermoanalytical curves of the irradiated polymer samples are presented in this chapter. The purpose of this chapter is to present and compare the observed degradation of polypropylene and polystyrene. All results in this chapter are presented as the mean of all measurements, with the standard error of the mean used as an estimate of the total error. Every absorption spectrum is drawn with two lines, presenting the upper and lower limits of the standard error of the mean of the five measured spectra.

The samples were irradiated with the method described before. The irradiation sequences for the thin films were 8–12 hours, after which the spectroscopic measurements were performed immediately, lasting approximately two hours. The irradiation sequences for the thicker sheets were 20–45 long, after which the DSC measurements were performed during the following day. All samples were irradiated for 140 hours, the same time as was plausible for the polypropylene thin films.

8.1 Photodegradation of polypropylene

The color of the polypropylene samples did not change during irradiation. Small surface cracks appeared in the thin films after approximately 70 hours of irradiation. The cracks grew with irradiation time and after 100 hours they extended from edge to edge of the sample. The planar samples also began to curve after approximately 80 hours of irradiation. After 140 hours of irradiation the polypropylene samples became very brittle and two of the five samples broke into smaller pieces during handling, making further irradiation and measurement sequences impossible.

8.1.1 Infrared spectra

The infrared absorption spectra measured for the five polypropylene samples before and after the irradiation cycle are presented in Figure 8.1.

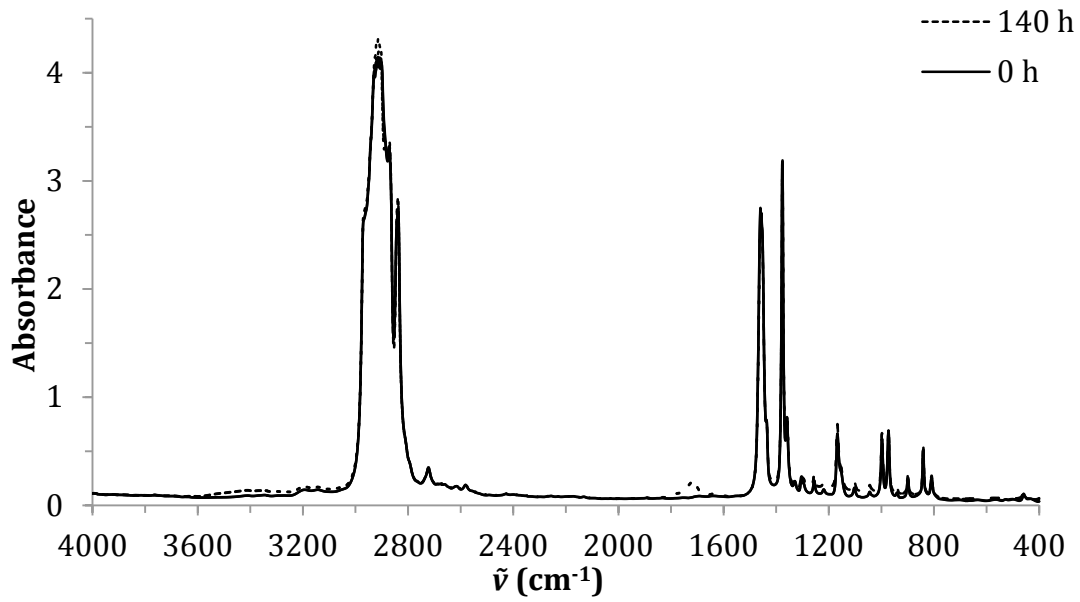

Figure 8.1 *Measured IR spectra for PP before and after irradiation.*

The changes that occur in the IR spectra due to photodegradation are limited to the hydroperoxide and hydroxyl groups $(\tilde{\nu} = 3600-3200\ \mathrm{cm}^{-1})$, carbonyl groups $(\tilde{\nu} = 1800-1650\ \mathrm{cm}^{-1})$ and the area associated with double bonds and the crystallinity of polypropylene $(\tilde{\nu} = 1300-800)$. The clearest changes are due to the formation of a wide carbonyl band. This suggests that carbonyl groups are the most plentiful product in the photodegradation of polypropylene, although carbonyl groups generally exhibit a larger IR absorption band than hydroperoxide or hydroxyl groups. A close-up of the carbonyl group absorptions at various irradiation times is presented in Figure 8.2.

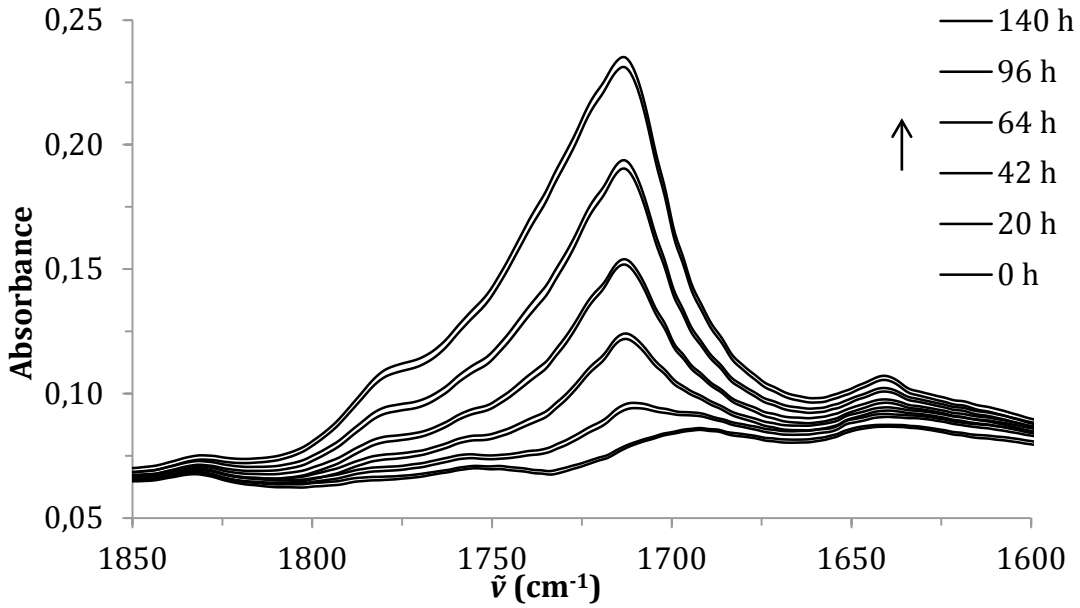

Figure 8.2 *Carbonyl group absorption area in the IR spectra measured after 0, 20, 42, 64, 96 and 140 hours of irradiation.*

The carbonyl band in Figure 8.2 is a superposition of numerous different types of carbonyl group bands, forming a wide band with numerous shoulders as local maxima. The maximum absorption of the carbonyl groups is located at $\tilde{\nu} = 1713\ \mathrm{cm}^{-1}$, which corresponds to a carboxylic acid group [22].

A close-up of the hydroxyl and hydroperoxide group absorptions at various irradiation times is presented in Figure 8.3.

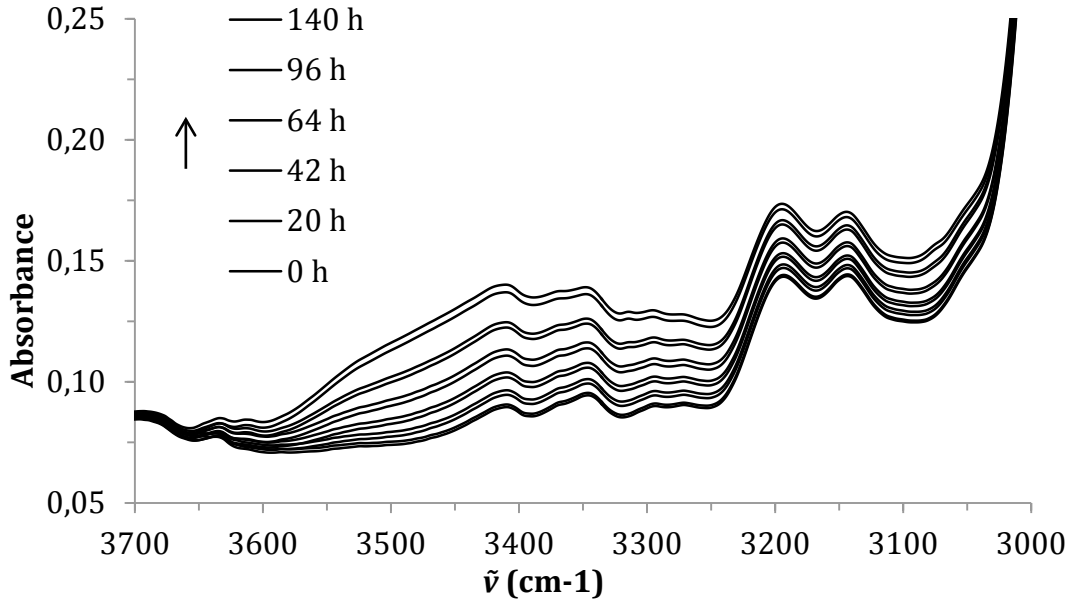

Figure 8.3 *Hydroxyl and hydroperoxide group absorption area in the IR spectra measured after 0, 20, 42, 64, 96 and 140 hours of irradiation.*

Clear absorption bands are not formed due to photodegradation in the hydroxyl absorption area. This is a specific property of the hydroxyl group, which forms a wide undefined absorption area due to hydrogen bonding. To calculate the degradation indices the absorption at $\tilde{\nu} = 3445\ \mathrm{cm}^{-1}$ is allocated to the hydroperoxide group and the absorption at $\tilde{\nu} = 3600\ \mathrm{cm}^{-1}$ is allocated to the hydroxyl group [10].

Any band at wavenumbers of 840, 974, 1166, 1455 and $2720\ \mathrm{cm}^{-1}$ can be used as a reference band to calculate the degradation indices. The most often used internal reference is the $\tilde{\nu} = 974\ \mathrm{cm}^{-1}$ band that corresponds to the rocking motion of the CH_3 groups. [10] This band is present in both fully atactic and melted isotactic polypropylene, which means that it corresponds to the amorphous sections in the polymer [12]. The reference band used ($\tilde{\nu} = 973\ \mathrm{cm}^{-1}$) and the band corresponding to the isotactic portion of the polymer ($\tilde{\nu} = 998\ \mathrm{cm}^{-1}$) are presented in Figure 8.4 at three irradiation times.

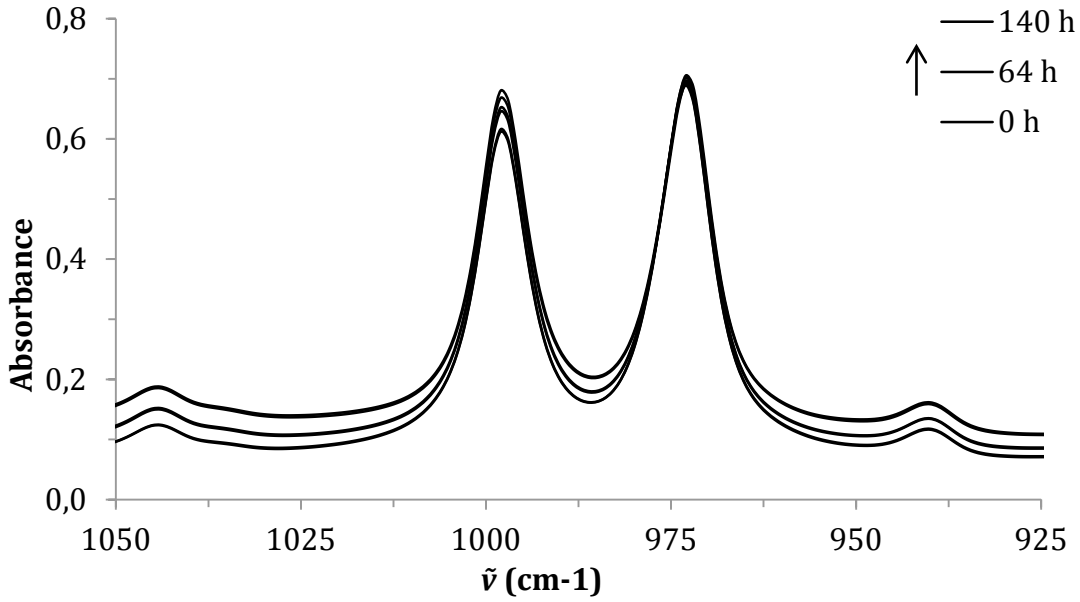

Figure 8.4 *Isotactic band at $\tilde{\nu} = 998\ cm^{-1}$ and reference band at $\tilde{\nu} = 973\ cm^{-1}$ in the IR spectra measured after 0, 64 and 140 hours of irradiation.*

The reference band remains very stable, as can be seen in Figure 8.4. Typically the calculation of the isotacticity index requires a baseline correction [12, 13] to correct for the changes in sample thickness, especially as the baseline around the bands changes in Figure 8.4. In this case the baseline change is due to photodegradation, not a true shift in the baseline as can be seen in Figures 8.1–8.3, where the general baseline outside the reference band area remains stable. The stability of the reference band confirms that the baseline remains stable, despite the change around the absorption bands in Figure 8.4. This means that implementing a baseline correction would distort the results, so no baseline correction is implemented in any of the calculations. The results obtained in this study are comparable to each other, especially because the same samples are measured throughout the irradiation cycle, but caution must be taken when comparing the obtained absolute values to other studies. The lack of a baseline correction gives slightly larger isotacticity index values, exaggerating the ItI by approximately 2 %.

The degradation indices from the IR spectra are calculated according to the following formulae:

$$CI = \frac{A(1713\ \mathrm{cm^{-1}})}{A(973\ \mathrm{cm^{-1}})} \tag{45}$$

$$HPI = \frac{A(3445\ \mathrm{cm^{-1}})}{A(973\ \mathrm{cm^{-1}})} \tag{46}$$

$$HI = \frac{A(3600\ \mathrm{cm^{-1}})}{A(973\ \mathrm{cm^{-1}})} \tag{47}$$

$$ItI = \frac{A(998\ \mathrm{cm^{-1}})}{A(973\ \mathrm{cm^{-1}})} \tag{48}$$

The degradation indices were calculated separately for each measured spectrum, after which they were averaged. The average results calculated with (45)–(48) are presented in table 8.1, with the standard errors of the means calculated as the errors.

Table 8.1 *Degradation indices of the polypropylene samples at various irradiation times. The results are averaged from the separate sample spectra with the standard errors of the means presented as the errors.*

Time (h)	CI	HPI	HI	ItI
0	0,1136 ± 0,0007	0,1185 ± 0,0009	0,1038 ± 0,0010	0,8892 ± 0,0021
8	0,1234 ± 0,0008	0,1217 ± 0,0008	0,1053 ± 0,0010	0,8926 ± 0,0020
20	0,1366 ± 0,0017	0,1255 ± 0,0014	0,1056 ± 0,0013	0,9000 ± 0,0019
30	0,1520 ± 0,0011	0,1301 ± 0,0012	0,1068 ± 0,0011	0,9048 ± 0,0020
42	0,1768 ± 0,0013	0,1348 ± 0,0014	0,1064 ± 0,0014	0,9140 ± 0,0020
52	0,1936 ± 0,0022	0,1397 ± 0,0015	0,1073 ± 0,0014	0,9189 ± 0,0020
64	0,2185 ± 0,0016	0,1472 ± 0,0018	0,1091 ± 0,0015	0,9276 ± 0,0021
74	0,2352 ± 0,0013	0,1523 ± 0,0015	0,1105 ± 0,0012	0,9329 ± 0,0021
86	0,2570 ± 0,0024	0,1584 ± 0,0020	0,1120 ± 0,0017	0,9394 ± 0,0021
96	0,2709 ± 0,0017	0,1614 ± 0,0013	0,1110 ± 0,0010	0,9441 ± 0,0021
108	0,2911 ± 0,0025	0,1678 ± 0,0022	0,1126 ± 0,0018	0,9498 ± 0,0023
118	0,3046 ± 0,0032	0,1718 ± 0,0029	0,1125 ± 0,0022	0,9558 ± 0,0015
130	0,3246 ± 0,0034	0,1830 ± 0,0032	0,1186 ± 0,0025	0,9613 ± 0,0019
140	0,3333 ± 0,0038	0,1861 ± 0,0032	0,1177 ± 0,0023	0,9642 ± 0,0015

The evolution of the carbonyl index of polypropylene as a function of irradiation time is presented in Figure 8.5.

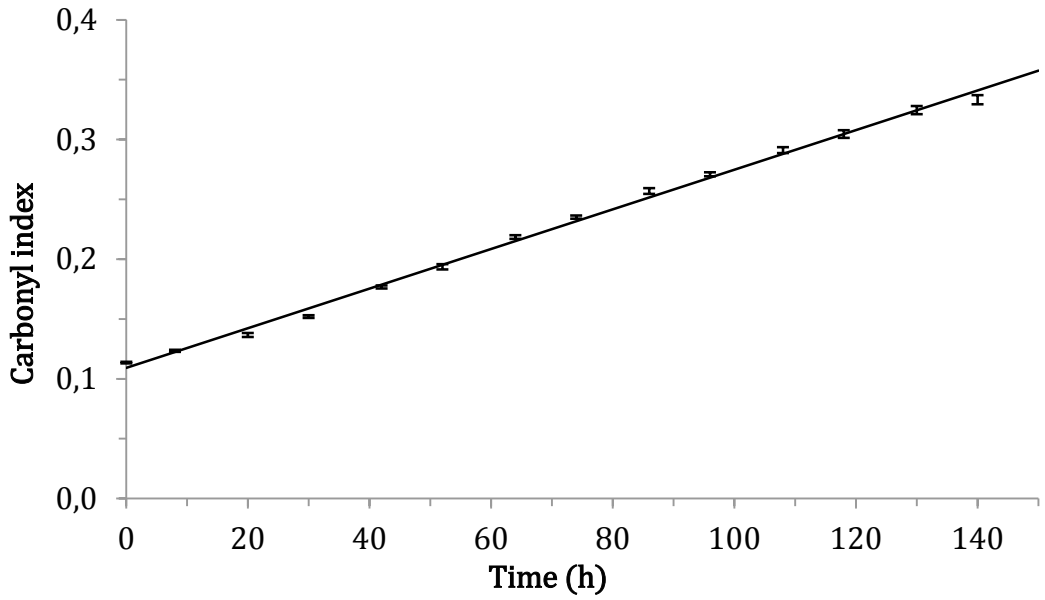

Figure 8.5 *Carbonyl index of polypropylene as a function of irradiation time.*

The carbonyl index rises linearly as a function of irradiation time with a linear fit of $CI = 0{,}0017 \times \mathrm{Time(h)} + 0{,}1091$. The squared correlation coefficient of the linear fit is $R^2 = 0{,}9969$, meaning that the linear fit is very accurate, although a short induction period, a steep propagation period and a termination period of slow rise can be seen in the evolution of the carbonyl index.

The evolution of the hydroperoxide index of polypropylene as a function of irradiation time is presented in Figure 8.6.

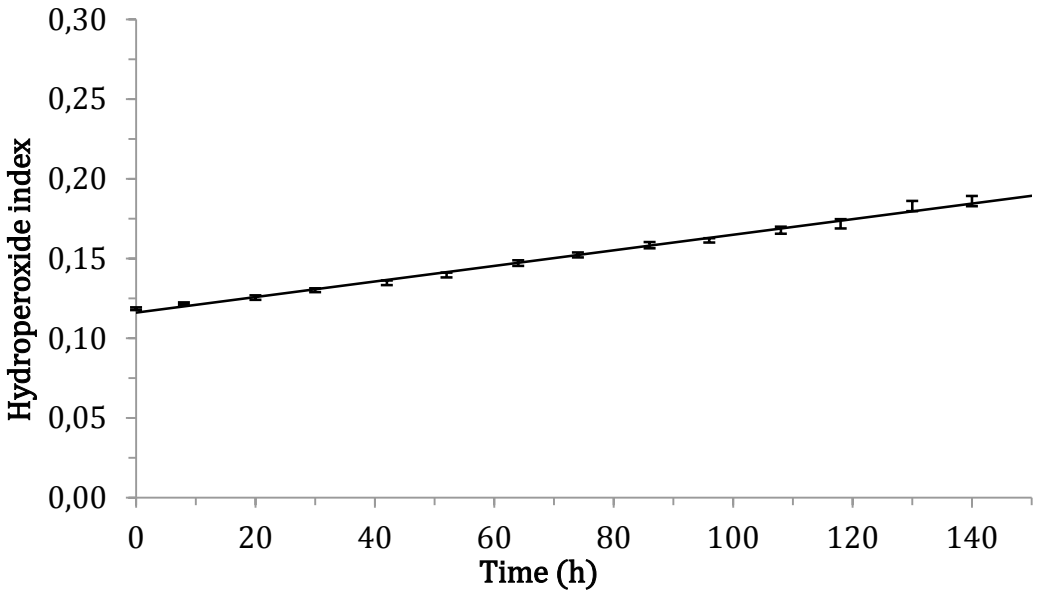

Figure 8.6 *Hydroperoxide index of polypropylene as a function of irradiation time.*

Like the carbonyl index, the hydroperoxide index rises linearly as a function of irradiation time with a linear fit of $HPI = 0{,}0005 \times \mathrm{Time(h)} + 0{,}1161$. The squared correlation coefficient of the linear fit is $R^2 = 0{,}9943$, meaning that the linear fit is as good as in the carbonyl index. The hydroperoxide index does exhibit a short induction period, a steep propagation period and a termination period of slow rise, although not as clearly as the carbonyl index. Generally the behavior of the carbonyl and hydroperoxide indices is similar, although the slope of the linear fit for the CI is over three times as large as the slope for the HPI.

The evolution of the hydroxyl index of polypropylene as a function of irradiation time is presented in Figure 8.7.

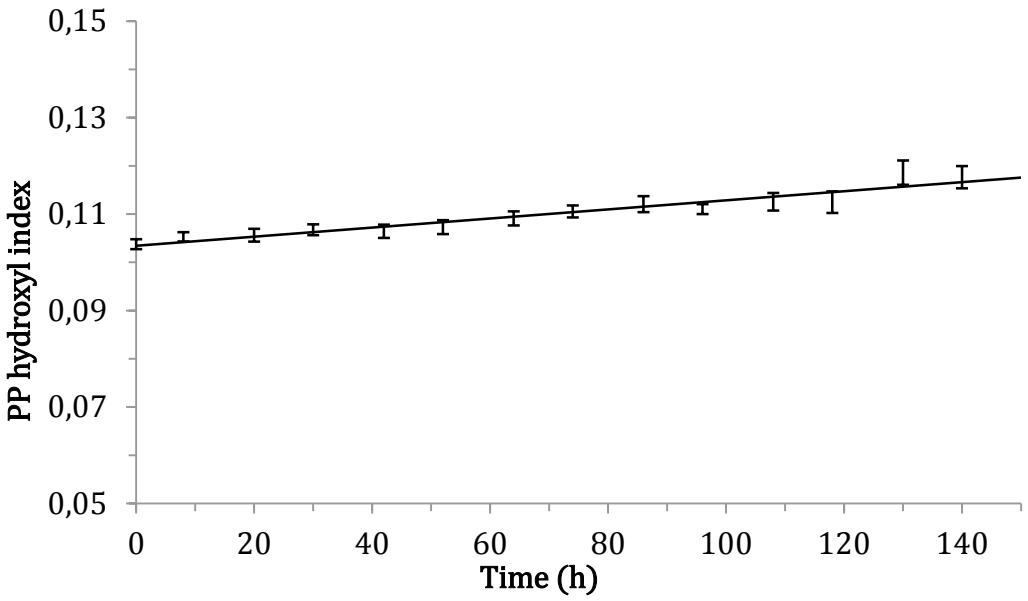

Figure 8.7 *Hydroxyl index of polypropylene as a function of irradiation time.*

The hydroxyl index does not exhibit a clear linear rise as a function of irradiation time. The linear fit to the hydroxyl index is $HPI = 0{,}00009 \times \mathrm{Time(h)} + 0{,}1034$ with a squared correlation coefficient of $R^2 = 0{,}9193$. The slope of the rise and the squared correlation coefficient are much weaker than with the carbonyl and hydroperoxide indices, with the slope being less than a fifth of the slope of the HI. This indicates that hydroxyl groups are not formed substantially in the photodegradation process or that they are dissociated by the low wavelength irradiation.

The evolution of the isotacticity index of polypropylene as a function of irradiation time is presented in Figure 8.8.

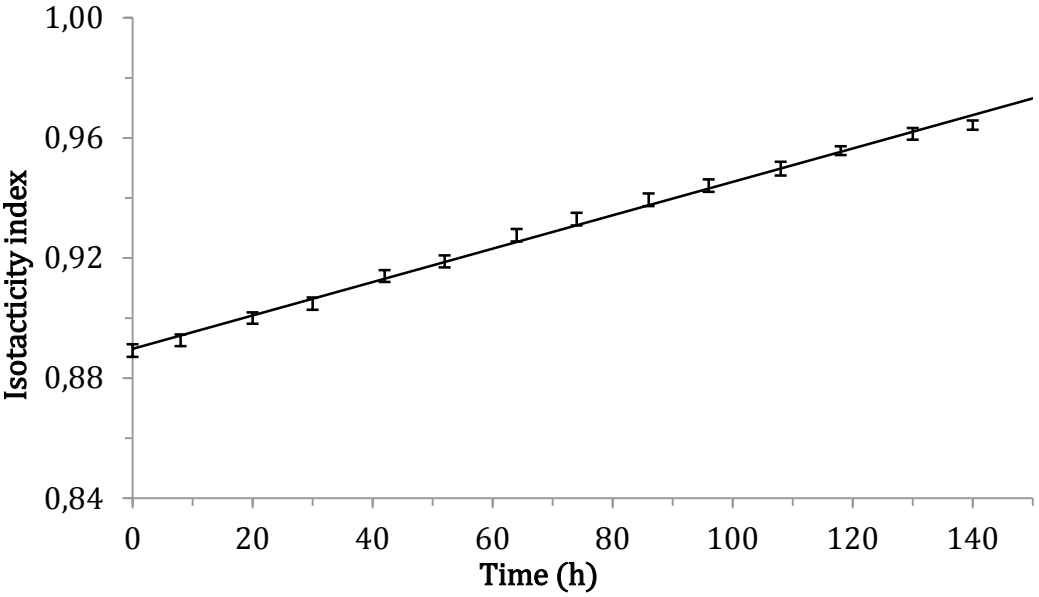

Figure 8.8 *Isotacticity index of polypropylene as a function of irradiation time.*

The isotacticity index exhibits a similar behavior during the photodegradation process as the carbonyl index with a short induction period, a steep propagation period and a termination period of slow rise clearly visible in Figure 8.8. The linear fit of the isotacticity index is $ItI = 0{,}0006 \times \text{Time}\ (h) + 0{,}8897$, with a squared correlation coefficient of $R^2 = 0{,}9961$, meaning that the linear fit is very good. The isotacticity index of polypropylene rises from 89 % up to 97 % during the irradiation cycle, indicating a noticeable increase in the crystallinity of the polymer samples due to photodegradation. This is an expected result, as the degradation process is largely contained in the amorphous regions of polypropylene.

8.1.2 Ultraviolet-visible spectra

The ultraviolet-visible absorption spectra measured for the five polypropylene samples before and after the whole irradiation cycle are presented in Figure 8.9.

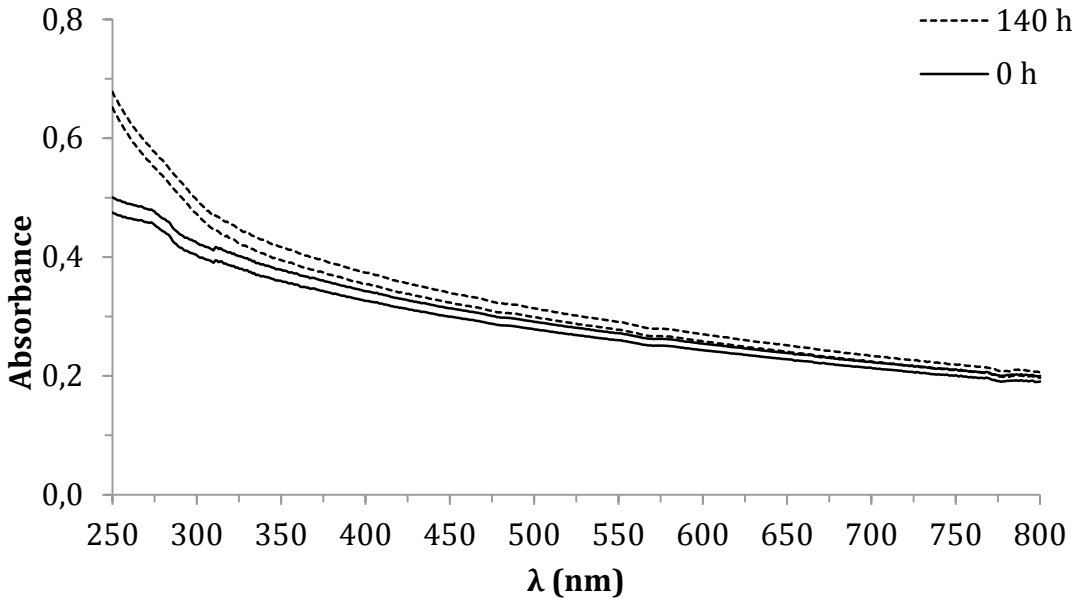

Figure 8.9 *UV-Vis spectra for PP before and after irradiation.*

The only observed change in the UV-Vis spectra of polypropylene samples due to photodegradation is the slightly increased absorbance in the $\lambda = 250–300$ nm wavelength range. This increase is due to the formation of carbonyl groups, which have an absorbance maximum approximately at $\lambda = 280$ nm.

The UV absorption spectra of the polypropylene samples are presented in Figure 8.10 at three irradiation times.

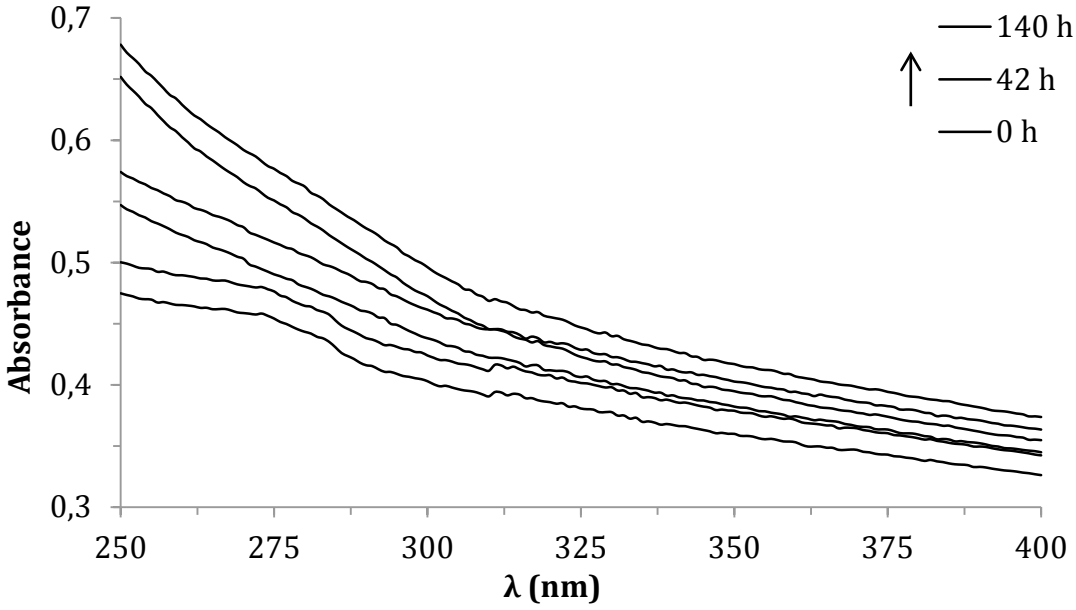

Figure 8.10 *UV spectra of polypropylene measured after 0, 42 and 140 hours of irradiation.*

It is clear from Figure 8.10 that the changes in the UV absorbance of polypropylene caused by photodegradation are barely larger than the errors of the spectra.

The absorbances of the wavelengths that correspond to conjugated double bonds are presented in table 8.2.

Table 8.2 *Absorbances of polypropylene at wavelengths of 312, 328 and 362 nm at various irradiation times. The absorbances correspond to sequences with two, three and four conjugated double bonds, respectively. The results are averaged from the separate sample spectra with the standard error of the mean presented as the errors.*

Time (h)	$A(312\ \mathbf{nm})$	$A(328\ \mathbf{nm})$	$A(362\ \mathbf{nm})$
0	$0{,}405 \pm 0{,}011$	$0{,}388 \pm 0{,}011$	$0{,}359 \pm 0{,}010$
8	$0{,}424 \pm 0{,}009$	$0{,}404 \pm 0{,}009$	$0{,}371 \pm 0{,}008$
20	$0{,}426 \pm 0{,}011$	$0{,}408 \pm 0{,}010$	$0{,}376 \pm 0{,}009$
30	$0{,}430 \pm 0{,}011$	$0{,}412 \pm 0{,}010$	$0{,}379 \pm 0{,}009$
42	$0{,}434 \pm 0{,}012$	$0{,}414 \pm 0{,}011$	$0{,}382 \pm 0{,}010$
52	$0{,}441 \pm 0{,}013$	$0{,}423 \pm 0{,}013$	$0{,}391 \pm 0{,}011$
64	$0{,}453 \pm 0{,}013$	$0{,}430 \pm 0{,}012$	$0{,}397 \pm 0{,}011$
74	$0{,}454 \pm 0{,}013$	$0{,}431 \pm 0{,}012$	$0{,}397 \pm 0{,}010$
86	$0{,}460 \pm 0{,}013$	$0{,}438 \pm 0{,}012$	$0{,}402 \pm 0{,}011$
96	$0{,}461 \pm 0{,}015$	$0{,}437 \pm 0{,}015$	$0{,}401 \pm 0{,}013$
108	$0{,}458 \pm 0{,}013$	$0{,}434 \pm 0{,}012$	$0{,}398 \pm 0{,}011$
118	$0{,}444 \pm 0{,}011$	$0{,}420 \pm 0{,}011$	$0{,}385 \pm 0{,}010$
130	$0{,}455 \pm 0{,}013$	$0{,}432 \pm 0{,}012$	$0{,}395 \pm 0{,}010$
140	$0{,}456 \pm 0{,}012$	$0{,}431 \pm 0{,}011$	$0{,}394 \pm 0{,}011$

The evolution of the absorbance of polypropylene at $\lambda = 312$ nm as a function of irradiation time is presented in Figure 8.11. The absorbance corresponds to sequences with two conjugated double bonds.

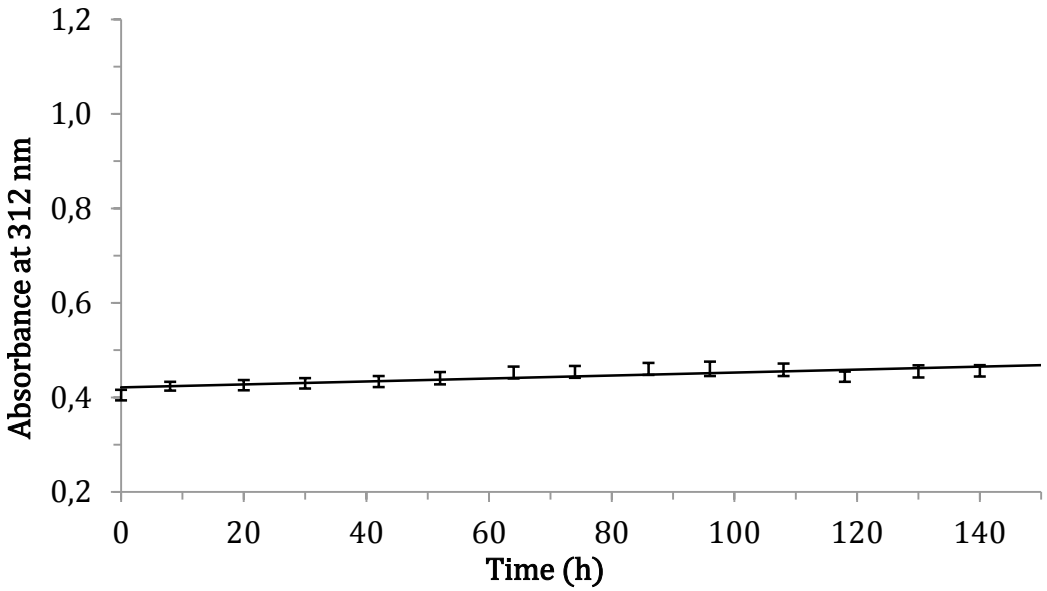

Figure 8.11 *Absorbance of polypropylene at $\lambda = 312$ nm as a function of irradiation time. The absorbance corresponds to sequences with two conjugated double bonds.*

The linear fit to the absorbance at $\lambda = 312$ nm as a function of time is $A(312\text{ nm}) = 0{,}0003 \times \text{Time (h)} + 0{,}4211$ with a squared correlation coefficient of $R^2 = 0{,}7144$. The evolution of the absorbance of polypropylene at $\lambda = 328$ nm as a function of irradiation time is presented in Figure 8.12. The absorbance corresponds to sequences with three conjugated double bonds.

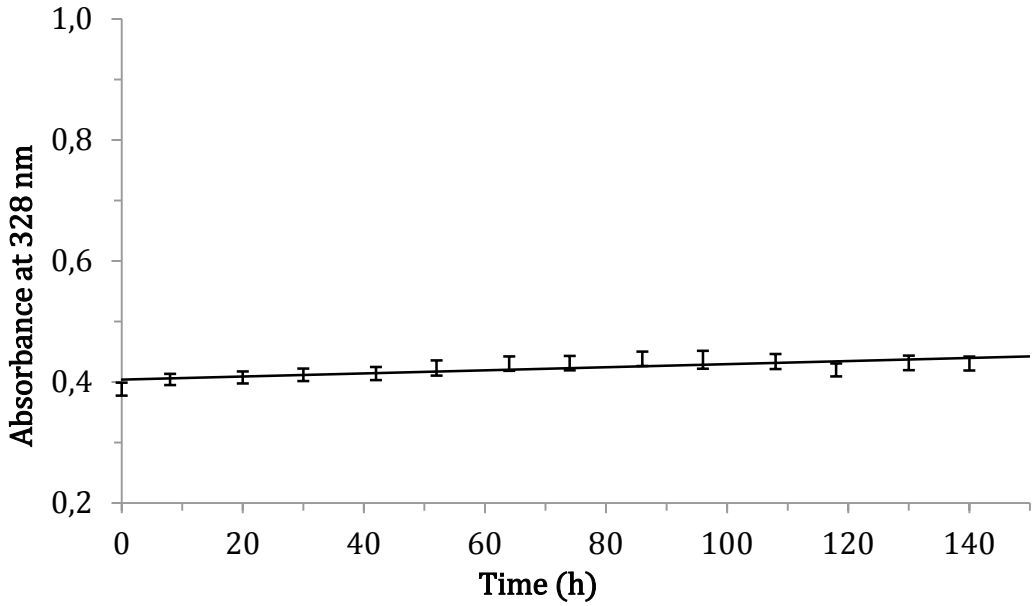

Figure 8.12 *Absorbance of polypropylene at $\lambda = 328\ nm$ as a function of irradiation time. The absorbance corresponds to sequences with three conjugated double bonds.*

The linear fit to the absorbance at $\lambda = 328$ nm as a function of time is $A(328\ \text{nm}) = 0{,}0003 \times \text{Time (h)} + 0{,}4039$ with a squared correlation coefficient of $R^2 = 0{,}6397$. The evolution of the absorbance of polypropylene at $\lambda = 362$ nm as a function of irradiation time is presented in Figure 8.13. The absorbance corresponds to sequences with four conjugated double bonds.

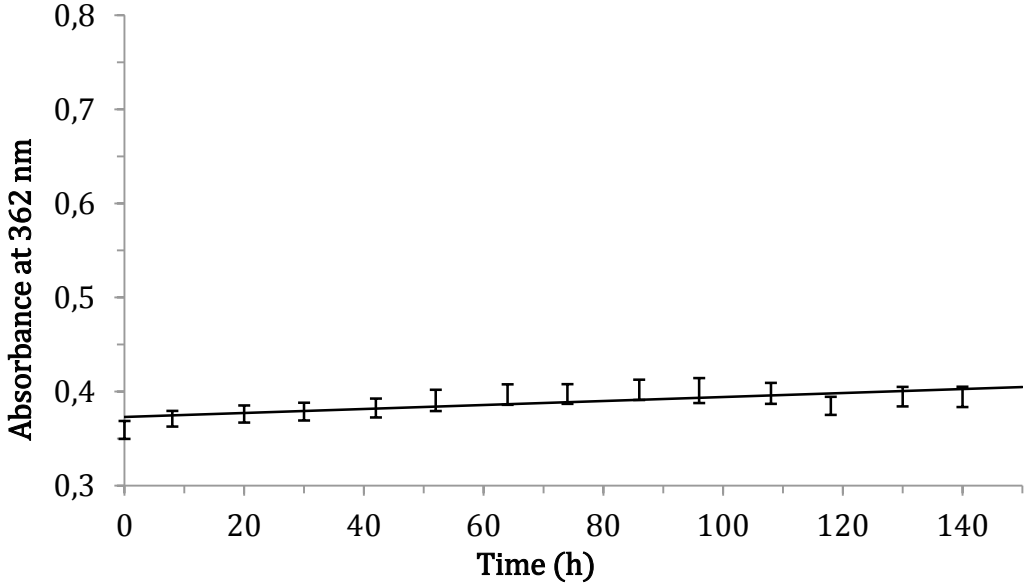

Figure 8.13 *Absorbance of polypropylene at $\lambda = 362\ nm$ as a function of irradiation time. The absorbance corresponds to sequences with four conjugated double bonds.*

The linear fit to the absorbance at $\lambda = 362$ nm as a function of time is $A(362\text{ nm}) = 0{,}0002 \times \text{Time (h)} + 0{,}3730$ with a squared correlation coefficient of $R^2 = 0{,}5781$.

The linear fits to the absorbances in Figures 8.11–8.13 all have a small slope and are quite poorly correlated. This indicates that the photodegradation of polypropylene does not involve the formation of conjugated double bonds in the polymer.

8.1.3 Melting temperature and enthalpy of polypropylene

The thermoanalytical melting curve of unirradiated polypropylene is presented in Figure 8.14.

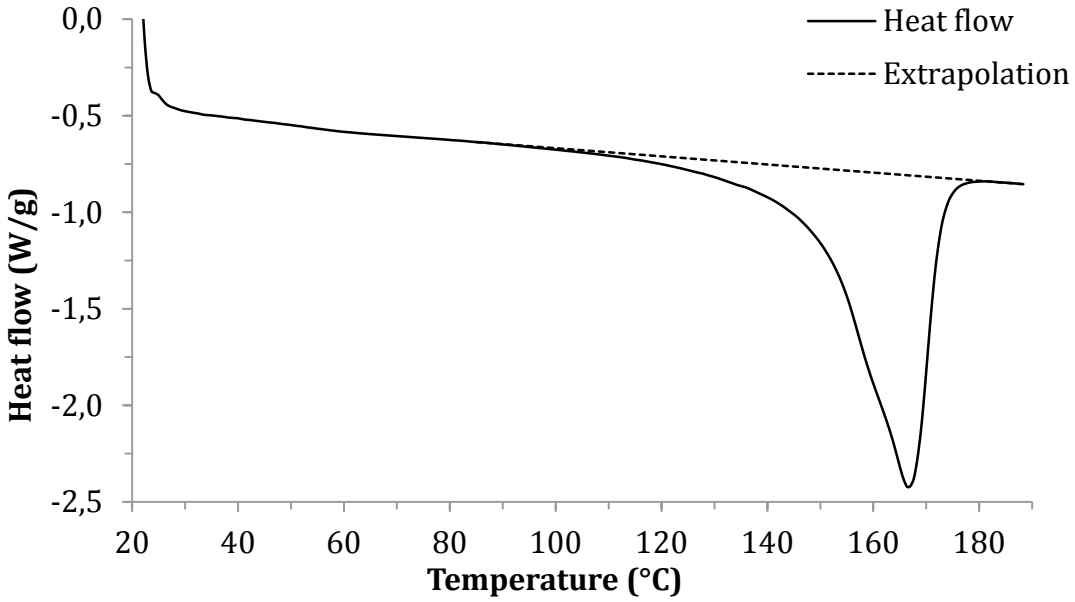

Figure 8.14 *Thermoanalytical melting curve of polypropylene.*

The melting temperature is determined as the peak temperature of the melting endotherm and the melting enthalpy is calculated from the area between the dashed linear extrapolation and the solid heat flow trace. The melting temperature and enthalpy of polypropylene at various irradiation times are presented in table 8.3.

Table 8.3 *Melting temperature and enthalpy of polypropylene at various irradiation times.*

Time (h)	$\boldsymbol{T_m}$ **(°C)**	$\boldsymbol{\Delta H_f}$ $\boldsymbol{(W/g)}$
0	$165{,}5 \pm 0{,}2$	$78{,}9 \pm 2{,}8$
20	$164{,}5 \pm 0{,}2$	$85{,}5 \pm 0{,}3$
45	$165{,}3 \pm 0{,}6$	$79{,}2 \pm 3{,}9$
92	$165{,}4 \pm 1{,}8$	$77{,}7 \pm 5{,}9$
140	$162{,}8 \pm 0{,}6$	$83{,}5 \pm 3{,}9$

During the first 92 hours of irradiation there is little change in the melting temperature of polypropylene. After 140 hours of irradiation the melting temperature drops noticeably. A possible reason for this drop in melting temperature is the shortening of the average PP chain length due to chain scission, which decreases the average molecular mass. The changes observed in the melting enthalpy appear to be stochastic, making the detection of crystallinity changes impractical. This may be due to the formation of polymer peroxides, which decompose at a temperature close to polypropylene's melting temperature.

8.1.4 Oxidation induction time

The thermoanalytical OIT curves measured at several different test temperatures for unirradiated polypropylene are presented in Figure 8.15.

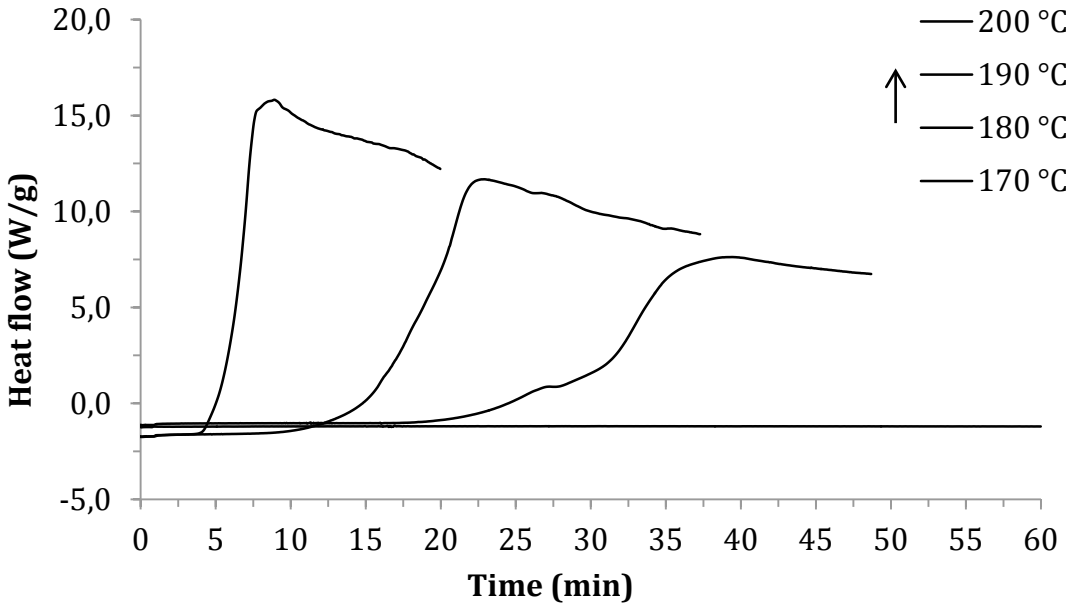

Figure 8.15 *Thermoanalytical OIT curves of polypropylene measured at temperatures of 170, 180, 190 and 200 °C.*

The standardized OIT should be measured at a temperature that results in an OIT between 10 and 60 minutes [19]. This means that from the OIT measurements presented in Figure 8.15 the measurements performed at 180 °C and 190 °C are suitable, with the OIT values of 39,1 and 24,7 minutes, respectively. The OIT measurements for the polypropylene samples were performed at a temperature of 190 °C, because it allowed for a more accurate determination of the melting range of polypropylene than the measurements performed at 180 °C. The full thermoanalytical OIT curve measured at 190 °C for polypropylene is presented in Figure 8.16.

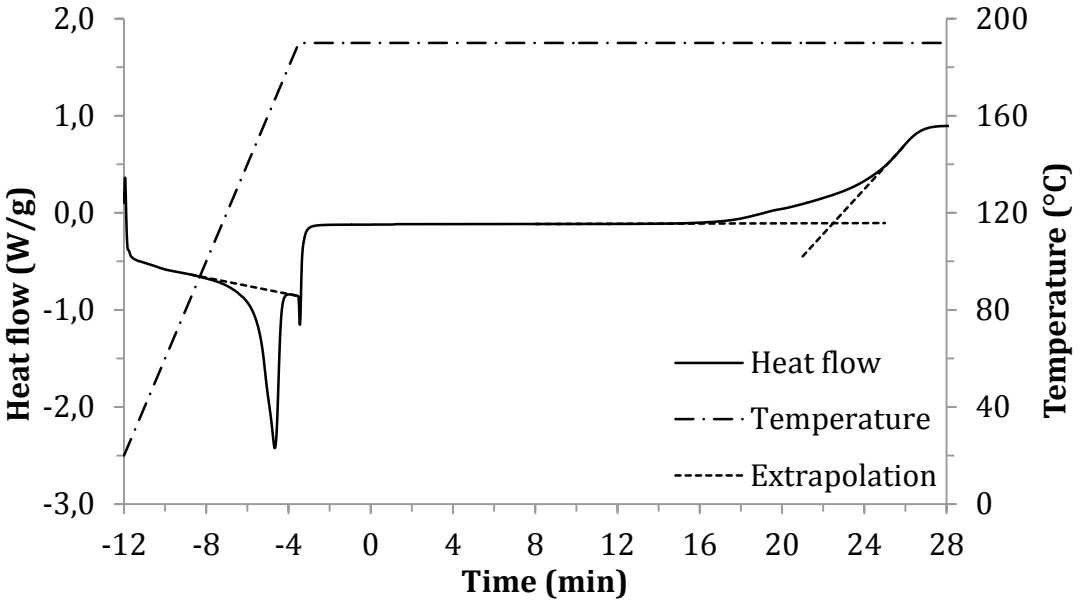

Figure 8.16 *Thermoanalytical melting and oxidation induction time curve of polypropylene.*

In Figure 8.16 the reference pan temperature is presented by the dotted line with the values on the right vertical axes, the heat flow trace is presented by the solid line with the values on the left vertical axes and the extrapolations used for the solving of the melting enthalpy and oxidation induction time are presented by the dashed lines above the melting endotherm and below the oxidation exotherm. Zero time in Figure 8.15 is the time of the gas change, meaning that the time at which the extrapolations before and after the oxidation exotherm intercept is directly the OIT.

The UV-OIT was measured with the same method as the OIT, with the DPC lamp shutter opened at the same time as the isothermal OIT test reached the test temperature, or at exactly −3 minutes using the notation in Figure 8.16. The thermoanalytical UV-OIT curve is presented in Figure 8.17.

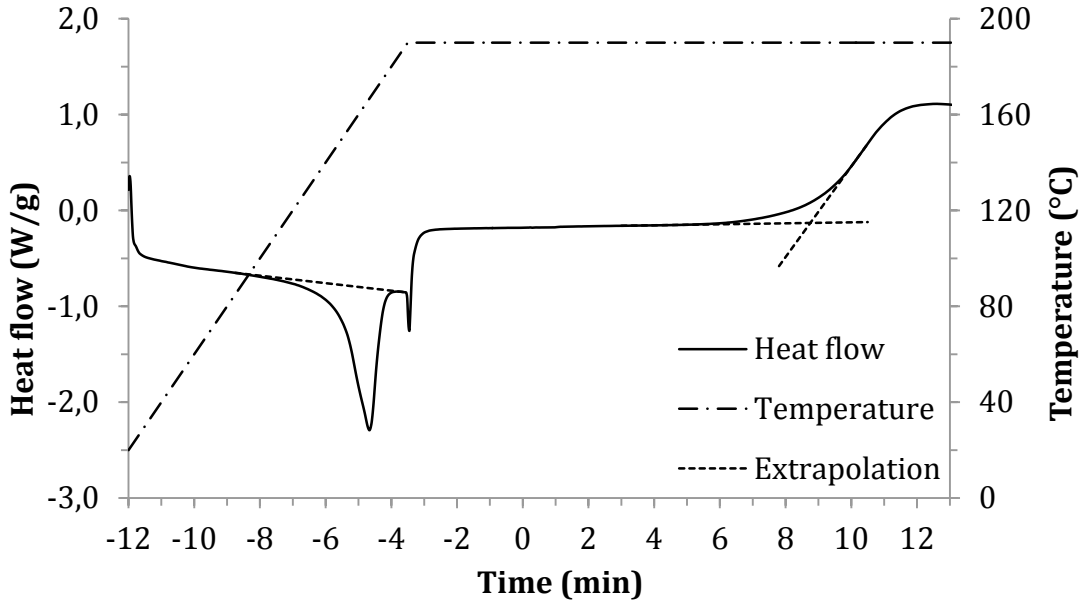

Figure 8.17 *Thermoanalytical melting and UV oxidation induction time curve of polypropylene.*

The thermoanalytical UV-OIT curve in Figure 8.17 is identical to the OIT curve in Figure 8.16, only with a lower value for the oxidation induction time.

The OIT and UV-OIT values measured for polypropylene samples at various irradiation times are presented in table 8.4.

Table 8.4 *OIT and UV-OIT of polypropylene at various irradiation times.*

Time (h)	***OIT* (min)**	***UV – OIT* (min)**
0	19 ± 2	$8{,}3 \pm 0{,}3$
20	$1{,}5 \pm 0{,}1$	$2{,}9 \pm 1{,}4$
45	$1{,}0 \pm 0{,}1$	$1{,}1 \pm 0{,}1$
92	$1{,}0 \pm 0{,}1$	$1{,}1 \pm 0{,}1$
140	$1{,}1 \pm 0{,}1$	$1{,}1 \pm 0{,}1$

Before irradiation the OIT is much larger than the UV-OIT for polypropylene samples. After 20 hours of irradiation the UV-OIT is larger than the OIT, which is an unexpected result. The higher value is due to one single measurement, with the other two measurements resulting in UV-OIT values similar to the OIT measurements. The discrepancy may be due to inhomogeneous photodegradation, because the divergent UV-OIT measurement's heat flow trace did not differ from the other measurements at the same irradiation time, and as such cannot be discarded as an outlier. After 45 hours of irradiation both the OIT and UV-OIT measurements resulted in practically immediate oxidation after the oxygen reached the furnace.

8.1.5 Oxidation induction temperature

The thermoanalytical curve from the oxidation induction temperature measurement for unirradiated polypropylene is presented in Figure 8.18.

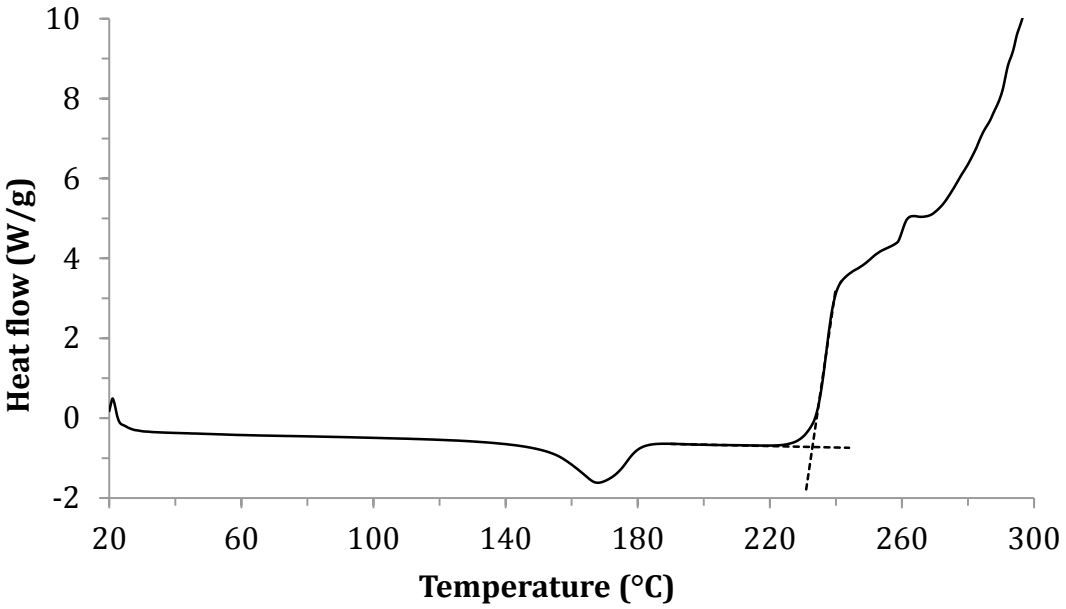

Figure 8.18 *Thermoanalytical oxidation induction temperature curve of polypropylene.*

The T_{ox} is defined as the onset temperature of oxidation, measured as the intercept temperature of the extrapolated heat flow traces onwards from both sides of the oxidation exotherm.

The UV-T_{ox} was measured with the same method as the T_{ox}, with the DPC lamp's shutter open from the beginning of the test. The thermoanalytical UV-T_{ox} curve is presented in Figure 8.19.

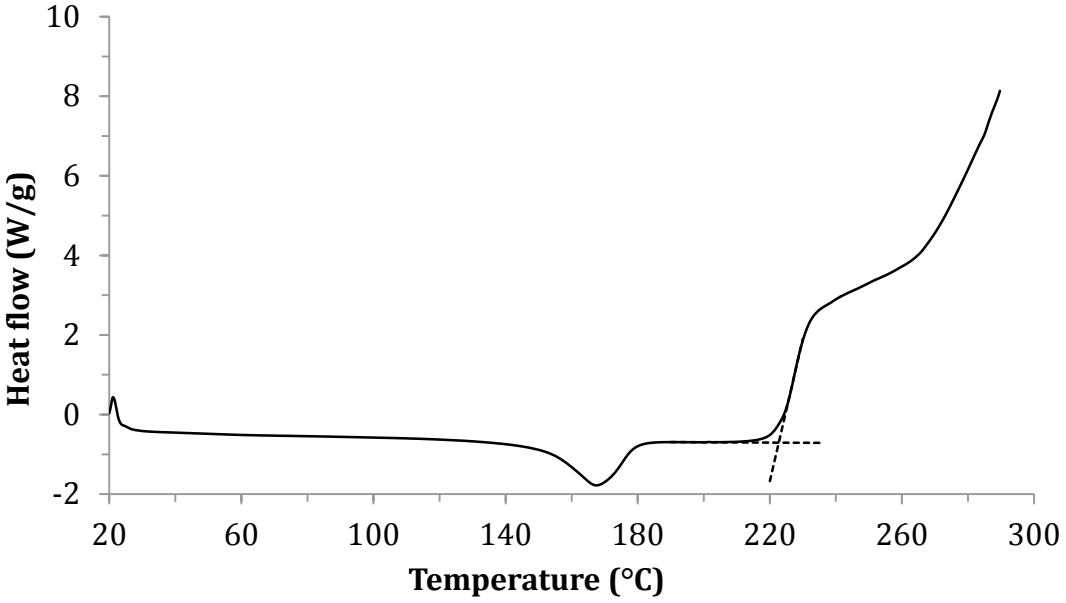

Figure 8.19 *Thermoanalytical UV oxidation induction temperature curve of polypropylene.*

The thermoanalytical UV-T_{ox} curve in Figure 8.19 is identical to the T_{ox}curve in Figure 8.18, only with a slightly smaller oxidation induction temperature.

The T_{ox} and UV-T_{ox} values measured for the polypropylene samples at various irradiation times are presented in table 8.5.

Table 8.5 *T_{ox} and UV-T_{ox} of polypropylene at various irradiation times.*

Time (h)	T_{ox} (°C)	UV-T_{ox}(°C)
0	$231{,}4 \pm 1{,}5$	$223{,}3 \pm 0{,}3$
20	$192{,}0 \pm 1{,}7$	$202{,}1 \pm 3{,}9$
45	$185{,}7 \pm 1{,}8$	$187{,}5 \pm 1{,}9$
92	$181{,}9 \pm 2{,}3$	$182{,}3 \pm 1{,}0$
140	$180{,}2 \pm 1{,}4$	$183{,}1 \pm 0{,}3$

Before irradiation the T_{ox} is higher than the UV-T_{ox}. After 20 hours of irradiation the T_{ox} decreased by 40 °C, twice the decrease that occurred in the UV-T_{ox}. The decrease was possibly due to chain scission, which lowers the average molecular mass. The T_{ox} was noticeably lower than UV-T_{ox} for all of the irradiated samples, which was an unexpected result not reported on before. It may be that the photodegradation reactions that occur in the melted samples hinder the thermal degradation in some manner.

8.2 Photodegradation of polystyrene

Polystyrene exhibited yellowing during irradiation. When all five irradiated thin films were layered on top of each other after 20 hours of irradiation, a slight yellowing was observed. After 50 hours of irradiation the individual films were clearly yellow. The color deepened with irradiation time. The polystyrene samples did not exhibit cracks or bend during irradiation like the polypropylene samples.

8.2.1 Infrared spectra

The infrared absorption spectra measured for the five polystyrene samples before and after the irradiation cycle are presented in Figure 8.20.

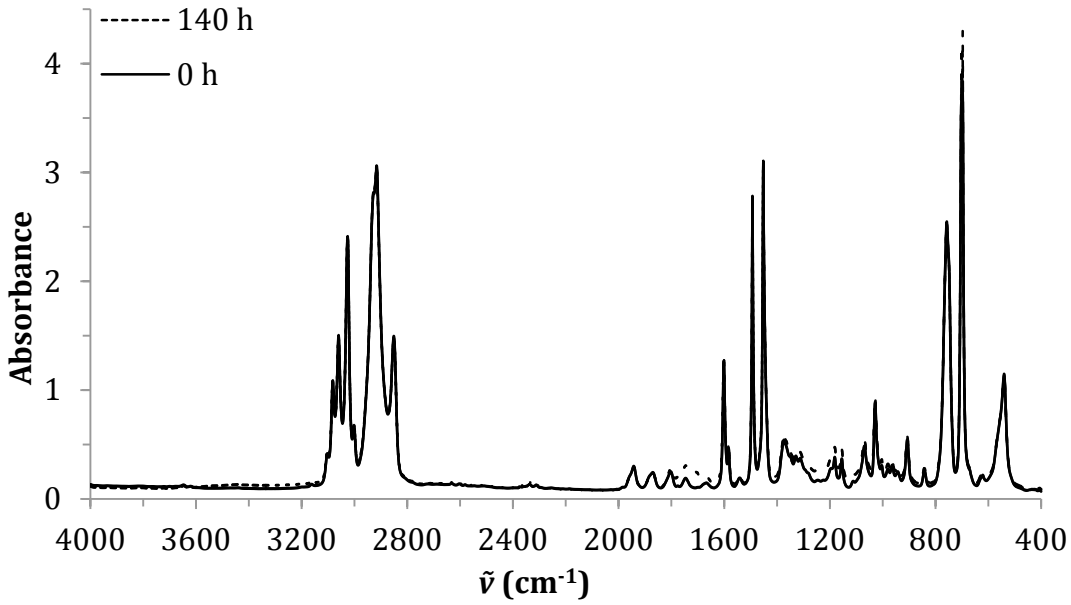

Figure 8.20 *Measured IR spectra for PS before and after irradiation.*

The changes that occur in the IR spectra due to photodegradation are limited to the hydroperoxide and hydroxyl groups $(\tilde{\nu} = 3600\text{–}3200\ \text{cm}^{-1})$, carbonyl groups $(\tilde{\nu} = 1800\text{–}1650\ \text{cm}^{-1})$ and the area associated with double bonds $(\tilde{\nu} = 1300\text{–}800)$. The clearest changes are due to the formation of a wide carbonyl band. This suggests that carbonyl groups are the most plentiful product in the photodegradation of polystyrene, although carbonyl groups generally exhibit a clearer IR absorption band than hydroperoxide or hydroxyl groups. The observation of the carbonyl band is slightly hampered by the out of plane bending of the benzene rings, which forms five absorption bands at $\tilde{\nu} = 1950\text{–}1650\ \text{cm}^{-1}$. A close-up of the carbonyl group absorptions at various irradiation times is presented in Figure 8.21.

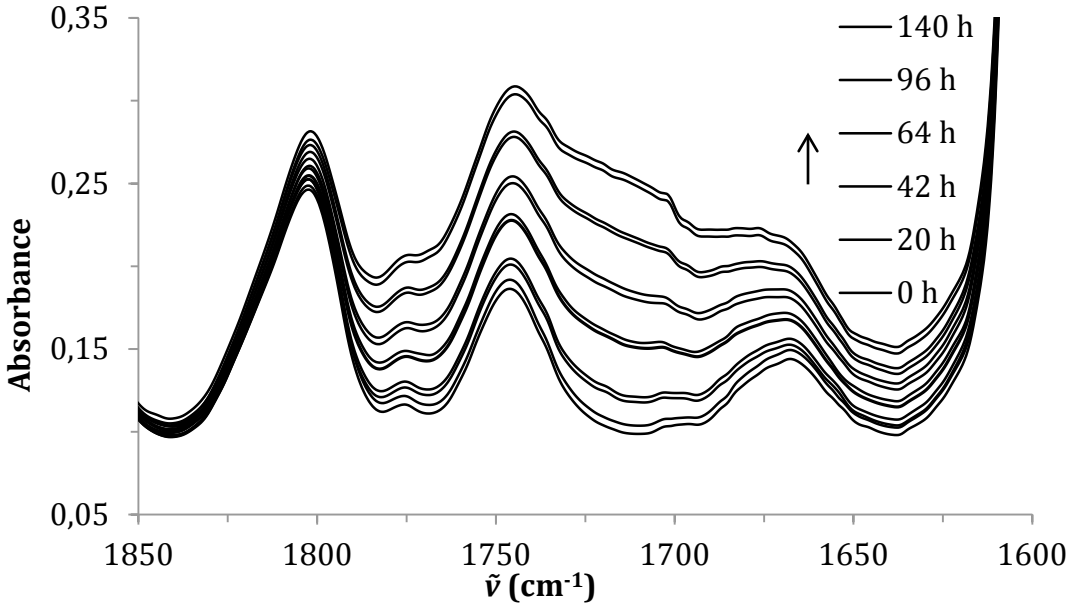

Figure 8.21 *Carbonyl group absorption area in the IR spectra measured after 0, 20, 42, 64, 96 and 140 hours of irradiation.*

The carbonyl band in Figure 8.21 is a superposition of numerous different types of carbonyl group bands, forming a wide band with numerous shoulders as local maxima. The maximum absorption of the carbonyl groups is located at $\tilde{\nu} = 1725\ \mathrm{cm}^{-1}$, which corresponds to an aliphatic ketone [11].

A close-up of the hydroxyl and hydroperoxide group absorptions at three irradiation times is presented in Figure 8.22.

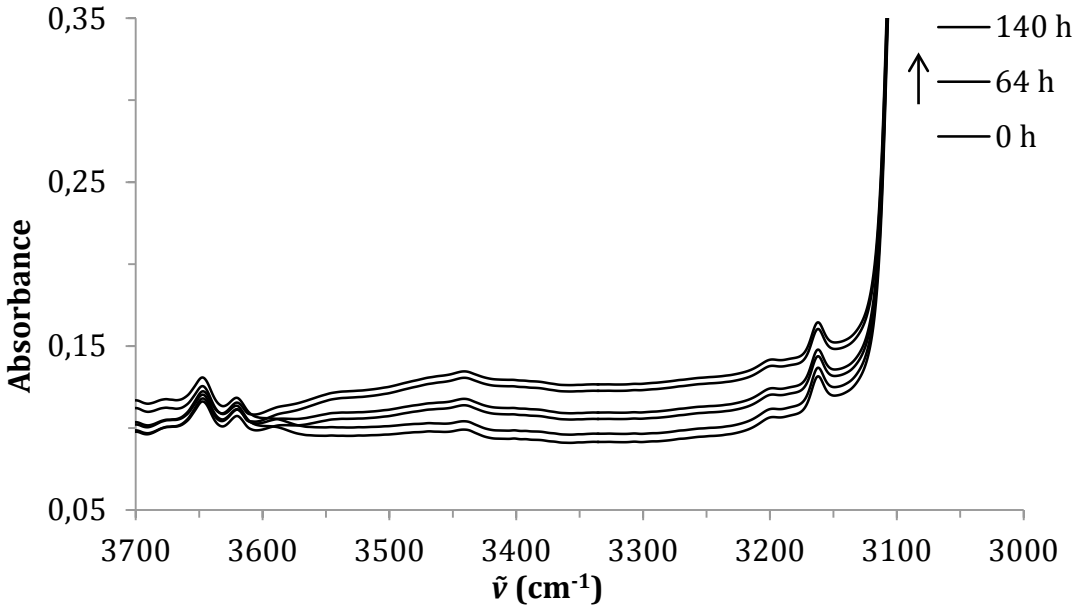

Figure 8.22 *Hydroxyl and hydroperoxide group absorption area in the IR spectra measured after 0, 64 and 140 hours of irradiation.*

Clear absorption bands are not formed due to photodegradation in the hydroxyl absorption area. This is a specific property of the hydroxyl group, which forms a wide undefined absorption area due to hydrogen bonding. To calculate the degradation indices the absorption at $\tilde{\nu} = 3450\ \mathrm{cm}^{-1}$ is allocated to the hydroperoxide group and the absorption at $\tilde{\nu} = 3540\ \mathrm{cm}^{-1}$ is allocated to the hydroxyl group [11].

The stretching band of the aliphatic CH group at $\tilde{\nu} = 2851\ \mathrm{cm}^{-1}$ is used as the reference band for the calculation of the degradation indices [23]. The reference band area is presented in Figure 8.23 at three irradiation times.

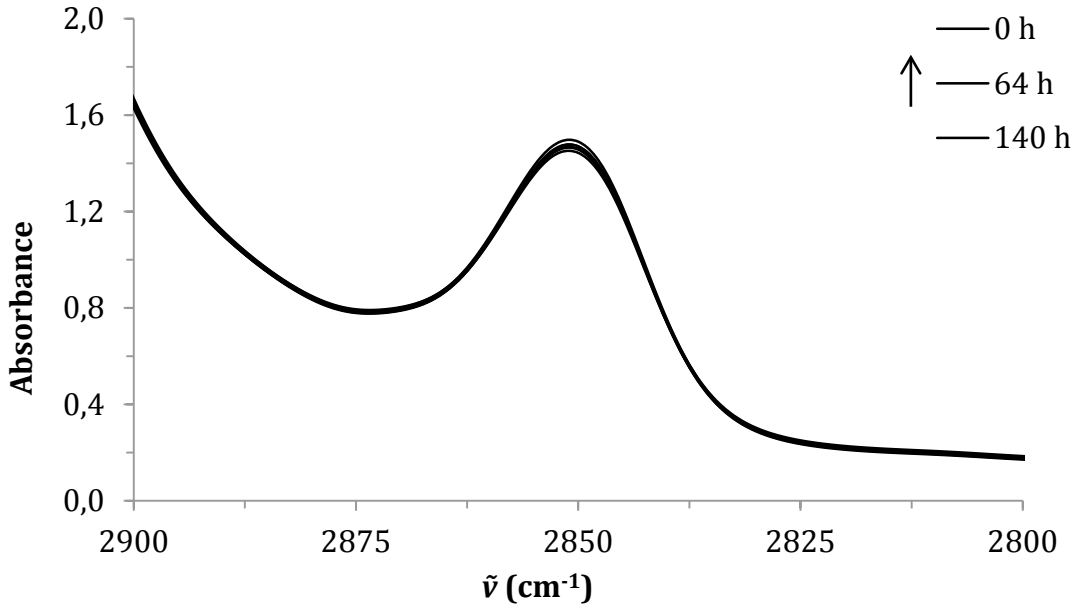

Figure 8.23 *Aliphatic CH_3 stretching band at $\tilde{\nu} = 2851\ cm^{-1}$ in the IR spectra measured after 0, 64 and 140 hours of irradiation.*

The absorbance of the reference band remains fairly stable throughout the irradiation cycle, although a small decrease is observed comparing the absorbance before and after irradiation.

The degradation indices from the IR spectra are calculated according to the following formulae:

$$CI = \frac{A(1725\ \mathrm{cm}^{-1})}{A(2851\ \mathrm{cm}^{-1})} \tag{49}$$

$$HPI = \frac{A(3450\ \mathrm{cm}^{-1})}{A(2851\ \mathrm{cm}^{-1})} \tag{50}$$

$$HI = \frac{A(3540\ \mathrm{cm}^{-1})}{A(2851\ \mathrm{cm}^{-1})} \tag{51}$$

The degradation indices were calculated separately for each measured spectrum, after which they were averaged. The average results calculated with (49)–(51) are presented in table 8.6, with the standard errors of the means calculated as the errors.

Table 8.6 *Degradation indices of the polystyrene samples at various irradiation times. The results are averaged from the separate sample spectra with the standard errors of the means presented as the errors.*

Time (h)	CI	HPI	HI
0	0,0711 ± 0,0010	0,0584 ± 0,0011	0,0560 ± 0,0011
8	0,0776 ± 0,0016	0,0612 ± 0,0016	0,0589 ± 0,0016
20	0,0893 ± 0,0011	0,0654 ± 0,0011	0,0627 ± 0,0012
30	0,1003 ± 0,0014	0,0683 ± 0,0014	0,0652 ± 0,0014
42	0,1128 ± 0,0010	0,0719 ± 0,0011	0,0681 ± 0,0011
52	0,1234 ± 0,0015	0,0748 ± 0,0014	0,0706 ± 0,0014
64	0,1335 ± 0,0014	0,0779 ± 0,0011	0,0730 ± 0,0011
74	0,1418 ± 0,0020	0,0790 ± 0,0016	0,0735 ± 0,0016
86	0,1516 ± 0,0011	0,0825 ± 0,0009	0,0766 ± 0,0009
96	0,1574 ± 0,0010	0,0830 ± 0,0010	0,0767 ± 0,0011
108	0,1652 ± 0,0012	0,0849 ± 0,0012	0,0781 ± 0,0012
118	0,1697 ± 0,0013	0,0848 ± 0,0013	0,0777 ± 0,0013
130	0,1766 ± 0,0014	0,0885 ± 0,0010	0,0811 ± 0,0010
140	0,1814 ± 0,0011	0,0898 ± 0,0012	0,0822 ± 0,0012

The evolution of the carbonyl index of polystyrene as a function of irradiation time is presented in Figure 8.24.

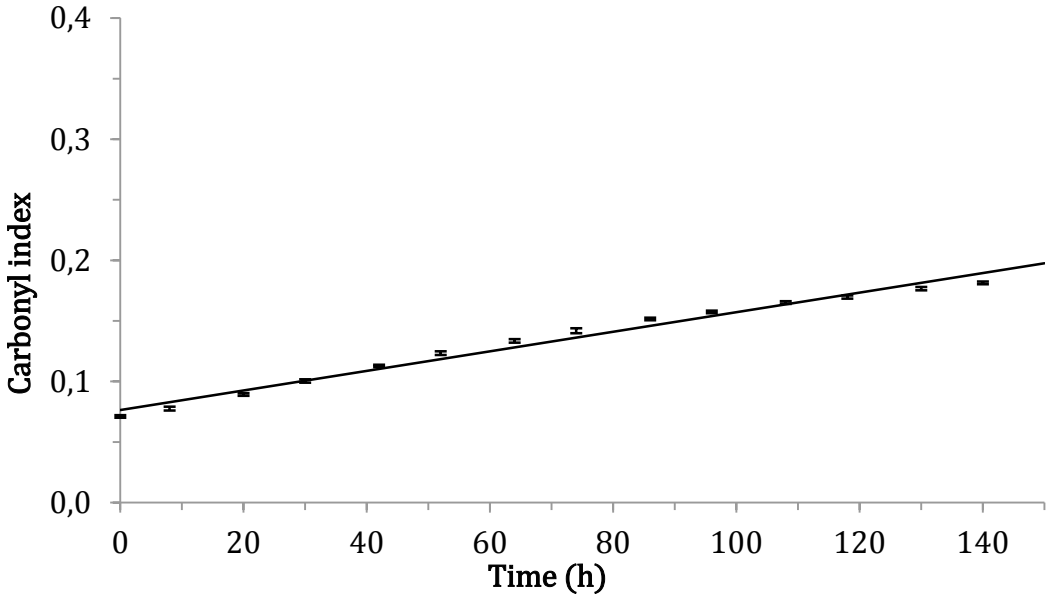

Figure 8.24 *Carbonyl index of polystyrene as a function of irradiation time.*

The carbonyl index rises linearly as a function of irradiation time with a linear fit of $CI = 0{,}0008 \times \mathrm{Time(h)} + 0{,}0764$. The squared correlation coefficient of the linear fit is $R^2 = 0{,}9835$, meaning that the linear fit is accurate. A short induction period, a steep propagation period and a termination period of slow rise can be seen in the evolution of the carbonyl index.

The evolution of the hydroperoxide index of polystyrene as a function of irradiation time is presented in Figure 8.25.

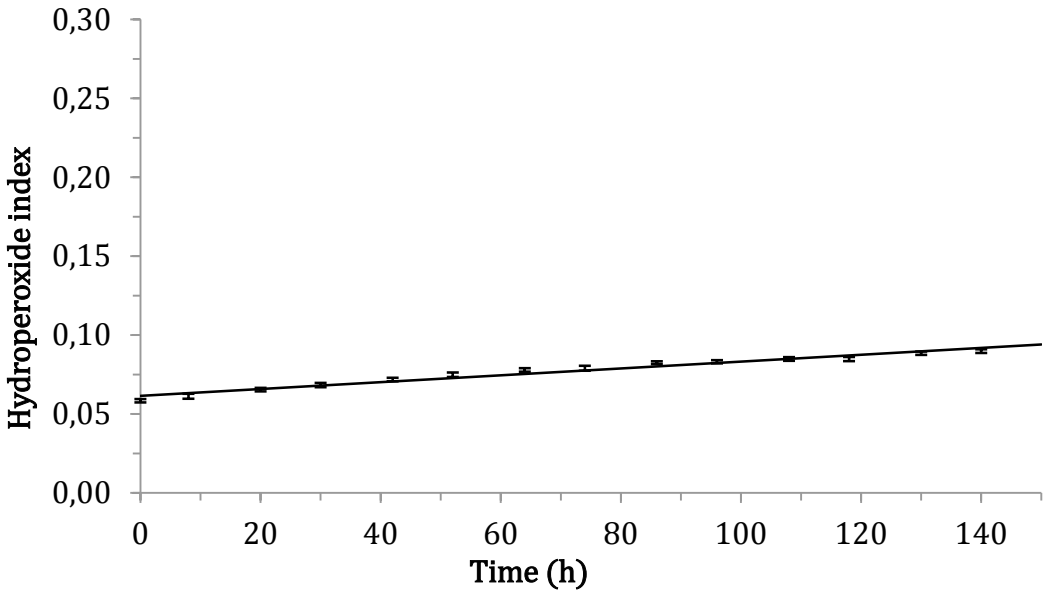

Figure 8.25 *Hydroperoxide index of polystyrene as a function of irradiation time.*

Like the carbonyl index, the hydroperoxide index rises linearly as a function of irradiation time with a linear fit of $HPI = 0{,}0002 \times \mathrm{Time(h)} + 0{,}0615$. The squared correlation coefficient of the linear fit is $R^2 = 0{,}9662$, meaning that the linear fit is almost as good as for the carbonyl index. The hydroperoxide index does exhibit a short induction period, a steep propagation period and a termination period of slow rise, although not as clearly as the carbonyl index. Generally the behavior of the carbonyl and hydroperoxide indices is similar, although the slope of the linear fit for the CI is four times as large as the slope for the HPI.

The evolution of the hydroxyl index of polystyrene as a function of irradiation time is presented in Figure 8.26.

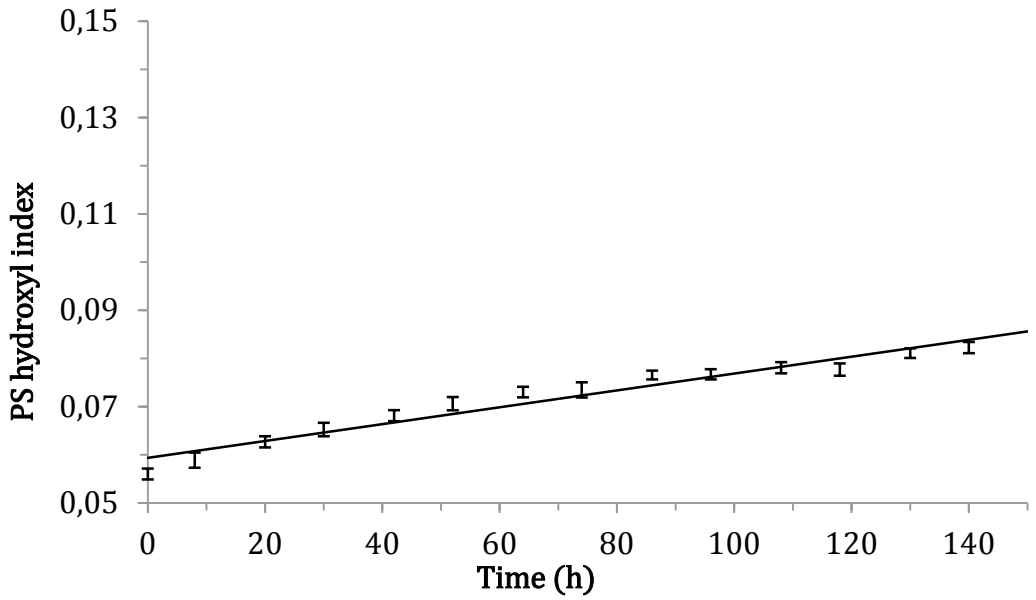

Figure 8.26 *Hydroxyl index of polystyrene as a function of irradiation time.*

The hydroxyl index also exhibits a clear linear rise as a function of irradiation time. The linear fit to the hydroxyl index is $HPI = 0{,}0002 \times \mathrm{Time(h)} + 0{,}0593$ with a squared correlation coefficient of $R^2 = 0{,}9507$. The slope of the rise and the correlation are practically the same as in the case of the hydroperoxide index.

8.2.2 Ultraviolet-visible spectra

The ultraviolet-visible absorption spectra measured for the five polystyrene samples before and after the whole irradiation cycle are presented in Figure 8.27.

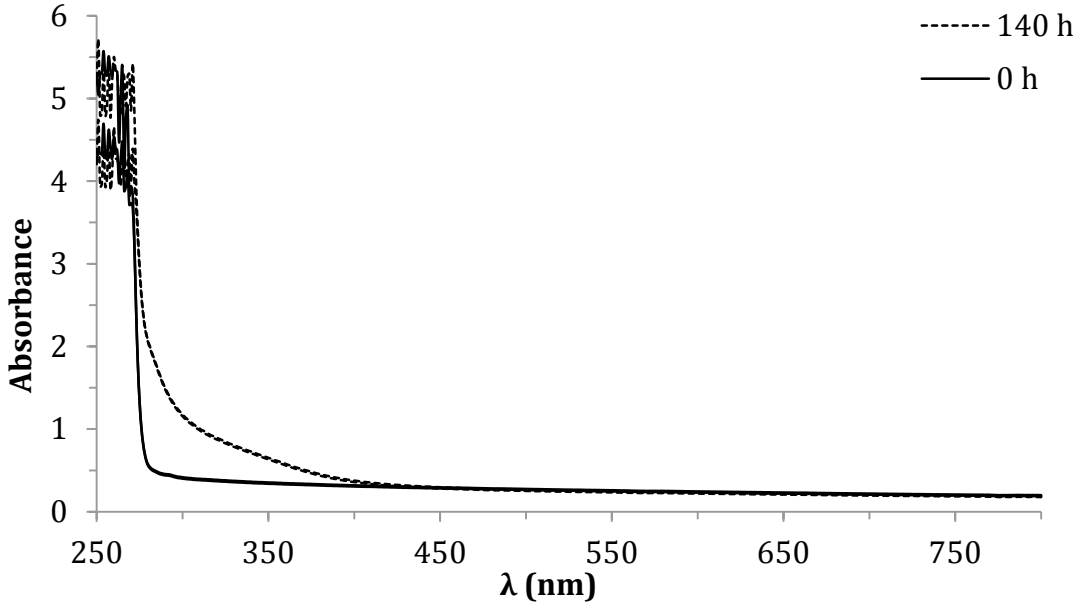

Figure 8.27 *UV-Vis spectra for PS before and after irradiation.*

A large increase in the UV absorbance of polystyrene is evident in the $\lambda = 270-400$ nm wavelength range. This increase is due to the formation of carbonyl groups and conjugated double bonds. The increased absorbance close to visible light is responsible for the yellowing observed in the polystyrene samples.

The UV absorption spectra of the polystyrene samples are presented in Figure 8.28 at various irradiation times.

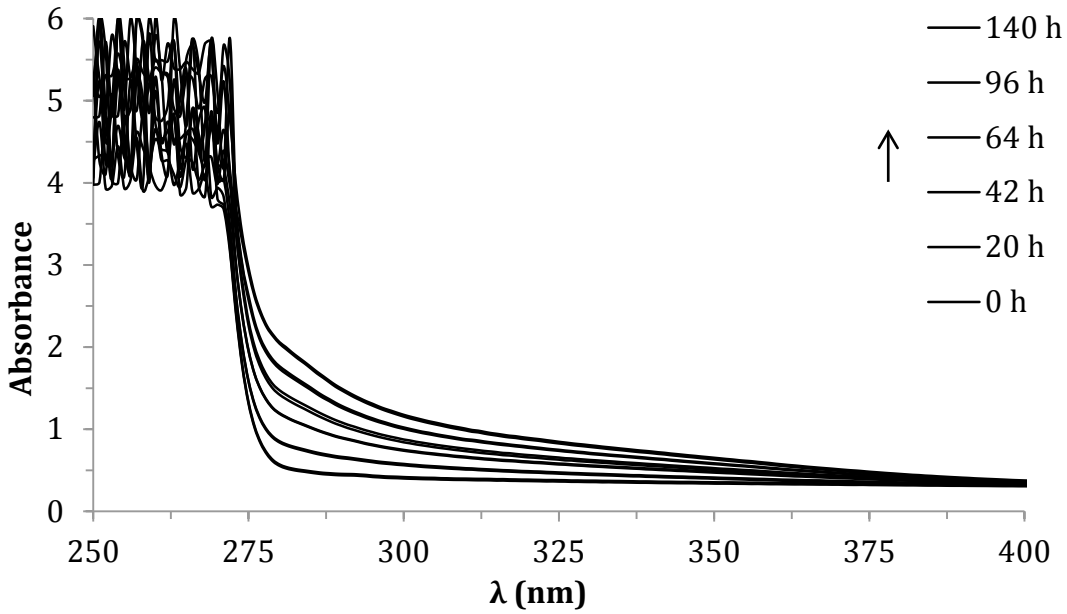

Figure 8.28 *UV spectra of polystyrene measured after 0, 20, 42, 64, 96 and 140 hours of irradiation.*

A close-up of the UV absorption spectra is presented in Figure 8.29.

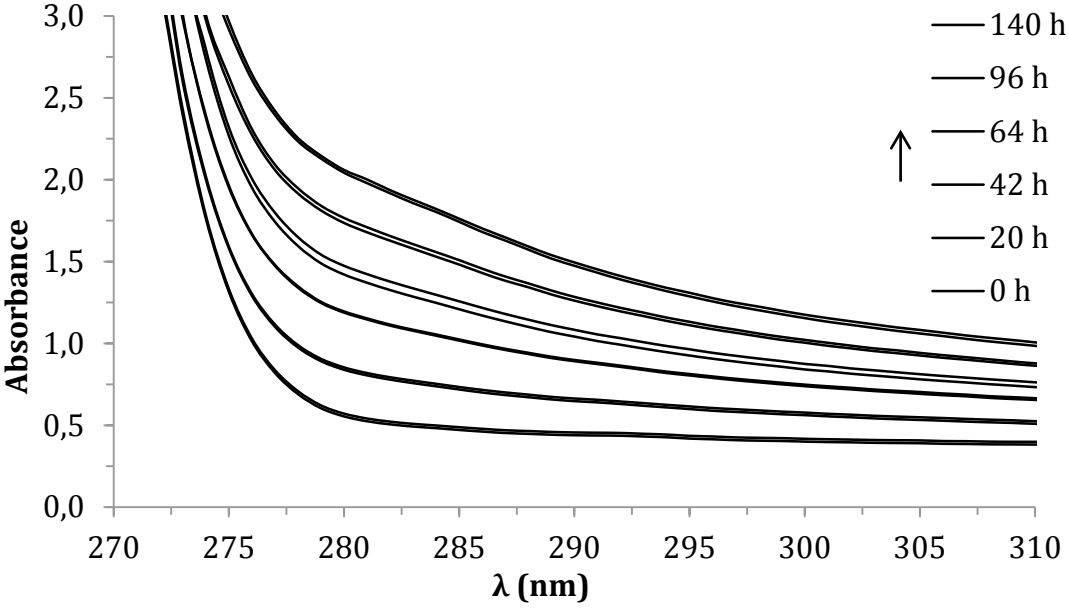

Figure 8.29 *UV spectra of polystyrene measured after 0, 20, 42, 64, 96 and 140 hours of irradiation.*

The largest change in the UV absorbance occurs at $\lambda = 280$ nm, where the absorbance increases from 0,5 to 2,0, corresponding to a change in the transmittance from 30 % to only 1 %. This increase is mostly due to the formation of carbonyl groups, which have an absorbance maximum at approximately $\lambda = 280$ nm.

The absorbances of the wavelengths that correspond with conjugated double bonds are presented in table 8.7.

Table 8.7 *Absorbances of polystyrene at wavelengths of 312, 328 and 362 nm at various irradiation times. The absorbances correspond to sequences with two, three and four conjugated double bonds, respectively. The results are averaged from the separate sample spectra with the standard error of the mean presented as the errors.*

Time (h)	$A(312\ \mathrm{nm})$	$A(328\ \mathrm{nm})$	$A(362\ \mathrm{nm})$
0	$0{,}387 \pm 0{,}009$	$0{,}368 \pm 0{,}008$	$0{,}337 \pm 0{,}008$
8	$0{,}437 \pm 0{,}007$	$0{,}402 \pm 0{,}007$	$0{,}349 \pm 0{,}006$
20	$0{,}510 \pm 0{,}007$	$0{,}458 \pm 0{,}007$	$0{,}379 \pm 0{,}007$
30	$0{,}578 \pm 0{,}016$	$0{,}512 \pm 0{,}014$	$0{,}409 \pm 0{,}013$
42	$0{,}646 \pm 0{,}005$	$0{,}563 \pm 0{,}005$	$0{,}436 \pm 0{,}006$
52	$0{,}685 \pm 0{,}013$	$0{,}591 \pm 0{,}012$	$0{,}448 \pm 0{,}012$
64	$0{,}730 \pm 0{,}015$	$0{,}625 \pm 0{,}013$	$0{,}461 \pm 0{,}009$
74	$0{,}781 \pm 0{,}007$	$0{,}665 \pm 0{,}007$	$0{,}484 \pm 0{,}007$
86	$0{,}837 \pm 0{,}012$	$0{,}710 \pm 0{,}011$	$0{,}509 \pm 0{,}010$
96	$0{,}855 \pm 0{,}008$	$0{,}720 \pm 0{,}006$	$0{,}508 \pm 0{,}004$
108	$0{,}900 \pm 0{,}007$	$0{,}758 \pm 0{,}006$	$0{,}532 \pm 0{,}006$
118	$0{,}907 \pm 0{,}008$	$0{,}760 \pm 0{,}006$	$0{,}528 \pm 0{,}006$
130	$0{,}959 \pm 0{,}011$	$0{,}804 \pm 0{,}010$	$0{,}554 \pm 0{,}010$
140	$0{,}972 \pm 0{,}010$	$0{,}810 \pm 0{,}010$	$0{,}555 \pm 0{,}009$

The evolution of the absorbance of polystyrene at $\lambda = 312$ nm as a function of irradiation time is presented in Figure 8.30. The absorbance corresponds to sequences with two conjugated double bonds.

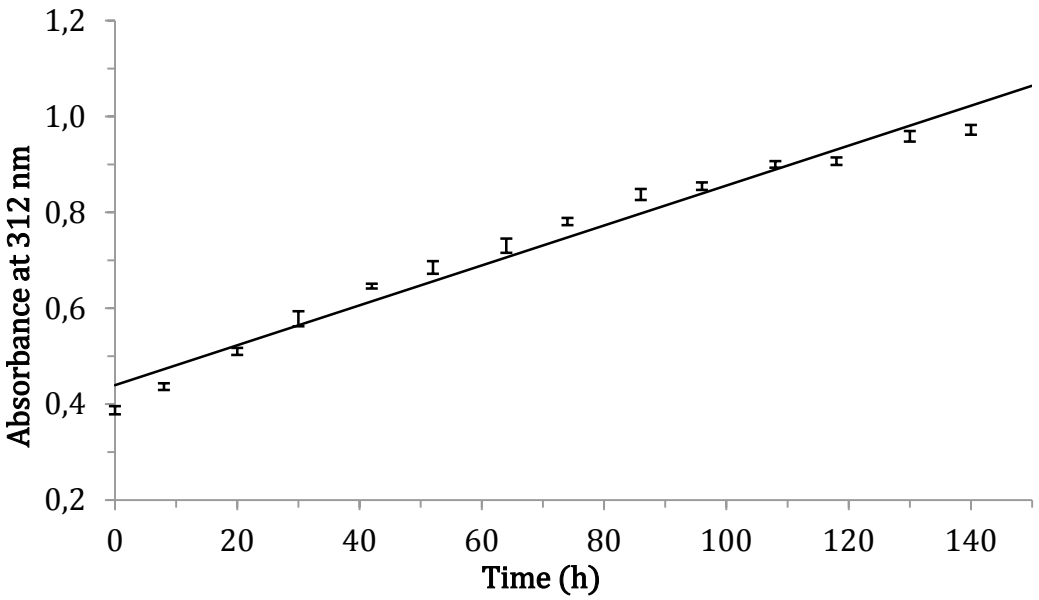

Figure 8.30 *Absorbance of polystyrene at $\lambda = 312$ nm as a function of irradiation time. The absorbance corresponds to sequences with two conjugated double bonds.*

The absorbance at $\lambda = 312$ nm rises linearly as a function of irradiation time with a linear fit of $A(312\text{ nm}) = 0{,}0042 \times \text{Time(h)} + 0{,}4395$. The squared correlation coefficient of the linear fit is $R^2 = 0{,}9722$, meaning that the linear fit is accurate. A steep propagation period and a termination period of slower rise are clearly visible in the evolution of the absorbance at $\lambda = 312$ nm, but an induction period visible in the evolution of the carbonyl index is missing.

The evolution of the absorbance of polystyrene at $\lambda = 328$ nm as a function of irradiation time is presented in Figure 8.31. The absorbance corresponds to sequences with three conjugated double bonds.

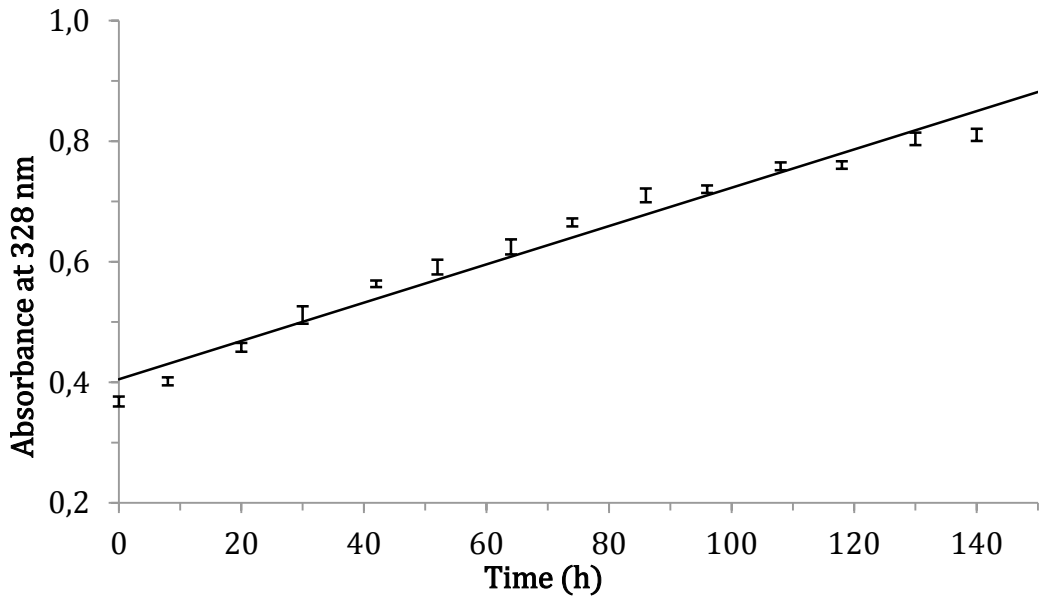

Figure 8.31 *Absorbance of polystyrene at $\lambda = 328$ nm as a function of irradiation time. The absorbance corresponds to sequences with three conjugated double bonds.*

The absorbance at $\lambda = 328$ nm rises linearly as a function of irradiation time with a linear fit of $A(328\text{ nm}) = 0{,}0032 \times \text{Time(h)} + 0{,}4051$. The squared correlation coefficient of the linear fit is $R^2 = 0{,}9725$. The slope is slightly smaller and the squared correlation coefficient practically the same as in the linear fit for the absorbance at 312 nm. The behavior of the absorbance at $\lambda = 328$ nm is similar to the behavior of the absorbance at 312 nm with a steep propagation period and a termination period of slower rise clearly visible in Figure 8.31.

The evolution of the absorbance of polystyrene at $\lambda = 362$ nm as a function of irradiation time is presented in Figure 8.32. The absorbance corresponds to sequences with four conjugated double bonds.

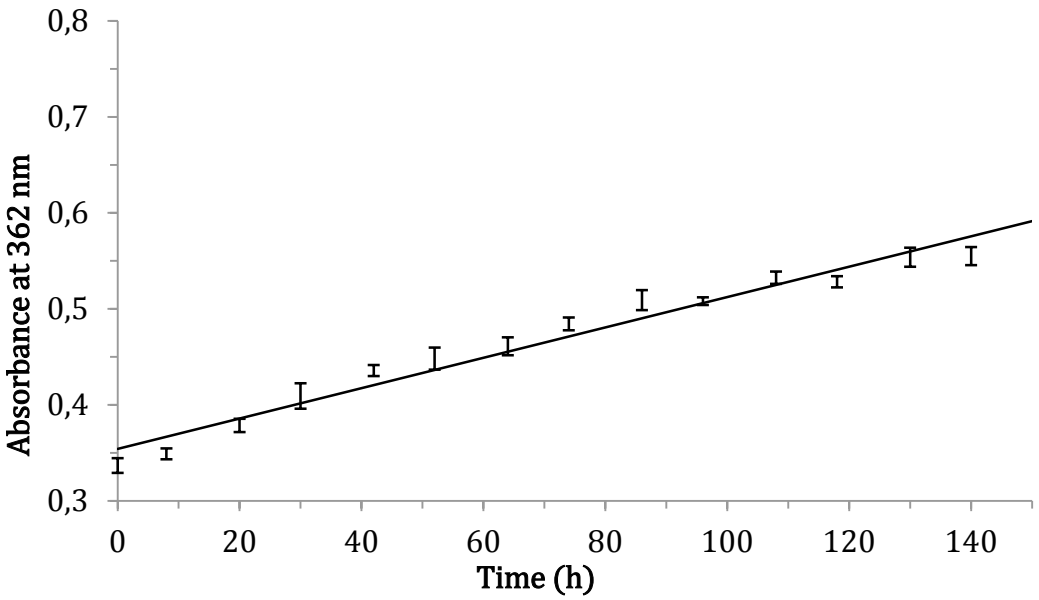

Figure 8.32 *Absorbance of polystyrene at $\lambda = 362\ nm$ as a function of irradiation time. The absorbance corresponds to sequences with four conjugated double bonds.*

The absorbance at $\lambda = 362$ nm rises linearly as a function of irradiation time with a linear fit of $A(362\text{ nm}) = 0{,}0016 \times \text{Time(h)} + 0{,}3543$. The squared correlation coefficient of the linear fit is $R^2 = 0{,}9666$. The slope is half of the slope for the linear fit for absorbance at 328 nm, but the squared correlation coefficient is practically the same as in the linear fits for the absorbances at 312 and 328 nm. The absorbance at $\lambda = 362$ nm exhibits a steep propagation period and a termination period of slower rise clearly in Figure 8.32.

8.2.3 Glass transition temperature of polystyrene

The two thermoanalytical glass transition curves of unirradiated polystyrene are presented in Figure 8.33.

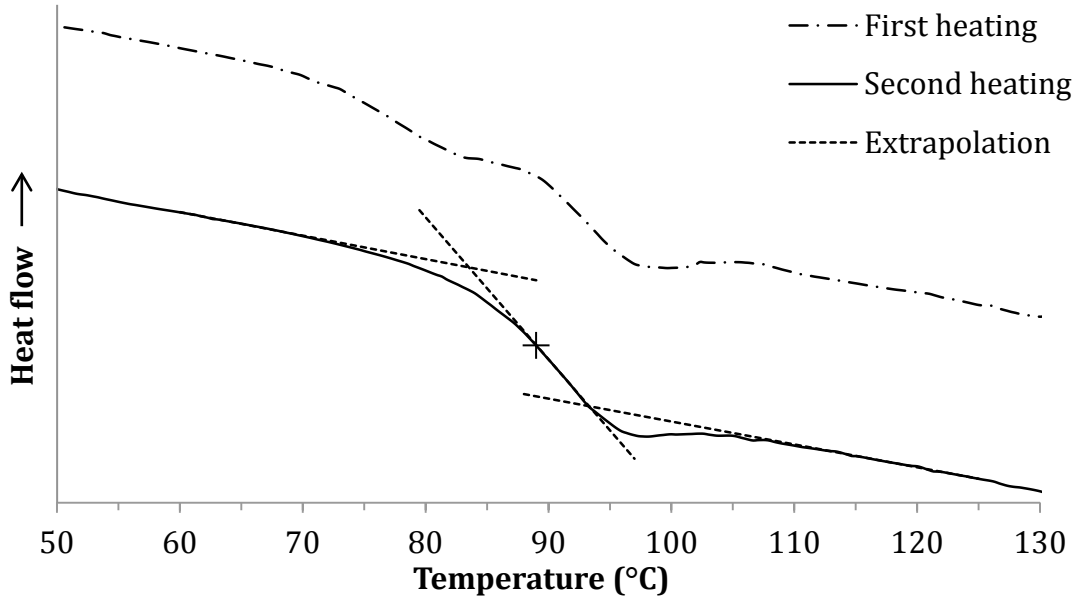

Figure 8.33 *Two thermoanalytical glass transition curves of polystyrene.*

The first heating in Figure 8.33 exhibits the characteristic relaxation band in the glass transition of polystyrene. The band disappears when the thermal history of the sample is erased after the first heating.

The glass transition temperature is measured from the second heating curve. It is determined by extrapolating the heat flow trace before and after the glass transition and of the steepest slope of the transition itself. The glass transition temperature is the temperature of the midpoint between the intercept points of the extrapolations, denoted with a cross in Figure 8.33.

The glass transition temperatures of polystyrene at various irradiation times are presented in table 8.8.

Table 8.8 *Glass transition temperatures of polystyrene at various irradiation times.*

Time (h)	T_g **(°C)**
0	$88{,}9 \pm 0{,}1$
20	$89{,}7 \pm 0{,}1$
45	$90{,}2 \pm 0{,}5$
92	$90{,}7 \pm 02$
140	$88{,}1 \pm 0{,}1$

The glass transition temperature of polystyrene rises by 2 °C in the first 92 hours of irradiation. This is probably due to crosslinking, which increases the average molecular mass. Between 92 and 140 hours of irradiation the glass transition temperature decreases by 3 °C. The large decrease in T_g is possibly due to either chain scission, which decreases the average molecular mass, or the photochain oxidation mechanism, which

decreases the molecular mass of and removes steric hindrances from the polymer chains.

8.2.4 Oxidation induction time

The thermoanalytical OIT curves measured at several different temperatures for unirradiated polystyrene are presented in Figure 8.34.

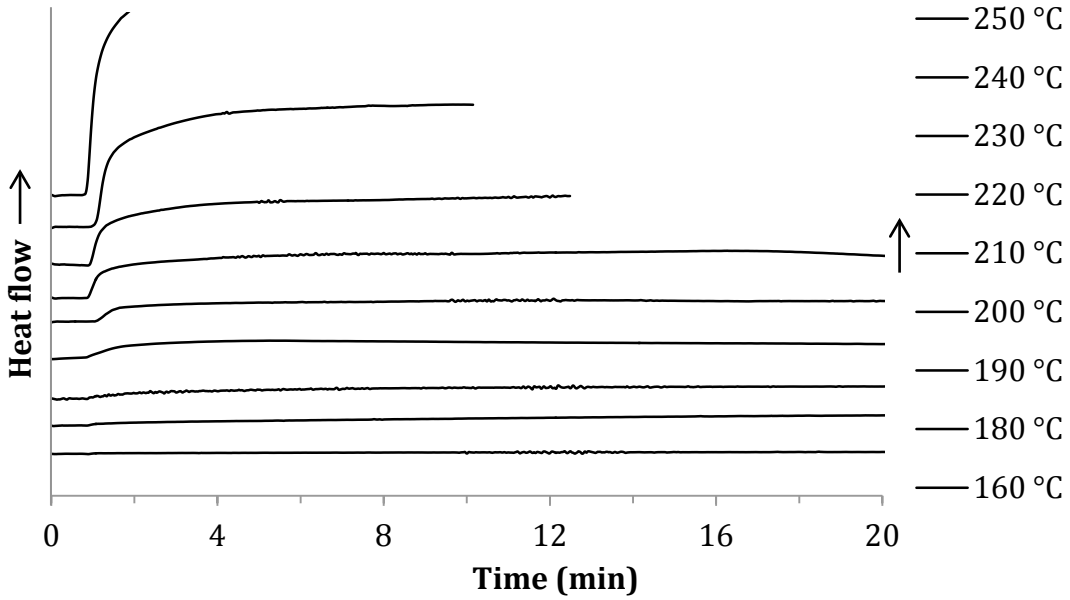

Figure 8.34 *Thermoanalytical OIT curves of polystyrene measured at temperatures of 160, 180, 190, 200, 210, 220, 230, 240 and 250 ºC.*

The thermoanalytical curves measured at temperatures under 200 °C do not exhibit an oxidation peak in the OIT curves. The thermoanalytical curves measured at 200 °C and upwards start to exhibit an exotherm at an OIT of approximately one minute, which corresponds to the dead volume of the gas line to the DSC. The whole thermoanalytical curve measured at 200 °C is presented in Figure 8.35.

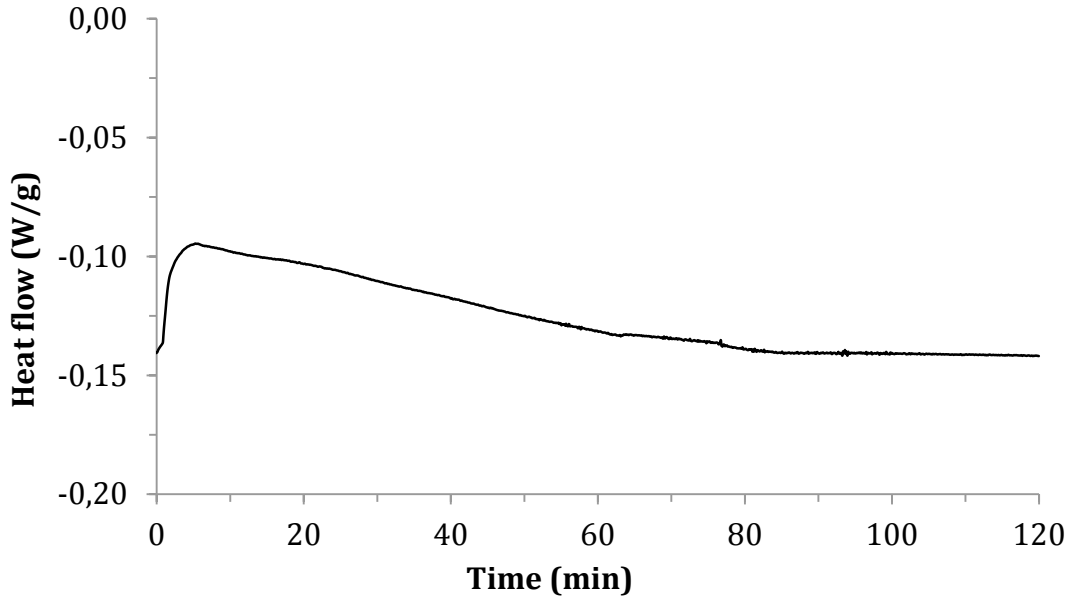

Figure 8.35 *Thermoanalytical OIT curve of polystyrene measured at a temperature of 200 ºC.*

The exotherm that is formed at test temperatures above 200 °C grows consistently as the test temperature increases and the onset time of the exotherm remains stable. This indicates that when the thermal activation energy of oxidation is exceeded, the oxidation occurs immediately. Thus the measurement of the oxidation induction time is not applicable to the polystyrene samples used in this study.

8.2.5 Oxidation induction temperature

The heat flow trace from oxidation induction temperature measurement for unirradiated polystyrene is presented in Figure 8.36.

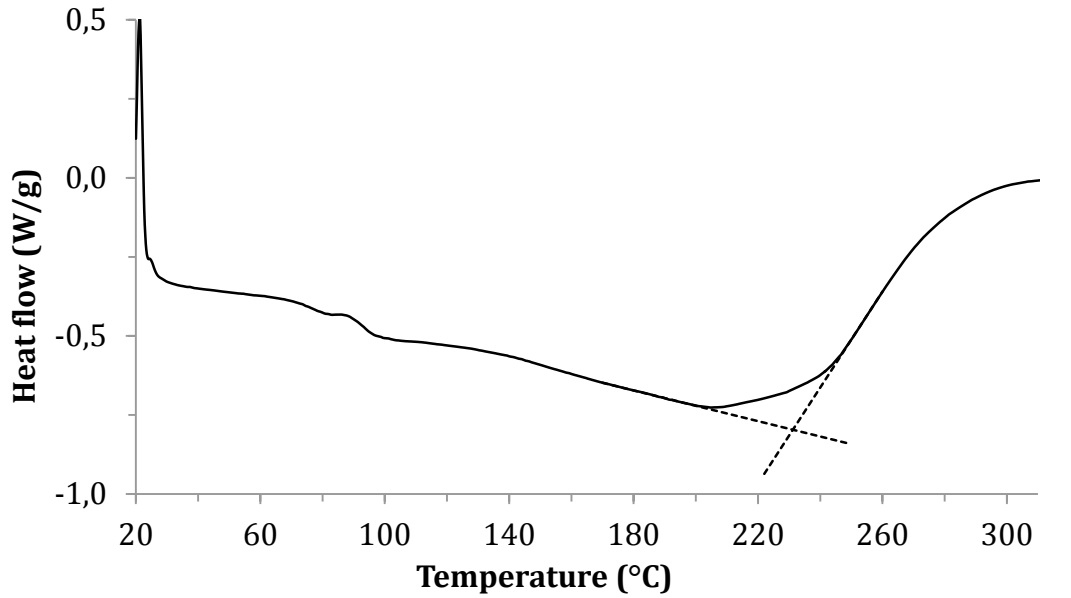

Figure 8.36 *Thermoanalytical oxidation induction temperature curve of polystyrene.*

The T_{ox} is determined in the same way as in chapter 8.1.5 for polypropylene.

The UV-T_{ox} was measured with the same method as the T_{ox}, with the DPC lamp's shutter open from the beginning of the test. The thermoanalytical UV-T_{ox} curve is presented in Figure 8.37.

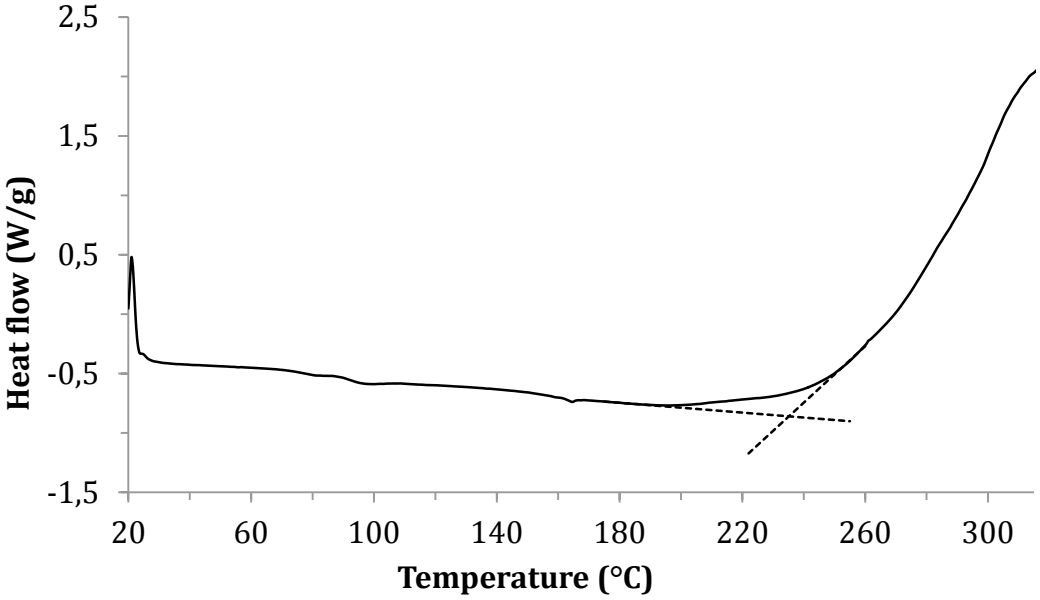

Figure 8.37 *Thermoanalytical UV oxidation induction temperature curve of polystyrene.*

The thermoanalytical UV-T_{ox} curve in Figure 8.37 is identical to the T_{ox} curve in Figure 8.36, only with a slightly higher oxidation induction temperature.

The T_{ox} and UV-T_{ox} values measured for the polystyrene samples at various irradiation times are presented in table 8.9.

Table 8.9 *T_{ox} and UV-T_{ox} of polystyrene at various irradiation times.*

Time (h)	T_{ox} (°C)	UV-T_{ox} (°C)
0	$231{,}3 \pm 0{,}4$	$247{,}1 \pm 0{,}3$
20	$235{,}8 \pm 6{,}7$	$260{,}2 \pm 1{,}1$
45	$240{,}7 \pm 1{,}7$	$252{,}0 \pm 1{,}2$
92	$265{,}3 \pm 0{,}9$	$242{,}4 \pm 4{,}0$
140	$272{,}9 \pm 1{,}3$	$253{,}3 \pm 1{,}6$

The T_{ox} rose consistently with irradiation time, rising by over 40 °C in 140 hours of irradiation. This was possibly due to crosslinking, which increases the molecular weight of the polymer chains. The UV-T_{ox} on the other hand either rose or dropped by approximately 10 °C between consecutive irradiation times. The behavior of the UV-T_{ox} seems to be rather stochastic, and no trend is clearly visible in the data.

8.3 Degradation comparison between polypropylene and polystyrene

The degradation indices, formation of double bonds and the oxidation induction temperature of polypropylene and polystyrene are compared in this chapter. The purpose of this chapter is to determine the best instrumental methods in the evaluation of polymer photodegradation.

8.3.1 Degradation indices

Figure 8.38 presents the carbonyl indices of polypropylene and polystyrene as a function of time.

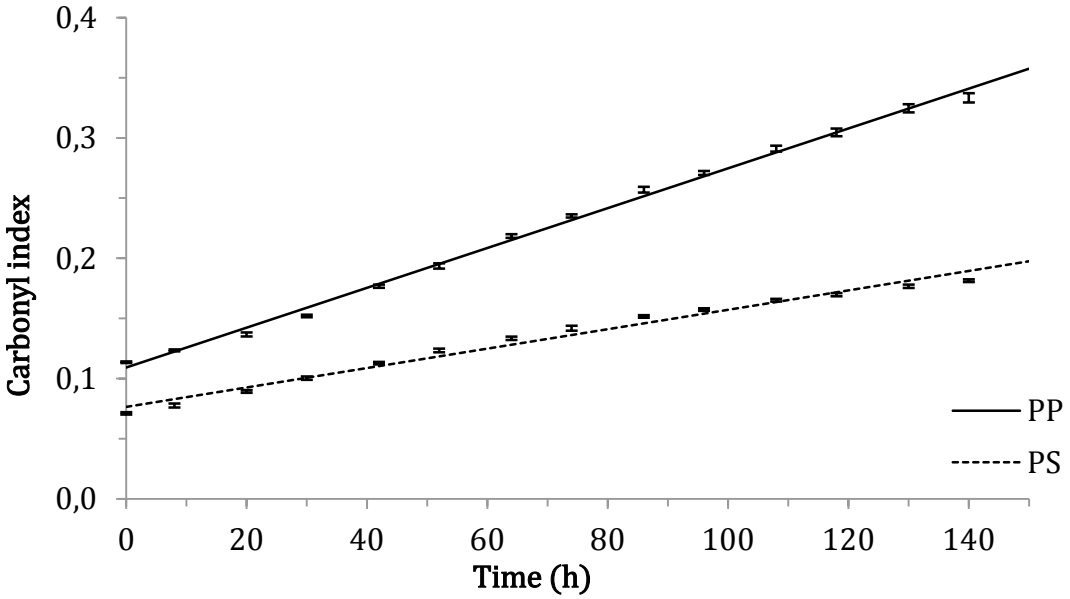

Figure 8.38 *Carbonyl indices of PP and PS as a function of time.*

The slope of the linear fit to the CI of PP is over two times larger than the slope of the CI of PS. This indicates that carbonyl groups are formed in PP much faster than in PS, making the detection of photodegradation faster for PP using the carbonyl index. This is an expected result, because unirradiated pure PP does not contain any absorption bands near the carbonyl group absorption area in IR spectroscopy.

Figure 8.39 presents the hydroperoxide indices of polypropylene and polystyrene as a function of time.

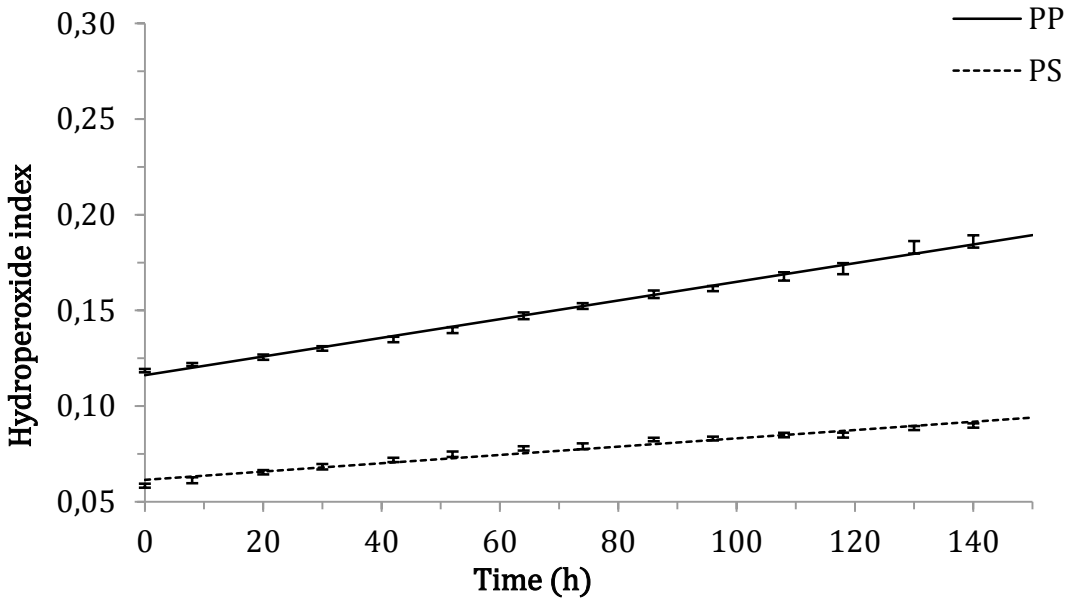

Figure 8.39 *Hydroperoxide indices of PP and PS as a function of time.*

The slope of the linear fit to the HPI of PP is 50 % larger than the slope of the CI of PS. This indicates that also hydroperoxide groups are formed in PP faster than in PS.

Figure 8.40 presents the hydroxyl indices of polypropylene and polystyrene as a function of time.

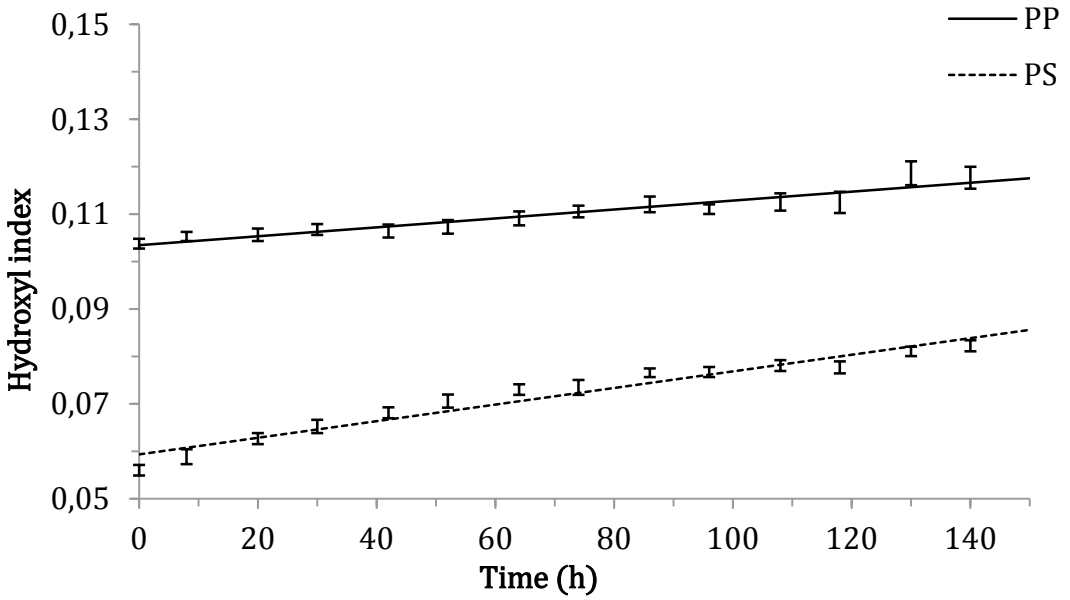

Figure 8.40 *Hydroxyl indices of PP and PS as a function of time.*

The slope of the linear fit to the HPI of PP is less than half of the slope of the CI of PS. This indicates that unlike the carbonyl and hydroperoxide groups, hydroxyl groups are formed in PP much slower than in PS.

In all of the degradation indices presented in Figures 8.38–8.40 the error bars for measurements of PS's indices are smaller. This indicates that PS may photodegrade in a more homogenous way when compared to PP.

8.3.2 Formation of double bonds

Figure 8.41 presents the UV absorbances of polypropylene and polystyrene at $\lambda = 312$ nm as a function of time.

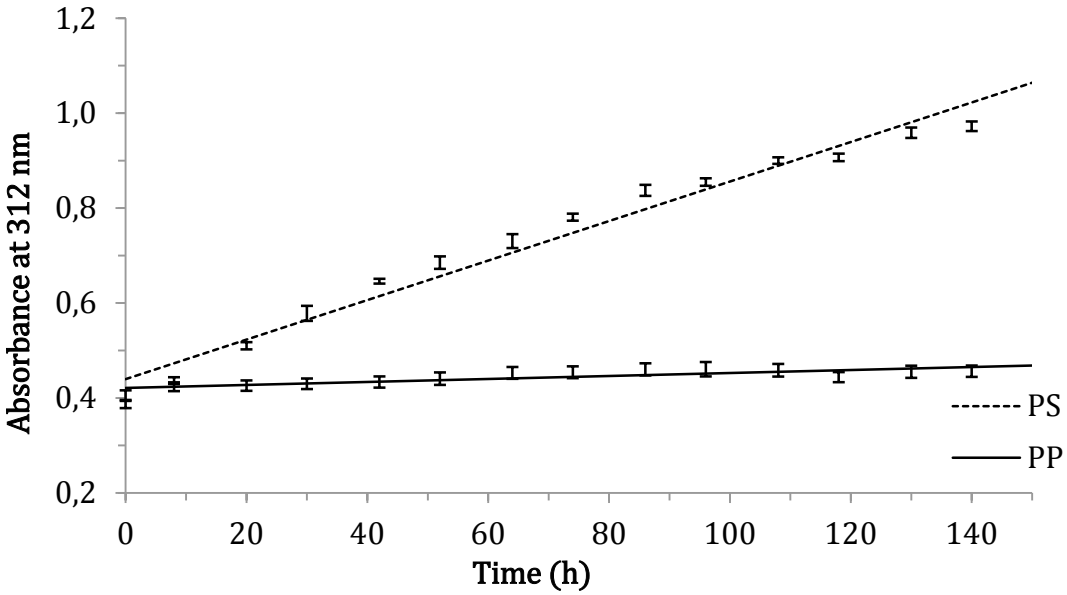

Figure 8.41 *UV absorbances of PP and PS at $\lambda = 312$ nm as a function of time. The absorbances correspond to sequences with two conjugated double bonds.*

The slope of the linear fit to the UV absorbance at $\lambda = 312$ nm of PS is 42 times larger than the slope of the UV absorbance at $\lambda = 312$ nm of PP. There is practically no trend in the results for PP when compared to the results for PS. This indicates strongly that conjugated dienes are not formed in the photodegradation of PP, whereas they are strongly formed in PS. This makes UV-Vis spectroscopy an important tool in the detection of photodegradation of PS, whereas it indicates only small changes in PP.

Figure 8.42 presents the UV absorbances of polypropylene and polystyrene at $\lambda = 328$ mn as a function of time.

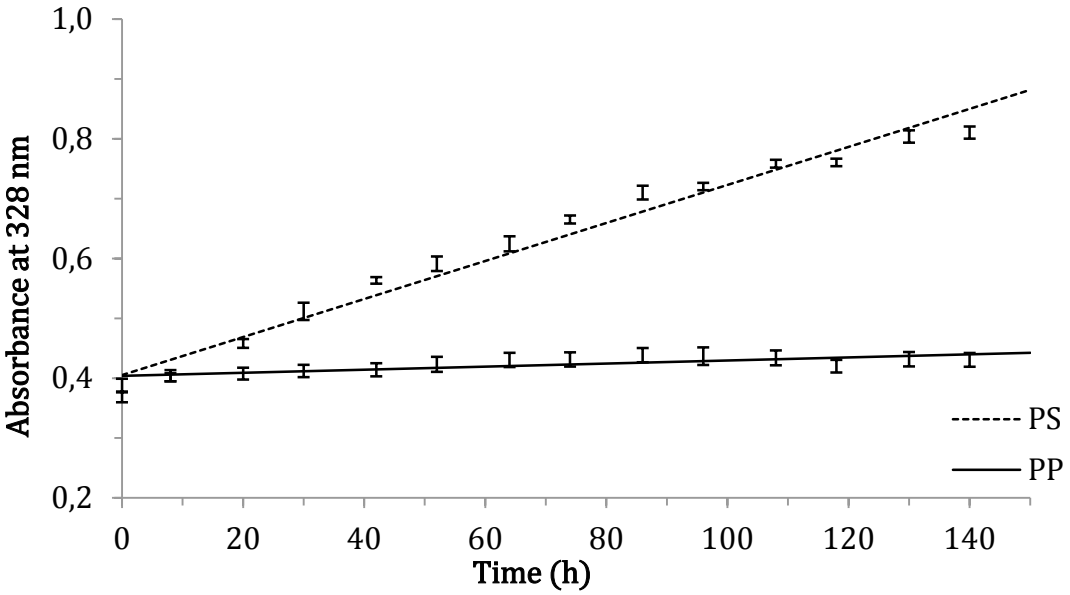

Figure 8.42 *UV absorbances of PP and PS at $\lambda = 328\ nm$ as a function of time. The absorbances correspond to sequences with three conjugated double bonds.*

The slope of the linear fit to the UV absorbance at $\lambda = 328$ nm of PS is over 30 times larger than the slope of the UV absorbance at $\lambda = 328$ nm of PP. There is practically no change in the slope for PP when compared to the results obtained for the UV absorbance at $\lambda = 312$ nm. This is expected, because when no conjugated dienes are observed the polymer samples cannot contain any conjugated trienes. Conjugated trienes are strongly formed in PS. For PS the slope for the UV absorbance at $\lambda = 328$ nm is a third smaller than the slope for the UV absorbance at $\lambda = 312$ nm.

Figure 8.43 presents the UV absorbances of polypropylene and polystyrene at $\lambda = 362$ mn as a function of time.

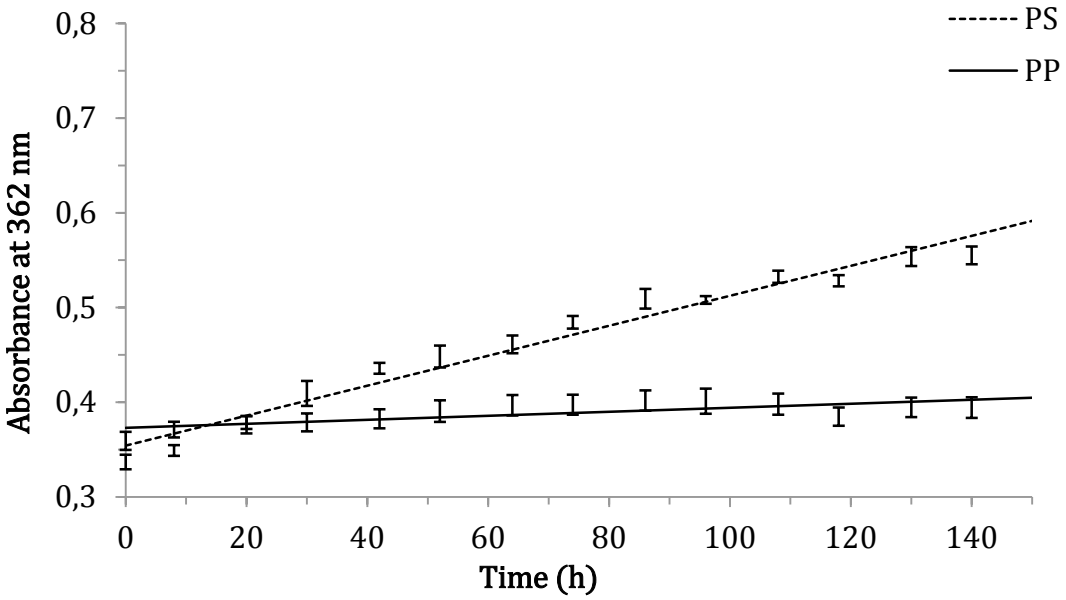

Figure 8.43 *UV absorbances of PP and PS at $\lambda = 362\ nm$ as a function of time. The absorbances correspond to sequences with four conjugated double bonds.*

The slope of the linear fit to the UV absorbance at $\lambda = 362$ nm of PS is 8 times larger than the slope of the UV absorbance at $\lambda = 362$ nm of PP. The slope for PP remains practically the same as in the UV absorbances at $\lambda = 312$ and $\lambda = 328$ nm. The slope for PS on the other hand is only a fifth of the slope for the UV absorbance $\lambda = 312$ nm. This indicates that conjugated tetraenes are formed in a much lesser amount than conjugated dienes or trienes.

The formation of conjugated double bonds in PS corresponds well with the yellowing of the samples observed during photodegradation. UV-Vis spectroscopy is a valuable tool in measuring the changes that occur in PS during photodegradation. It is a precise measurement, which can indicate changes in the UV absorption spectrum much faster than the changes in color are observable in the samples.

8.3.3 Oxidation induction temperature

The oxidation induction temperature is the only DSC measurement that was applicable for both polypropylene and polystyrene. This enables a direct comparison of the changes observed in the T_{ox}. The T_{ox} results are presented in table 8.10.

Table 8.10 *Oxidation induction temperatures for PP and PS as a function of irradiation time.*

Time (h)	***PP* - T_{ox} (°C)**	***PS* - T_{ox} (°C)**
0	$231{,}4 \pm 1{,}5$	$231{,}3 \pm 0{,}4$
20	$192{,}0 \pm 1{,}7$	$235{,}8 \pm 6{,}7$
45	$185{,}7 \pm 1{,}8$	$240{,}7 \pm 1{,}7$
92	$181{,}9 \pm 2{,}3$	$265{,}3 \pm 0{,}9$
140	$180{,}2 \pm 1{,}4$	$272{,}9 \pm 1{,}3$

The evolution of the oxidation induction temperature is significantly different for polypropylene and polystyrene. The T_{ox} drops consistently for PP as a result of irradiation, whereas it rises for PS. This is probably due to the different photodegradation mechanisms of PP and PS. The different behavior of the T_{ox} for PP and PS can possibly be explained by a lowering of the molecular mass of the PP chains and an increase in the molecular mass of the PS chains. The changes in the polymer's molecular masses in these directions are supported by the results obtained for the melting temperatures of PP and the glass transition temperatures of PS.

9. OVERVIEW AND CONCLUSIONS

The photodegradation of polypropylene and polystyrene was studied in this thesis using FTIR spectroscopy, UV-Vis spectroscopy and DSC. The polymer samples were artificially weathered by irradiating them with a xenon arc lamp, and the measurements were performed at suitable time intervals during the irradiation cycle. FTIR spectroscopy was used to observe the changes occurring in the polymer structure and the formation of new functional groups. UV-Vis spectroscopy was used to observe the formation of double bonds and the changes in the color of the polymer samples. DSC was used to observe the changes in the thermal properties and oxidative stability of the polymers. DPC was used as a novel approach to measure the oxidative stability of the polymers with simultaneous irradiation. The DPC results were compared to the oxidative stability results obtained with regular DSC.

The largest change observed in the polymer samples during irradiation was the formation of a carbonyl group absorption band in the IR spectra, with the band maximum located at $\tilde{\nu} \approx 1720\ \mathrm{cm}^{-1}$ corresponding to the formation of a carboxylic acid for polypropylene and an aliphatic ketone for polystyrene. The carbonyl band was clearly visible after only 20 hours of irradiation for both polymers and it was the first observed change during photodegradation. The formation of hydroperoxide and hydroxyl groups was much less pronounced in the IR spectra, although hydroperoxides are the primary photodegradation products. Hydroperoxide groups are probably decomposed rapidly in reactions with energetic low wavelength radiation at $\lambda < 300\ \mathrm{nm}$.

A substantial change observed during irradiation was the increase in the UV absorbance of polystyrene between $\lambda = 270\text{–}350\ \mathrm{nm}$. The increase in the absorbance at $\lambda = 280\ \mathrm{nm}$ is due to the formation of the carbonyl groups observed also in the IR spectra. The increase in absorbance at higher wavelengths is due to the formation of conjugated double bonds in the polystyrene chain, mostly consisting of two and three conjugated bonds. The formation of conjugated double bonds was the reason for the yellowing observed in the polystyrene samples during irradiation. The UV absorbance of polypropylene changed only slightly between $\lambda = 250\text{–}300\ \mathrm{nm}$, which was assigned to the formation of the carbonyl group.

The absorbances used to determine the degradation indices and formation of double bonds grew linearly with time. According to the Lambert-Beer law absorbance is linear with the concentration of the absorbing agent, so the linear growth of the absorbances implies a linear growth of the photoproduct concentrations. Because the photoproduct concentration is expected to grow logarithmically, the linear growth implies an early stage of degradation, where a linear approximation is valid. The evolution of the degra-

dation indices and formation of double bonds can possibly be studied further using thicker samples, which can endure mechanical degradation better than the thin samples used in the spectroscopic studies of this thesis.

The thermal properties of both polypropylene and polystyrene changed during irradiation. The melting temperature of polypropylene remained fairly stable for the first 92 hours and decreased noticeably between 92 and 140 hours of irradiation. This change was assigned to a decrease in the average molecular mass due to chain scission. The glass transition temperature of polystyrene rose steadily for the first 92 hours, but decreased noticeably between 92 and 140 hours of irradiation. The increase was assigned to crosslinking, which increases the average molecular mass, and the decrease was assigned to either chain scission, which decreases the average molecular mass, or the photochain oxidation mechanism, which removes steric hindrances and also decreases the average molecular mass.

The oxidation induction time measured with DSC and DPC decreased rapidly with exposure time for polypropylene. The OIT decreased over 90 % within the first 20 hours of irradiation, with the oxidation occurring practically immediately for the irradiated samples. The UV-OIT was less than half of the OIT before irradiation, also occurring practically immediately after irradiation. The OIT test was not applicable for the polystyrene samples.

The oxidation induction temperature of polypropylene also decreased rapidly within the first 20 hours of irradiation, after which the T_{ox} continued to decrease steadily. The T_{ox} was higher than the UV-T_{ox} for unirradiated polypropylene, but for all of the irradiated samples the situation reversed, which was an unexpected result not reported before. It may be that the photodegradation reactions that occur in the melted samples hinder the thermal degradation in some manner, but further research is needed to resolve this mechanism. The T_{ox} of polystyrene increased quite steadily for the whole irradiation cycle. These results indicate that the thermal oxidative stability of polypropylene decreases whereas the stability of polystyrene increases due to photodegradation. This may be due to changes in the average molecular mass, with a decrease in mass indicating a decrease in the oxidative stability and vice versa.

Of the instrumental methods used in this study FTIR spectroscopy is the fastest way to directly detect the early chemical changes that are due to the photodegradation of polymers. UV-Vis spectroscopy is mainly useful as a method for supplementary analysis, but is especially important if the polymer contains pigments for stabilization or coloring. DSC is valuable as a fast means to measure the thermal properties and the thermal oxidative stability of polymers. The effect of photodegradation on the thermal stability of polymers needs to be studied further, in order to solve the mechanism that appears to inhibit thermal degradation when the sample is exposed to simultaneous UV irradiation.

REFERENCES

[1] Fried, J. R. 2003. *Polymer science and technology*, 2nd ed. New Jersey, Pearson Education, Inc. Publishing as Prentice Hall Professional Technical Reference. 582 p.

[2] Jenkins, A. D., Kratochvíl, P., Stepto, R. F. T. & Suter, U. W. *Glossary of Basic Terms in Polymer Science*. Pure & Applied Chemistry 68(1996)12, pp. 2287–2311.

[3] Frank, H. P. 1968. *Polypropylene*. New York, Gordon and Breach, Science Publishers, Inc. 134 p.

[4] *Sähkömagneettisen säteilyn spektri*. In: Seppänen, R., Kervinen, M., Parkkila, I., Karkela, L. & Meriläinen, P. MAOL-taulukot. 2. painos. Helsinki 2005, Matemaattisten Aineiden Opettajien Liitto MAOL ry. and Kustanneosake-yhtiö Otava. p. 145.

[5] Table 1.1 Energy Conversion Table. In: Turro, N. J. *Modern Molecular Photochemistry*. 1st ed. Menlo Park 1978, The Benjamin/Cummings Publishing Company, Inc., p. 8.

[6] Rånby, B. G. & Rabek, J. F. 1975. *Photodegradation, Photo-oxidation and Photostabilization of Polymers*. London, John Wiley & Sons, Inc. 573 p.

[7] Carlsson, D. J. & Wiles, D. M. *The Photodegradation of Polypropylene Films. II. Photolysis of Ketonic Oxidation Products.* Macromolecules 2(1969)6, pp. 587–597.

[8] Kuzina, S. I. & Mikhailov, A. I. *Chain and Photochain Mechanisms of Photooxidation of Polymers*. High Energy Chemistry 44(2010)1, pp. 39–53.

[9] Silverstein, R. M. & Webster, F. X. 1997. *Spectrometric Identification of Organic Compounds*. 6th ed. John Wiley & Sons, Inc. 496 p.

[10] Rajakumar, K., Sarasvathy, A., Thamaraichelvan, A., Chitra, R. & Vijayakumar, C. T. *Effect of Iron Carboxylates on the Photodegradability of Polypropylene. I. Natural Weathering Studies*. Journal of Applied Polymer Science 118(2010), pp. 2601–2612.

[11] Mailhot, B. & Gardette, J.-L. *Polystyrene Photooxidation. 1. Identification of the IR-Absorbing Photoproducts Formed at Short and Long Wavelengths*. Macromolecules 25(1992), pp. 4119–4126.

[12] Burfield, D. R. & Loi, P. S. *T. Approaches to the Problem of Tacticity Determination in Polypropylene*. Studies in Surface Science and Catalysis 25(1986), pp. 387–406.

[13] Sundell, T., Fagerholm, H. & Crozier, H. *Isotacticity determination of polypropylene using FT-Raman spectroscopy*. Polymer 37(1996)15, pp. 3227–3231.

[14] Blais, P., Carlsson, D. J. & Wiles, D. M. *Surface changes during polypropylene photo-oxidation: a study by infrared spectroscopy and electron microscopy.* Journal of Polymer Science 10(1972)A-1, pp. 1077–1092.

[15] Kaczmarek, H., Kamińska, A., Świątek, M. & Sanyal. S. *Photoinitiated degradation of polystyrene in the presence of low-molecular organic compounds*. European Polymer Journal 36(2000), pp. 1167–1173.

[16] Torikai, A. & Sibata, H. *Photodegradation of polystyrene: Effect of polymer structure on the formation of degradation products*. The Arabian Journal for Science and Engineering 27(2002)1C, pp. 11–24.

[17] Gabbott, P., editor. 2008. *Principles and Applications of Thermal Analysis.* Blackwell Publishing Ltd. 464 p.

[18] SFS-ISO 11357-1. *Plastics — Differential scanning calorimetry (DSC) — Part 1: General principles*. Helsinki 2009, Suomen standardoimisliitto. 31 p.

[19] ISO 11357-6. *Plastics — Differential scanning calorimetry (DSC) — Part 6: Determination of oxidation induction time (isothermal OIT) and oxidation induction temperature (dynamic OIT).* 2008. 12p.

[20] Tabelle 3.3 Zusammenfassende Darstellung der mit GPC-MALLS ermittelten Molmassenmittelwerte und Polydispersitäten aller untersuchten Polypropylene mit Ausnahme der Blends. In: Stange, J. *Einfluss rheologischer Eigenschaften auf das Schäumverhalten von Polypropylenen unterschiedlicher molekularer Struktur*. Dissertation. Erlangen 2006. University of Erlangen-Nuremberg, Faculty of Engineering. p. 41.

[21] Kaci, M., Remili, C., Bruzaud, S. & Grohens, Y. *Effect of Photooxidation on Polystyrene/Cloisite 15A Nanocomposites Under Accelerated UV Exposure.* Academic Journal of Manufacturing Engineering 8(2010)1, pp. 61–66.

[22] ISO 10640. *Plastics — Methodology for assessing polymer photoageing by FTIR and UV/visible spectroscopy*. 2011. 29 p.

[23] Kemp, T. J. & McIntyre, R. A. *Influence of transition metal-doped titanium(IV) dioxide on the photodegradation of polystyrene.* Polymer Degradation and Stability 91(2006), pp. 3010–3019.